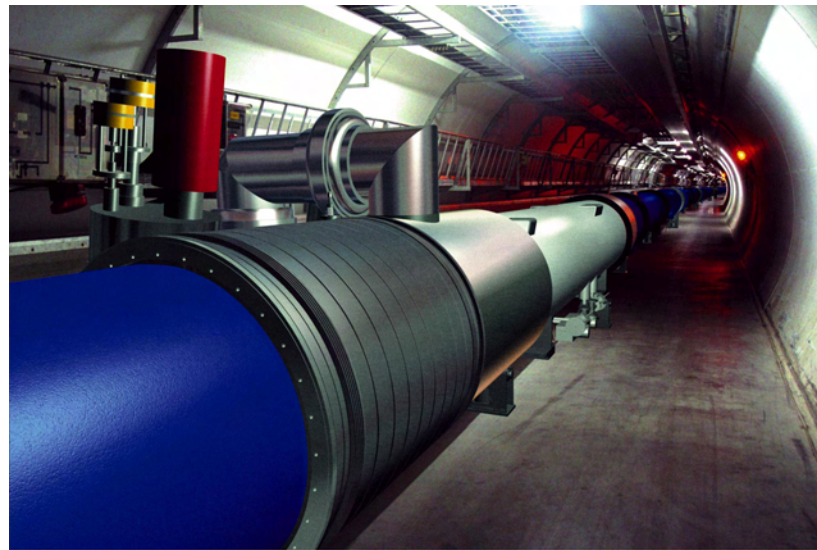


Torbjørn Houge

Mobile remote surveillance system for the CERN LHC cryogenic system

Trondheim August 2006

NTNU
Norwegian University of Science and Technology
Faculty of Information Technology, Mathematics and
Electrical Engineering
Department of Engineering Cybernetics



TORBJØRN HOUGE

Mobile remote surveillance system for the CERN LHC cryogenic system

Trondheim, August 2006

Academic supervisor: Jan tommy gravdahl

External supervisor: Luigi Serio



CERN - EUROPEAN ORGANIZATION FOR NUCLEAR RESEARCH



NORWEGIAN UNIVERSITY OF SCIENCE AND TECHNOLOGY
Faculty of Information Technology, Mathematics and electrical Engineering
Department of Engineering Cybernetics

NTNU
Norwegian University of
Science and Technology

CERN
European Organization for
Nuclear Research

Faculty of Information Technology,
Mathematics and Electrical Engineering
Department of Engineering Cybernetics

AT-ACR
Accelerator technology
Cryogenics for Accelerators



MASTER THESIS

Name of candidate: Torbjørn Houge

Program: Cybernetics Engineering

Title of thesis: Mobile, remote surveillance of underground cryogenic equipment

Assigned task:

Plan and build a mobile, remote surveillance system for monitoring of the cryogenic equipment in one sector of the CERN LHC tunnel. Each sector is 3.3 km in length. The camera has to use as much of the existing infrastructure as possible, and not interfere with operation of the LHC or other maintenance tasks. The system will use a specified camera, of the type already in use in other locations at CERN.

1. Make a technical specification based on equipment and technical constraints.
2. Research the technologies that can be used for this system. Especially consider using the powered overhead rail for supplying both power and communications.
3. Investigate limitations for this system. Find solutions on how to handle these limitations.
4. Make a detailed proposal for the surveillance system.
5. Propose a positioning system with feedback control based on modeling and simulations of the total surveillance system.
6. Simulate the total system with the proposed controller.

Assignment given: 1. February 2006

Due: 9. August 2006

Handed in: 9. August 2006

Accomplished at CERN and NTNU, Department of Engineering Cybernetics
Supervisor CERN: Luigi Serio

Supervisor NTNU: Jan Tommy Gravdahl

Preface

It is common sense to take a method and try it. If it fails, admit it frankly and try another. But above all, try something.

- Franklin D. Roosevelt

Several good people have given me a helping hand or two during my work on this thesis. First of all, I will thank my supervisor at CERN, Luigi Serio, whom has kept me focused on the project at hand, reminding me of the deadlines we have set, and not shown too much disappointment when I did not meet them.

Also, my supervisor at NTNU, Jan Tommy Gravdahl, has done the job of guiding me so that I also am able to fulfill the requirements from NTNU.

There are several other people at CERN that I would like to thank. Guiseppe Gubello, for his support in helping me with finding background information about the project, and general help in how things work at CERN. Benoit Civel, for making the PCB layout from my schematics for the communication device. Also, I thank Anders Vestnes and Øyvind Aakvik, fellow technical students, for acting as electronic design consultants when I needed it most. Without you, I would not have been able to complete the design of the circuit.

Contents	ix
List of Figures	xiii
List of Tables	xv
Summary	xvii
1 Introduction	1
1.1 Outline of this thesis	1
1.2 Contributions of this thesis	2
1.3 Publication of results from this thesis	3
2 Background	5
2.1 About CERN	5
2.2 Large Hadron Collider - LHC	5
2.2.1 Cryogenics	6
2.2.2 Hazards	6
2.2.3 Description of the tunnel	9
2.2.4 Tunnel surveillance	10
3 Requirements	11
3.1 Camera	11
3.2 Trolley	12
3.3 Power	14
3.4 Communications	14
3.5 Summary	15
4 Technology	17
4.1 Camera	17
4.1.1 Axis 213 PTZ	17
4.1.2 External light source	18
4.2 Trolley	18
4.2.1 Prefabricated	18
4.2.2 Modifications to the prefabricated trolley	19

4.3	Power	20
4.3.1	FABA power rail	20
4.3.2	Battery power	22
4.4	Communications	22
4.4.1	Wired communication technologies	22
4.4.2	Wireless communication technologies	23
4.5	Proposal	26
4.5.1	Camera	29
4.5.2	Trolley	29
4.5.3	Communication	29
4.5.4	Power	30
4.6	Limitations	31
5	Design and assembly	33
5.1	Hardware	33
5.1.1	Camera	33
5.1.2	Trolley	33
5.1.3	Power	33
5.1.4	Communication	33
5.2	Software	35
5.2.1	Camera	36
5.2.2	Microcontroller for the trolley	36
6	Modeling and simulation	39
6.1	Modeling	39
6.1.1	Dimensions to consider	39
6.1.2	Mathematical model of the motor	40
6.1.3	Model of the trolley	41
6.1.4	Verifying the system model	43
6.2	Controller design and stability	44
6.2.1	Linearization	45
6.2.2	Nonlinear stability	48
6.3	Simulations	52
6.3.1	Go to a specified setpoint	53
6.3.2	Follow a changing setpoint	54
6.3.3	Following an oscillating reference	55
6.3.4	Following a constant speed reference	56
6.3.5	Varying voltage supply and a constant reference position	57
6.3.6	Varying voltage supply and constant speed reference	58
7	Discussion	59
7.1	Testing	59
7.2	Prototype plan and results from tests	59
7.2.1	Prototype modules	59
7.2.2	Simulations	61

8 Conclusion	63
8.1 Camera	63
8.2 Trolley	64
8.3 Power	64
8.4 Communication	65
9 Future Work	67
9.1 The prototype	67
9.2 More functionality	67
List of references	69
A 400V 3-phase AC current	I
B Design of the communication device	III
B.1 P-CAD output	III
B.2 The finished board	XIII
C Software for the motor controller	XV
D MatLab and Simulink code and diagrams	XVII
D.1 MatLab code	XVII
D.2 Simulink diagram	XXI
E Project presentation	XXIII
F Video and files	XXVII

List of Figures

2.1	Overview of the LHC tunnel	6
2.2	The basic layout of the QRL	7
2.3	The magnet and the QRL in the tunnel, visualized open-ended	8
2.4	Cross section of the tunnel	9
3.1	A section of the tunnel, with some measurements noted. The numbers refer to table 3.1	12
4.1	Axis 213 network camera system	17
4.2	TKS trolley	18
4.3	The DC motor	19
4.4	Atmel AVR MC100 motor controller	20
4.5	The FAB100 power collector shoe	21
4.6	The FAB100 power rail mounted in the LHC tunnel, alongside the monorail	21
4.7	Car batteries	22
4.8	RJ-11 socket used for VDSL	23
4.9	Attenuation for the leaky feeder cable	25
4.10	Conceptual sketch	27
4.11	Visualization of the proposed system	28
4.12	Concept sketch of the powerline to Ethernet device	29
4.13	Concept sketch of the power-distribution	30
5.1	The simplified high-pass filter	34
5.2	Bode diagram of the high-pass filter transfer function	35
5.3	The camera interface in Internet Explorer	37
6.1	The motor and trolley in Simulink	39
6.2	Motor model in Simulink	41
6.3	Free mass diagram	42
6.4	Trolley model in Simulink	43
6.5	Motor performance with no load	44
6.6	Motor speed for the total system, with full input voltage	45
6.7	Bode plot of the system	47
6.8	The controller implemented in Simulink	48

6.9	Sensitivity and complimentary sensitivity	49
6.10	The Lyapunov function	50
6.11	The time derivative of the Lyapunov function	51
6.12	Simulations with a constant reference at 1650m into the tunnel.	53
6.13	Simulations with a variable reference.	54
6.14	Simulations with an oscillating reference.	55
6.15	Simulations with a constantly increasing reference.	56
6.16	Simulations with a constant reference at 1650m into the tunnel, and varying available voltage for the controller.	57
6.17	Simulations with a constant reference at 1650m into the tunnel, and varying available voltage for the controller.	58
8.1	A surveillance camera in the LHC	63
A.1	The 3 phases in the top plot, the difference between phase 1 and 2 in the bottom plot	II
B.1	Schematics for the powerline to ethernet device, made in P-CAD, page 1	IV
B.2	Schematics for the powerline to ethernet device, made in P-CAD, page 2	V
B.3	PCB layout for the powerline to ethernet device, made in P-CAD, page 1	VI
B.4	PCB layout for the powerline to ethernet device, made in P-CAD, page 2	VII
B.5	PCB layout for the powerline to ethernet device, made in P-CAD, page 3	VIII
B.6	PCB layout for the powerline to ethernet device, made in P-CAD, page 4	IX
B.7	List of components for the powerline to ethernet device, made in P-CAD, page 1	X
B.8	List of components for the powerline to ethernet device, made in P-CAD, page 2	XI
B.9	List of components for the powerline to ethernet device, made in P-CAD, page 3	XII
B.10	The PCB, finished with the components mounted	XIII
D.1	The overall system	XXI
D.2	The motor model	XXI
D.3	The trolley model	XXI
D.4	The controller	XXII
D.5	The block for choosing inputs to simulate	XXII
D.6	The input made from the signal builder block	XXII

List of Tables

3.1	The meaning of the numbers in figure 3.1	13
4.1	Link budget for radiating coax for 900, 1900 and 2400MHz	25
6.1	Motor parameters	41
6.2	Parameters in the model of the trolley	43
6.3	Change of parameters and notation	45
6.4	Controller parameters	47
C.1	List of Commands	XVI

Summary

This thesis documents the research, planning and partial implementation of a remote surveillance system for use in the CERN LHC machine tunnel. The system is planned to provide surveillance of the cryogenic system in the LHC, eliminating the need for the personnel to go personally to look at a piece of possible faulty equipment.

For this project, the complete system is planned. The system will be controlled via an Ethernet connection. This is fed into a 400V power line as a powerline communication signal, and picked up by the surveillance system. Then it is decoded into an Ethernet signal again, and sent to a camera with an on board web server. The power is transported by the same powered rail as used for communication, so that the system can take power and communication along the whole tunnel.

The thesis describes the goals of the system and explains the requirements it needs to meet. Several solutions, especially technologies for communication, are considered, and details about them are described. A solution that can fulfill the requirements is proposed. The concept of internal communication is proven in laboratory testing, as well is the camera. The powerline communication device is designed and a prototype is being manufactured.

The communication system is built, but not fully tested, and therefore not yet operational.

Also, the dynamics of the system is modeled and simulated, and a controller for the positioning system is developed. This controller is tested in Matlab Simulink, where the results indicate that it works.

The simulations tell that the motor will be exposed to an unnecessary amount of wear, so some further development of the controller will be needed. The same is true for the model, which can be made more accurate if parameters are measured of a real prototype. An analysis of the planned system reveals that not all requirements will be met, but the most important ones will be satisfied.

For the future, it is recommended to finish the prototype, and use precise measurements to improve the theoretical model.

1.1 Outline of this thesis

Chapter 1, Introduction

This chapter sums up the contents of each chapter, giving a brief introduction to what has been planned and accomplished in the thesis work. It also describes what innovations that have been done in this work.

Chapter 2, Background

An explanation of what CERN is and what the organization does is offered, as well as descriptions of the LHC and the cryogenic system in the LHC machine. This ends with a motivation of the surveillance project as well as the basic requirements related to surveillance of the cryogenic system in the machine.

Chapter 3, Requirements

The requirements of the system are explained. Here, the task is divided into 4 modules, each with its own requirements. These are the camera, trolley, power and communications.

Detailed descriptions of what the different modules need to be able to do and withstand is offered in this chapter.

Chapter 4, Technologies

Possible technical solutions are considered in all areas. In some areas, as for the trolley and camera, only one solution is considered. In other areas, where the technologies are more diverse, more than one solution is considered and described.

The positive and negative properties of the technologies are considered, and a recommendation for the full system is made at the end of the chapter. Ultimately, there is also considered some limitations that are already known based on the technological solutions that are chosen.

Chapter 5, Assembling the system

Because it was discovered that not all parts of the system would be available at the time of this thesis work, the available components were assembled one at a time, and connected together to verify that they would work.

Chapter 6, Modeling and Simulations

A model of the DC motor to be used for control of the trolley was made, and the motor parameters estimated based on the manufacturer's datasheet.

The system was modeled in Simulink, and simulated for several series of input commands, and variations on supply voltage. The Simulink models included the simple controller.

Chapter 7, Discussion

A discussion of the findings in the tests and analysis that has been done.

Chapter 8, Conclusion

Conclusions about what the findings mean. A conclusion about what parts of the project that are working, and what needs to be researched more, or replaced.

Chapter 9, Future Work

The parts of the project that still needs more work, and what to do about it. Also, suggestions of how to continue the project.

1.2 Contributions of this thesis

Planning and research of large-area remote surveillance system

In this thesis, research and planning of the total remote surveillance system is explained. This system is planned so that one single camera can cover 3.3km in length in a reasonable short time, without sacrificing speed and accuracy of the results from the camera.

Circuit design of communication device

All off-the-shelves products used to communicate with high bandwidth using power lines as signal carrier, are designed for standard home usage. This usually means either 230V or 110V. The available system installed in the LHC tunnel is 400V, and therefore this needs to be custom made. Circuit design was done in P-CAD.

Planning the use Ethernet for communicating with real-time system

The usual problem using Ethernet for communicating with a real-time system is that real-time systems most often require predictable timing, and the unpredictable delays experienced using Ethernet is not very desirable. By making the control system autonomous, real-time control will not be needed, and Ethernet will be sufficient for communication.

Full system modeling and simulations

The complete system is modeled, both the DC motor and the trolley system, with the motor voltage as the input and the trolley position and speed as the setpoint to the controller. Stability of this system is proven, and a simple controller is made.

1.3 Publication of results from this thesis

Since this thesis is based on project work performed at CERN, the results and this thesis is published at CERN at 3 occasions:

- As an internal note at CERN AT-ACR group
- In the CERN Thesis database
- The main results are presented at CERN AT-ACR group meeting, the presentation can be found in Appendix E. This presentation also covered some research into inspection of cryogenic pipelines

In this chapter, some key elements are explained, as well as the scope of this thesis.

2.1 About CERN

CERN is the European Organization for Nuclear Research (Organisation Européenne pour la Recherche Nucléaire), the world's largest particle physics centre. The organization was established in part to reclaim European scientists that emigrated to the USA during World War II. It is located across the French-Swiss border close to Geneva. CERN exists to give researchers the tools they need in order to study the building blocks of matter, and the forces holding them together. These tools are accelerators and detectors. The organization was founded in 1954, and is one of the oldest joint venture organizations in Europe. It now includes 20 member states (CERN, 2006*a*, Encyclopædia Britannica, 2006*a*).

2.2 Large Hadron Collider - LHC

A hadron is a subatomic particle made up of quarks. Protons are one of the hadron types (Encyclopædia Britannica, 2006*c*), and is most known for making up the atom nucleus together with neutrons, which are also a type of hadrons.

The Large Hadron Collider, LHC, is the particle accelerator that is currently being built at CERN. It is planned to start working in 2007. Then it will collide beams of protons at energies of 14TeV, which is not much energy, but it is compressed 10^{12} times. Later, the machine will also collide beams of lead nuclei. It will attempt to recreate the conditions right after the Big Bang, in a microscopic scale.

The LHC consists of a ring of magnets, mounted together in an underground tunnel, 27km long. By cooling the magnets, they become superconducting. The magnets are made of a niobium-titanium alloy, that starts to be superconducting when cooled below 10K (Schiver, 1986). They are then able to accelerate the beams up to a speed extremely close to the speed of light (CERN, 2006*b*).

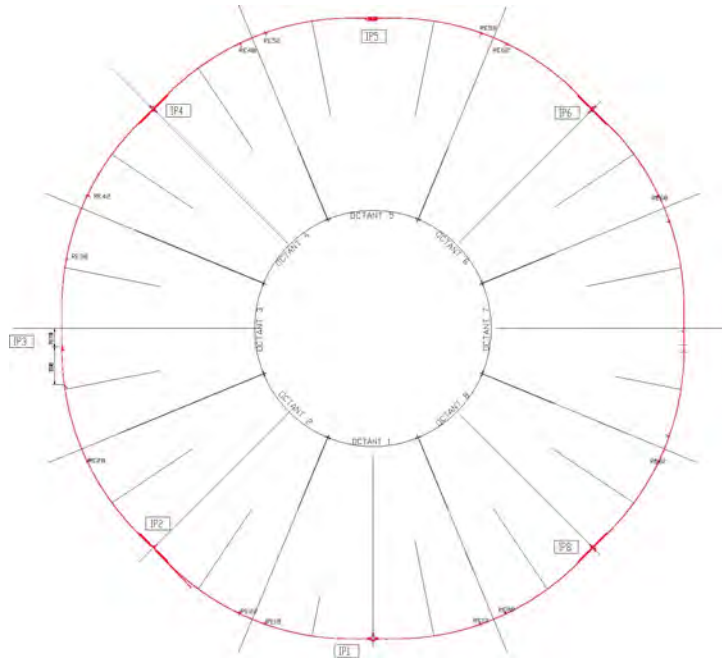


Figure 2.1: Overview of the LHC tunnel

2.2.1 Cryogenics

Cryogenics is the study and use of very low temperatures. In the case of the LHC, the cryogenic system is installed to cool the magnets down to superconducting state. The system consists of equipment for cooling down to 4.5K, and 1.8K, where 0K is the absolute zero temperature, just below -273°C . The available cooling power for the whole accelerator is 140kW at 4.5K equivalent. The magnets are cooled in a bath of pressurized helium (1.3bar) at 1.9K (CERN, 2004a).

Helium is used to exploit its low temperature boiling point, which is as low as 4.3K. For comparison, nitrogen has a boiling point of 77K (Bryson, 1999).

When helium is cooled down below 2.2K, it enters a state called superfluid, where the viscosity is significantly lower than for ordinary liquid helium. Also, the apparent thermal conductivity of superfluid helium is many orders of magnitude larger than liquids and even high-conductivity solids (Schiver, 1986).

The system is divided into 8 sectors, where 5 cooling stations are providing cooling. When cooled down, 4.5K helium will flow through the cryogenic distribution line (QRL) that goes alongside the magnets in the tunnel. Every 109m, there is a connection from the QRL that feeds the cooling pipes to the magnets with cooling fluid. This system is designed to work automatically for 9 months consecutively, before a 3 month scheduled shutdown every year for maintenance (CERN, 2004a).

2.2.2 Hazards

In a machine as big as the LHC, there are several potential hazards. The four types most relevant to this project are described in this section.

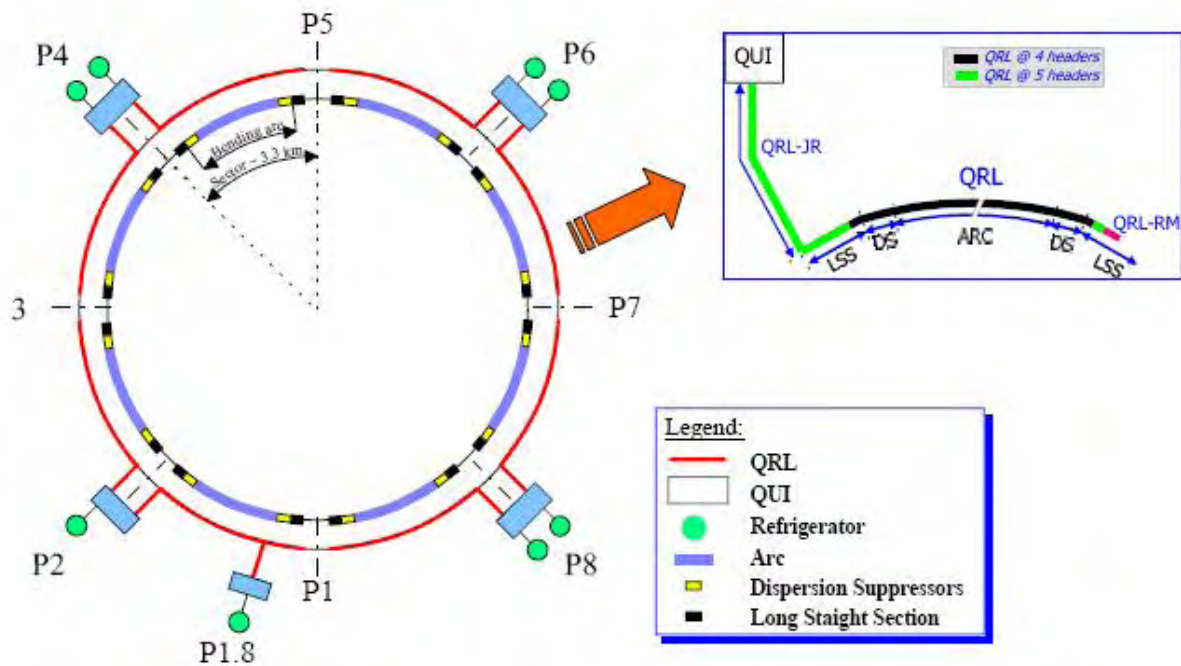


Figure 2.2: The basic layout of the QRL

Liquid gas

Liquid gas will not pose a significant danger to the surveillance system itself, but is important for people operating in the tunnel. If there are indications of a leak, the tunnel is to be evacuated. In such a situation, it will be helpful to be able to inspect the site of the leak with a remotely operated camera. When liquid helium or matter that is cooled with this comes in contact with skin, it can cause freezing, and result in damage to the skin tissue similar to that of a heat burn. This is called a cold burn, or "cryogenic burn" (Weisend II, 1998). In addition to this immediate damage, hypothermia is also a possible hazard if one is exposed to cold temperatures for a period of time.

Oxygen deficiency

When a volume of liquefied gas heats up to room temperature, it evaporates. When this happens it expands, and starts to displace or dilute the breathable air in the area. If a person is close by, the lack of breathable air cause asphyxiation (Weisend II, 1998). The safety of people in this regard is already considered to a great degree, with oxygen deficiency monitors around the tunnel. Also, the fact that helium is lighter than air, and therefore the deficiency will first take place at the ceiling, is in itself increasing the safety. If a person loses consciousness, he/she will fall to the floor, where there still is enough oxygen for him/her to crawl to safety.

Radioactive hazard

When the machine is in operation, personnel are not allowed into the tunnel. This is largely because of radiation created by beam leakage, which is as high as 30% at some points. The radiation can reach dangerous levels at several places in the tunnel. For some areas, the existing 5m concrete walls are not considered well enough for shielding. In general, the radiation fields in



Figure 2.3: The magnet and the QRL in the tunnel, visualized open-ended

the tunnel are considered very similar to cosmic radiation fields. The components in the tunnel will be handled as radioactive once the machine has been operated for the first time with beam. Due to cost considerations and speed, use of off-the-shelves electronic components is widespread. The electronics are tested, and are not expected to downgrade quickly, but single event errors are expected as soon as a circulating beam is present in the machine (CERN, 2004b, Ch.4).

The significant radiation consists of gamma and neutron-radiation. Simulations indicate that after 200 days of operation, and 1 day of cooling, radiation levels in the walkway aside the magnets can reach 10mSv/h. Closer to the magnets, the level increases to 2300mSv/h. These values indicate that any intervention into the area needs to be planned carefully, since the levels are dangerously high. At other points in the tunnel, the level is lower, but planning and care is important (Silari and Menzel, 2004).

Electromagnetic energy build-up

During run, the magnets will contain huge amounts of stored electromagnetic energy. If the cryogenic system fails, the magnets will heat up, leave the superconducting state, and start to build up a high voltage. There are installed quench protection systems that will drain this energy in case of a fault in the electric system or the cryogenic system, but this risk is still a reason for remote monitoring to be desirable (CERN, 2004a, Ch.9).

2.2.3 Description of the tunnel

In order to get an impression of the physical conditions in the LHC machine, some data describing the tunnel is found in the LHC Design Report (CERN, 2004a) and the LEP Design Report (CERN, 1984). The Large Electron-Positron storage ring, LEP, was the predecessor of the LHC, and was the original purpose of the tunnel. After it was used, the magnets were taken out, and the LHC machine will be using the same tunnel, but will have a lot more power.

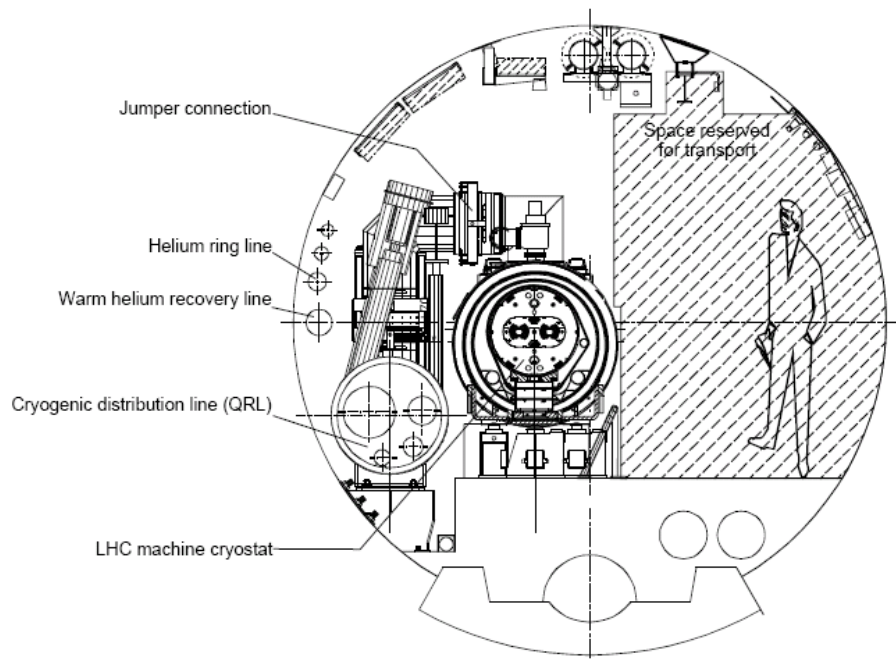


Figure 2.4: Cross section of the tunnel

The tunnel is exactly 26658.883m in circumference, and is shaped like an octagon with rounded corners. It is divided into 8 sectors of about 3.3km in length. Each sector contains a curved section of around 2800m, and starts and ends with a straight section of 250m in each end of the curved part. This gives us about 4000m straight part, and 22400m curved tunnel. The tunnel is made on an inclined plane with a maximum slope of maximum 1.4%. This is done in order to reduce the depth of the tunnel at the points where the ground is at its highest.

As drawn in figure 2.4, the QRL is positioned along the wall on the outside of the tunnel (left in the figure). Moving inward, we see the magnets, and then the walkway at the right.

Internally, the height is approximately 3.5m, and the width is about 4m. Right above the walkway, there is a rail placed for guiding the vehicles in use for transport of the magnets. This rail hangs about 2.5m above the floor (Bachy, 1989).

2.2.4 Tunnel surveillance

When getting ready for a beam run of the LHC, the tunnel will be closed for personnel, or access will be severely restricted. The critical equipment is equipped with sensors, but this is not always sufficient. In cases where one wish to inspect some of the equipment, it is not always likely that personnel can reach it, and a remote solution is desirable. Such a system must be able to go to an area where i.e. a valve alarm has triggered, or a temperature rise is observed, to perform a visual or audiovisual inspection. It is important that this solution does not interfere with either machine operation or maintenance. Because of cost considerations, it is not necessary for the system to be in operation during machine operation. Instead, the system will be located in a shielded position.

In this chapter, the requirements for the system will be described and justified. It will be noted which is of critical importance and which requirement that can be dropped if there is no practical solution present. The planning of the project is sectioned into 4 key elements. First we have the camera that will view the point of interest. Then the trolley will serve as the platform for mounting the system parts on, and moving them to the assigned place. The power supply will provide powering for the system, and backup power if the main power source fails. At last we have the communication device will give the system the capabilities it needs to send and receive commands, and send surveillance data to the operator.

3.1 Camera

Zoom capabilities for viewing objects of 1cm or less in distance of 3m

Since the objective is to inspect valves, it is important that the system enables the operator to see even small details on the valves. This is the single most important property of the camera, since no kind of automation will help if the images are not good enough.

Ability to implement automatic response to alarms and movement

In a later version of the surveillance system, it might be relevant to program automated tasks for the camera, using image recognition, in order to reduce the work load on the operator.

Needs sufficient lighting conditions

For the present time, the lighting in the tunnel is sufficient. However, in the future it can be considered running the camera at times closer to LHC machine runs, when the tunnel main lights are turned off. In those cases, it will be important to enable the surveillance system to provide its own lighting.

3.2 Trolley

Large area of operation

The overall goal is to monitor each sector, 3.3km in length. It is important that the trolley can handle the distance, and that it is not likely to get stuck far into the tunnel.

Must be kept small

The trolley must not interfere with maintenance operations, installation procedures, and general movement in the tunnel. From the tunnel drawings, it is measured that it should build less than 50cm in height, so that there is room for people to walk underneath. From figure 3.1, we can see that the system must avoid being too wide at the uppermost parts, but can afford to widen out further down. Still, a small as possible cross sectional area is desirable.

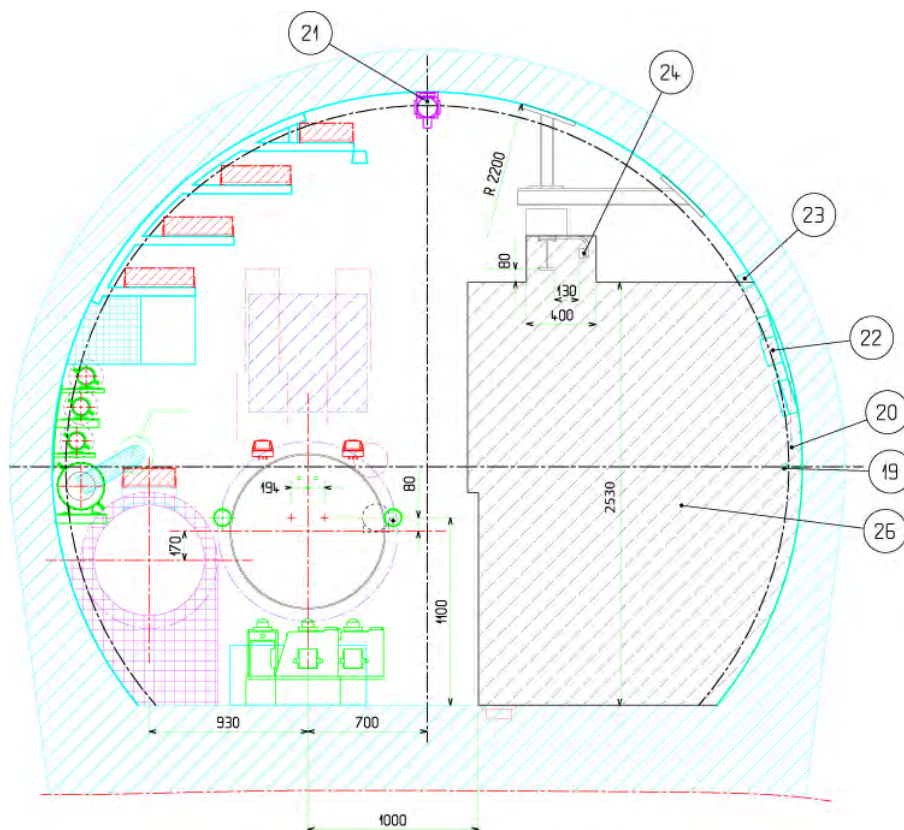


Figure 3.1: A section of the tunnel, with some measurements noted. The numbers refer to table 3.1

Material considerations

Because the overhead rail in the tunnel is coated with zinc, it is a requirement that the wheels of the trolley are made of polyurethane material (Kershaw, 2006). The reason for this is to prevent damage to the rail. This is a highly durable type of plastic material, commonly used in shopping carts and industrial applications where metal is not desired.

19	Communications antenna cable
20	Safety information
21	O ₂ deficiency monitors and warning lights
22	Emergency phones
23	Lighting
24	Electrical powering for transport
26	Space reserved for transport

Table 3.1: The meaning of the numbers in figure 3.1

Speed requirements

The alternative to using the trolley for surveillance is to use people moving in the tunnel. If we disregard the safety issue on this, we want the trolley to be faster than a man walking/cycling in the tunnel would be. Also it is very boring for an operator to wait for long periods of time, so we define the desired waiting time to be less than 10 min. This means that the trolley would need to travel up to 3.3km in less than that time, which corresponds to a speed of approximately 20km/h. Since this is a very high speed, we can consider lowering this to 12km/h, which is still faster than walking speed, and about the same as biking speed in the tunnel.

Need to know position in the tunnel

In order for the trolley to be able to go autonomously to a specified valve (which are located every 100m) it needs to know its position. Because of the length of the tunnel, it is desirable that the operator simply indicates which valve he wants to look at, and then the trolley moves to that spot autonomously. Considerations related to communications, as described in section 3.4, also points towards making the trolley highly autonomous.

Safety measures

In order to prevent problems due to human error, we can see that some points will need to be programmed as points of low speed or not accessible for the trolley. Especially the endpoints of the sector are places where the operator should not be allowed to drive it too fast.

The speed should be automatically controlled. In order to reduce the chance of human error, the operator should only be able to set a setpoint position, or to reduce the traveling speed.

Reestablish communication if lost

If the communication is not continuous, the trolley should be able to park in a position where it has a network connection. This means it should be intelligent enough that after it has reached its destination, it will go back or continue to the nearest point where it will be online.

Easy accessibility and shielding

It is desired that the device is operational just after a beam ends or whenever there is no beam in the LHC, without anyone locally present to start it. This also means it needs to be placed in the tunnel, and therefore needs to be shielded during LHC machine operation. Since the radiation is significant during beam operation, all unnecessary systems will be turned off. Both power and communication in the tunnel is off. In addition, the system will be made of commercially available off-the-shelves components that are not tested to withstand high levels of radiation. Therefore the trolley needs to have an assigned position where it is safe from radiation.

3.3 Power

Ability to operate for a long period of time

The surveillance system is planned to be working especially right before and after a run of the LHC machine, when it is still not allowed with human presence in the tunnel. It is therefore important that the system has enough power to operate for a long period of time without the need for change of batteries or other maintenance related to power. The system cannot be in operation during LHC operation, due to radiation. This means that when the LHC machine is in operation, the surveillance will be off, and the power can be shut down.

Operation without external power

If the power supply goes down, the system can be located up to 3.3km from its resting position. If this happens right before a LHC run, it is important that the system has enough power to make its way back into the shielded position, without any external aid.

Due to distances, a power cord is not possible to use

Considering the long distance in question, it is obvious that a power cord is impossible to use. It would also compromise the safety of the people working in the tunnel, as well as the machinery, if the surveillance system were to drag 3.3km power cables behind it.

3.4 Communications

Remotely controlled by computer

It is important that the system can be controlled from a computer at the CERN Control Centre (CCC), where the rest of the LHC systems are controlled from. It is also an advantage if it can be controlled from other locations as well.

Streaming video requires high bandwidth communications

Since most digital video cameras need high bandwidth in order to provide good quality real-time streaming, we need to design the system so that it can provide this. We could attempt to design the system with just enough bandwidth to our camera, but in case we wish to change the camera in the future, this is not a sufficient solution.

For real-time control of the trolley, there should be no delay

If we choose to implement real-time control of the trolley, that is that the operator controls it with i.e. a joystick, then the communication system needs to meet hard real-time requirements (Krishna and Shin, 1997). If we choose to fit the trolley with a more sophisticated control system, then the real-time requirements reduces and we have a soft real-time system, and can then handle delays in the communication. We therefore choose to aim for a trolley with a control system that enables it to go autonomous once it gets the control commands. This way, we can make it even if we have a delay in the communications.

Physical wire problem, due to the distance

For the same reason as for the power supply, a 3.3km signal wire is not an option.

The system should have continuous coverage

It is desirable for the system to have continuous coverage along the whole tunnel, since errors can occur at unexpected locations, and if they do, we wish to be able to observe them, no matter where they are. On the control side of this, we observe that any non-continuity in the coverage will impose a delay in the communications, again pointing to the importance of a certain degree of autonomy of the trolley.

3.5 Summary

Considering our requirements, we see that it will be simple to find a good camera. The trolley has some special requirements, and it also needs to be made autonomous to a certain degree. The communication system needs to be robust and have high bandwidth due to the camera requirements. Ideally it should be without delays also, but due to the high bandwidth requirements, a compromise will have to be made. Since limitations on the bandwidth will have a direct effect on the image quality and update frequency, it is not good to reduce this. A better control system on the trolley will reduce the significance of any delays.

For the total system it is required that it builds less than 50cm in height and weighs less than 20kg, so that it is not interrupting people walking below, and one man is able to disconnect it and carry it. Due to the high speeds requested, it is also smart to keep the weight down to reduce the impact of possible accidents. Also the general requirements to all material in the LHC tunnel apply. This means that it should not contain any heavy gasses or be easily flammable.

This chapter will outline the technologies that are relevant to this project. Possibilities and limitations will be considered at the end of this chapter. The parts of the complete system are described in sections similar to the ones of the previous chapter. These are the camera, trolley, power and communications.

4.1 Camera

4.1.1 Axis 213 PTZ

The camera used for surveillance of the other parts of the cryogenic system is the Axis 213 PTZ network camera. There exists many different types of cameras, but this has the advantage that the user interface will be well known to the operator, since it already is in use. The camera satisfies the requirements, and has some extra features that are nice to have.



(a) The Axis 213PTZ network camera

(b) The connection module

Figure 4.1: Axis 213 network camera system

Specifications

The camera has 26x optical zoom. A simple test shows that even small print on the valves are easy to read from a distance of more than 5m. Control of the camera is done over the Ethernet. Axis 213 PTZ has an embedded web-server that can implement automatic responses to alarms and movement, as well as communicate with external devices using several input and output lines, as well as RS-232, when connected to the Axis 213CM connection module. The camera is already set up for simple communication using URL-commands to tell the camera what to send over the IO-lines and RS-232. The specifications states that the camera can operate in conditions down to 1 lux (Axis Communications, 2006).

Power requirements are 13V DC, with a minimum of 1.8A. It comes with an adapter for normal 230V AC power.

4.1.2 External light source

Since it is not thought to be important with external lighting for the operation at this point, the possibilities for fitting the system with an on-board light system are not researched. What is most relevant, however, is to use standard flood lights for video cameras to provide lighting. Another possibility is to use an LED lamp. LED has the advantage that it is more robust than traditional lighting systems.

4.2 Trolley

4.2.1 Prefabricated

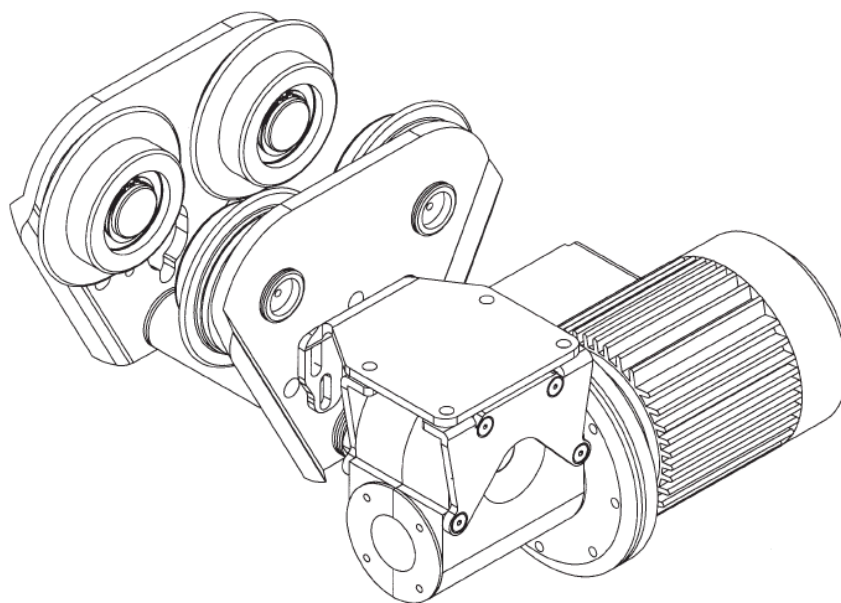


Figure 4.2: TKS trolley

In order to make the system as small as possible, the research has been focused on small trolleys to be mounted on an IPN-rail that is already in place in the LHC tunnel. The type of trolleys used to carry pulleys and cranes for industrial applications are easily available. According to TKS, a manufacturer of such trolleys, their trolley is capable of speeds up to 282m/min, which is just below 17km/h (Bilstad, 2006). The weight of the trolley is not specified, but a rough

estimate based on the weight of the individual parts in the datasheet tells us it will weigh about 20kg. The total weight of the full system will then exceed the requirements set up in section 3.5. It is clearly possible to exchange the wheels with polyurethane wheels of the exact same dimensions (TKS AS, 2006). However, it has not been possible to find any supplier to provide custom made wheels for this project at the time this thesis is written.

The motor originally mounted on the trolley use 230V or 400V AC. This provides 3000rpm. It is possible to purchase the trolley without a motor, and fit it with one that fulfills our requirements.

4.2.2 Modifications to the prefabricated trolley

Because of the special requirements to this system, we cannot use the trolley as it is. It needs to be modified.

Because of the requirement of polyurethane wheels, the trolley will need to change the wheels with some that are custom made so they can be exchanges with the ones on the trolley.

Since we wish to apply a more sophisticated control strategy to this project, we need to exchange the original AC motor with a DC motor, because this gives us better speed control.

Also, in order for us to be able to control the trolley to where we want it to go, we need to fit it with some type of positioning system.

It appears that it is possible to design and make a trolley that would satisfy our requirements fully. This has not been done, mainly because mechanical design of this kind is beyond the scope of this thesis.

Motor

The Chinese manufacturer Shenzhen Unite Industries Co Ltd. makes the motor called MY1018E2-500W. This provides a maximum torque of 2.69Nm, and a speed up to 3000rpm. It operates at 48V where it can give a power of 500W. The motor is originally intended to be used in electric scooters.



Figure 4.3: The DC motor

Motor controller

For control of the trolley, both PLC and microcontroller are possible to use. PLCs are simple to set up and program for this purpose, but are larger and use more power. They also have a significantly higher cost. Microcontrollers are cheap and have low power usage. For motor control, Atmel has made an evaluation board/development kit called AT-AVRMC100 (Atmel, 2006). This kit controls a 12V DC motor, and can easily be modified to control more powerful motors. The microcontroller onboard also has enough capacity to be programmed with a sophisticated controller. In addition, this system is already ready to use RS-232 for communication with other devices.



Figure 4.4: Atmel AVR MC100 motor controller

Positioning

There are several possible solutions available for positioning. The best solution would be to use a solution that could give an absolute position at some points, and an onboard system that is in use in between the points. For the prototype, it is possible to use an internal estimator based on the input into the motor. Later, this can easily be expanded with measurements from an accelerometer, or from an external positioning system.

4.3 Power

The trolley needs a supply of power, can acquire power from the powered rail system already installed in the tunnel. The rail system is already in use for installation of the magnets, where it is supplying the installation vehicles with power.

4.3.1 FABA power rail

The installed power rails are of the type FABA 100 (Magnetek Electromotive Systems, 2003), and do not carry any weight. There are 4 conducting rails, carrying 400V AC between conductors L1, L2, and L3. There is also present a PE conductor. There is no N-conductor available (Chevalley, 2006). Most 400V power supplies and chargers are set up to have the N-conductor as a reference.

Between any L-conductor and N, it is 230V. Between the conductors, there is a 120 degree phase shift. Between two L-conductors, there is 400V shifted -30 degrees (A).

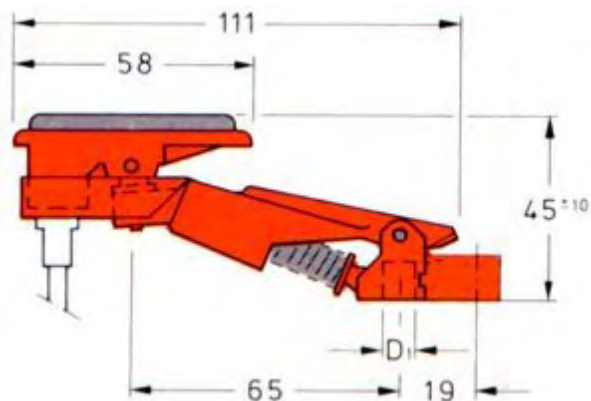


Figure 4.5: The FABA100 power collector shoe

The specification for the power rail indicates a max speed of 400m/min, which is the same as 24km/h. This is more than enough for our usage, since it is clearly above the capabilities of the trolley. However, the distance from the power rail to the IPN-beam in the tunnel is not fixed. Additionally, the bends in the tunnel makes it more complicated to have a steady power supply at all times (CERN, 2004*b,c*, Fahrleitungsbau GmbH, 2002). Testing done on the equipment already using the power rail has shown that the power collector shoes jump out of the rail at speeds as slow as 3-4km/h (Kershaw, 2006). This is significantly slower than our target speed, but at this time, there seems to be no alternative, except batteries, which is more of a supplement than an alternative as power supply.



Figure 4.6: The FABA100 power rail mounted in the LHC tunnel, alongside the monorail

4.3.2 Battery power

Because the power rail does not perform well at high speeds, we will fit the trolley with batteries to use when it is not powered by the rail. This will enable it to run faster once it has a setpoint to go to, and then connect to the power rail once moving slowly or stopping. Also, in case of a power shortage, it is important that the trolley is able to go to its resting position by its own stored power.

Which types of batteries to use, depends on several factors. Initially, car batteries are recommended, due to their durability and low cost. The major drawback they have is their weight. For later prototypes, other types of batteries should be considered. More modern battery technologies can provide lighter and more powerful batteries.



Figure 4.7: Car batteries

4.4 Communications

FABA has a system for communication along the rails, supporting several movable devices working simultaneously, but this is not installed in the LHC tunnel. The bandwidth of this system is unknown, but is most likely only for signaling and control, not for high bandwidth video streaming. Therefore we need to look at other solutions.

In this section, there is described several technologies in addition to the one ultimately chosen. This is done in order to explain how the final choice is motivated, and because this area was the one where there was most uncertainty as to what would work best.

4.4.1 Wired communication technologies

Powerline networking (OFDM)

Powerline networking is most known for being used to fit buildings with network connection throughout, without the need of installing new cabling infrastructure. The basic function is that it adds the high frequency network signal on the top of the 50Hz AC wave in the power lines. After the growth of wireless networks, this technology is not widely used. All commercially available systems using this technology tend to use either 110V or 230V power lines. Our system will need to transmit on a 400V system, since we have no N-conductor available, as explained in section 4.3.1. Since appendix A shows that the frequency still is 50Hz, even in the 400V case, we can use powerline networking in this case. Because the power rail is sectioned and each section has its own power supply, the transmission distance will be sufficiently short so that signal loss should not be a problem. Since our case uses a 400V system, there are no

off-the-shelves products that we can use, but we can design our own that uses a separate power supply.

Maxim makes the MAX2986 chip, which can transmit signals over power lines with bandwidth of up to 14Mbps. It adds a signal in the frequency band 4.49MHz to 20.7MHz to the carrier wave in the power line. Because it uses such high frequencies, most other systems on the power lines disregards it as noise, while a similar system can extract it and use it. The powered rail is not continuous, but is subdivided, so range is not that critical (Maxim Integrated Products, 2004).

There are dead zones of 35cm where two different power zones meet, so the signal needs to be injected at several points along the tunnel. Each zone can then be thought of as a wall-outlet for a normal Ethernet line. When nothing is plugged in, nothing happens. When a device plugs in, then it can start using it quickly. One implementation issue will be the problem if the trolley stops in a dead-zone or if there is a faulty zone with no power. It then has to be able to go back to the previous point where it can get power and communication.

VDSL

For the purpose of installation, there are installed a VDSL-network in the LHC underground area. VDSL stands for Very high data rate Digital Subscriber Line (Encyclopædia Britannica, 2006b), and are many places used to provide broadband.

In the tunnel, it is installed outlets every 106m. Originally, it was planned that this system was to be turned off when the LHC is started. This system supplies Ethernet connection with broadband speed, and good quality. It is made with off-the-shelves components, which are inexpensive and easy to get. Due to this, they are not expected to have a long life span, and will need frequent replacement, even though they will be turned off during LHC machine operation (CERN, 2004b, Ch.6.2). Using VHDL will require the surveillance system to plug in and out of the outlets when moving the camera. For this, the system would need a separate robotic arm, and many moving parts that make it highly complicated. Although this would give a very reliable connection, the customization of that many components would take this beyond the scope of this project.

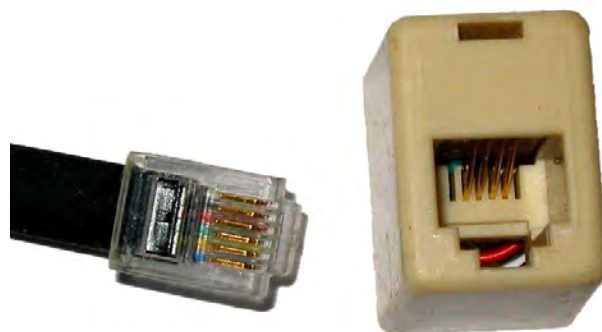


Figure 4.8: RJ-11 socket used for VDSL

4.4.2 Wireless communication technologies

WLAN (802.11)

Wireless LAN is considered cheap to install for most purposes. Therefore it needs to be considered for this application as well. It is well known that WLAN can provide high bandwidth, and

works reasonably well with varying distance from the base station. On commercially available access points, the specified range is given to be somewhere between 30m to about 300m in ideal conditions (Wi-Fi Alliance, 2006) . At best, we will be able to hope for coverage as long as there is a clear line of sight in the tunnel. The line of sight in the curved sections of the tunnel is about 100m, which makes one access point able to cover a distance of 200m. An estimate then tells us that we would need about 150 access points to provide the entire tunnel with WLAN coverage. All these units could be connected through the VDSL-network. This solution seems to be very expensive, and also it is not very robust when it comes to faults due to radiation damage. Shielding 150 boxes will be too expensive for the scope of this project.

The surveillance system will need a WLAN bridge unit in order to be in touch with the Ethernet.

GSM

Presently, there already is a GSM 900 network in the LHC underground areas. This installed both for practical purposes, and to increase security within the tunnel. This system will be maintained and will be operational during the lifetime of the LHC machine. It will be turned off only during LHC machine operation (CERN, 2004*b*, Ch.6.2-6.3). In the GSM system, the routines for hand-off between base stations are well developed, which makes for smooth and stable transmission. In addition to voice transmissions, the GSM network at CERN can provide up to 55kbps GPRS transmissions. With the Axis 213 network camera as an example, this will enable 2-4 images pr minute, with about 15 seconds delay. By reducing the image quality, a higher frame rate is possible, but then the quality will be too low. There also exist GSM-Ethernet bridges that are easy to use, and commercially available. Though this solution will work, the bandwidth will be too low to be of good use.

Radiating coaxial cable

This is not a wireless technology as the two former, but rather a method for transmission of the signals. It is mentioned because it provides an interesting possibility for this project.

This is the system used today for transmitting the GSM signals in the LHC underground areas. It works like an antenna stretched out along the tunnel. Instead of sending all its power from a small area, it "leaks" a small amount of radiation all along its whole length, providing a large coverage area with a reliable signal. The system is easy to turn off, and the electronics does not have to be radiation resistant, since they can be placed in a shielded position. Only the antenna will be exposed to the harmful radiation, and is not affected by it when the system is shut down during LHC machine operation (CERN, 2004*b*, Faugeras, 2002).

Radiating coaxial cable is used in the tunnel for GSM for the internal communication system used by the CERN Fire Brigade. This way, several systems utilize the same cable, but with different frequencies. In theory, we could insert a WLAN signal in this as well.

To find out if it is feasible to use this solution to equip the tunnel with WLAN, we can look at the transmission power needed with radiating coax cable. In order to find this, we can set up a simple link budget in table 4.1. How to do calculations on such system is explained in detail in McClaning and Vito (2000). With a link budget, we use that the gains and losses, expressed in dB, can be added together to get a resulting lower bound for transmission power needed for the transmission to work. For this case, we take the total attenuation along the cable, and subtract the values of the antenna gain and sensitivity at the receiver. The resulting value tells us what power is needed on the input, to be able to transmit all the way. When using dB

values, the result will be in dBm, which is related to transmit power in Watts according to this equation:

$$P_{dBm} = 10 \log \left(\frac{P_{Watts}}{0.001} \right) \quad (4.1)$$

$$P_{Watts} = 0.001 \cdot 10^{P_{dBm}/10} \quad (4.2)$$

In our calculations, we use values for WLAN, GSM1900 and GSM900 (which is already in use in the leaky feeder cable). In the link budget, we add up the lines with a + in front, and subtract the lines with a -. This gives us a lower bound on transmission power, measured in dBm, which we can convert to Watts. The cable installed in the tunnel, is the Radiaflex

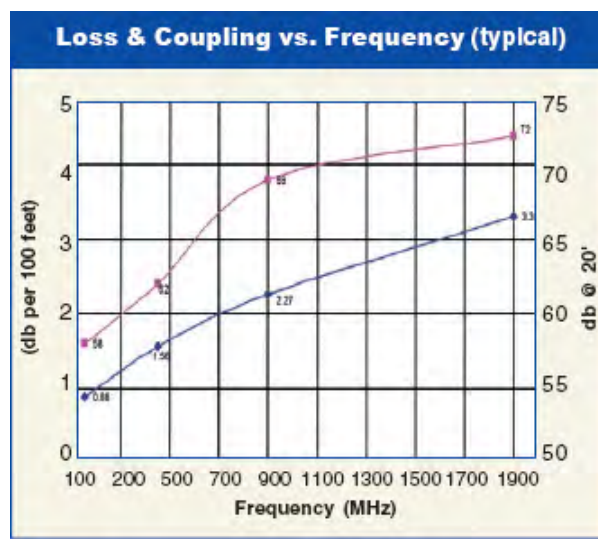


Figure 4.9: Attenuation for the leaky feeder cable

	900MHz	1900MHz	2400MHz
Attenuation per 100m [dB/100m]	7.44	10.84	12
Total attenuation for 1600m [db]	55.3	173.4	192
- Receiver antenna gain [dBi]	0	5	5
+ Receiver sensitivity [dBm]	-109	-95	-95
= Lower bound on transmission power [dBm]	-53.7	73.4	92
= Lower bound on transmission power	4.27nW	21.9kW	1.58MW

Table 4.1: Link budget for radiating coax for 900, 1900 and 2400MHz

RLKW11450JFL (Guerrero, 2006). This cable is unable to transmit at over 1950MHz, according to its specifications (Radio Frequency Systems, 2006). Since WLAN uses 2400MHz, this will not work, but it can be interesting to look at it in theory. The attenuation of the cable (also known as the longitudinal loss) is given as 3.46dB/100m at 900MHz, and 10.84dB/100m at 1900MHz. Based on how it seems to develop, we can estimate it to be more than 12dB/100m at 2400MHz.

The total attenuation is found by dividing the attenuation pr 100m by 100, and multiplying with the antenna stretch of 1600m. In table 4.1, the gain and sensitivity for the WLAN device is given for the D-Link DWL-7700, which is a powerful WLAN bridge unit (D-Link, 2006). For the GSM900-calculation, it is assumed that the antenna is omni directional, and therefore has 0dB gain. The receiver sensitivity is not a property that is publicly announced by the mobile

phone makers, but a typical value is given in Loke and Ali (2002) as -109dBm. The lower bound on transmission power is given by taking the attenuation, adding the receiver sensitivity, and subtracting the receiver antenna gain. The power requirements will most likely be higher than this calculation shows, because there will be a loss when the signals propagate through the air before it reaches the antenna or cable. For comparison, we also calculate the values for a thought system with the same properties as the WLAN, but with 1.9GHz frequency instead of 2.4GHz.

The results in the link budget tells us that the GSM900 net demands a significantly lower transmission power than the WLAN net if it were to be installed in the tunnel. Since not all losses are taken into account, like the losses when the signals go through the air, all of the frequencies need more power than the link budget states. Even the 1.9GHz frequency gives us a lot more positive result. It is obvious that a power usage of 1.6MW is not possible, especially when considering that there are 16 such sectors to be covered, i.e. a total of 25.6MW needed power to cover the entire tunnel at the same time. Also, if this were to be used, a similar power requirement would be imposed on the mobile device. Alternatively, the base station receiver could use significantly lower receiver sensitivity, but this would increase the disturbance. For the GSM900, the results are supported by the fact that the system already is in use and working in the tunnel. The total power needed is not much, and the power requirement is easily met with standard commercially available mobile phones.

It clearly shows that under these conditions, using this leaky feeder cable in example to supply a WLAN in the tunnel is not feasible. If, however, cables with better characteristics are used, then this can be feasible. As we can see, just a little bit lower attenuation makes the system demand significantly less transmission power.

4.5 Proposal

An effort is made to utilize the best solutions outlined in chapter 4. In this chapter, a proposal for which technologies to use is made, and the plan for the prototype is presented. The proposal is to follow the concept sketched in figure 4.10. That means to use the camera as an interface to the system, using the onboard web-server on the camera to handle internal messaging. By designing powerline to Ethernet communication devices adapted to the 400V power network, the communication can utilize infrastructure that is already present.

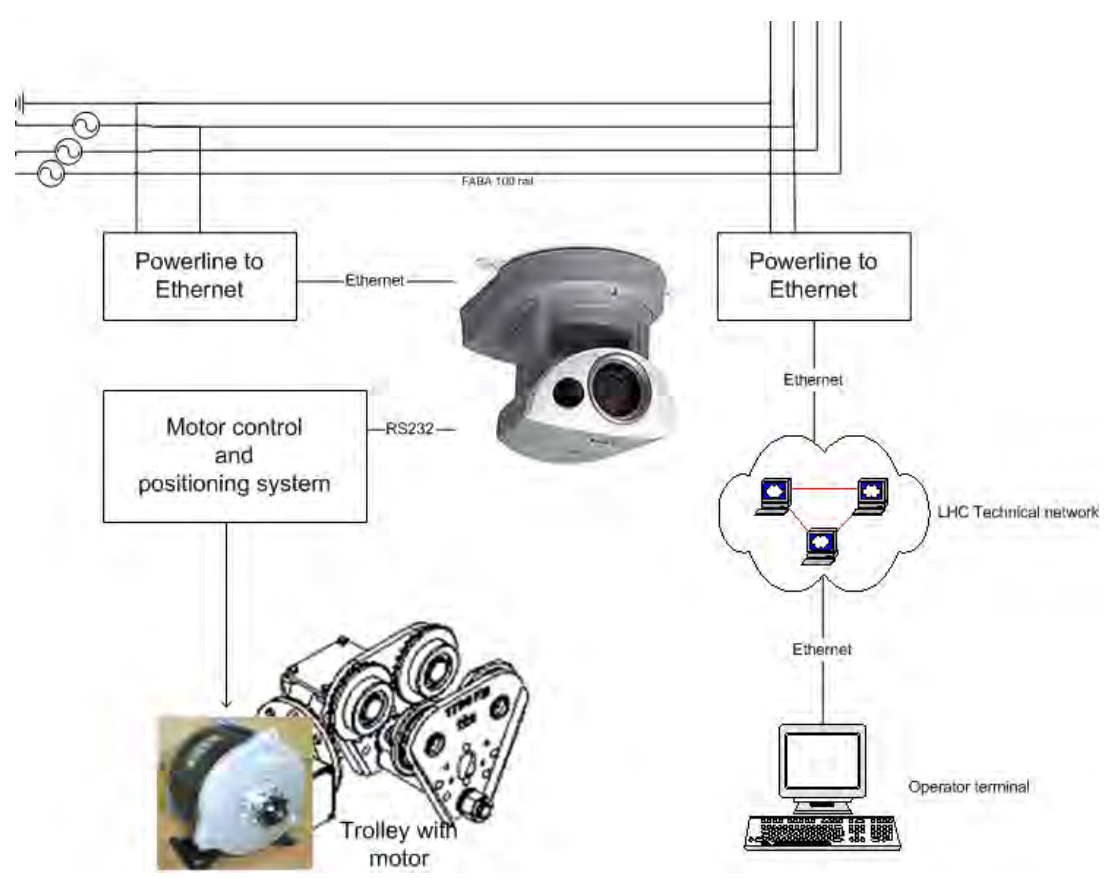
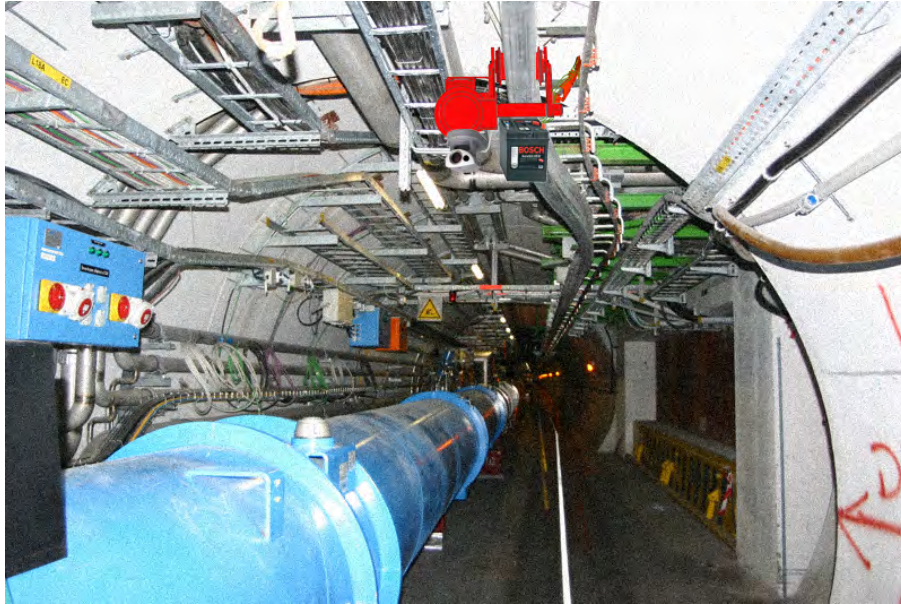
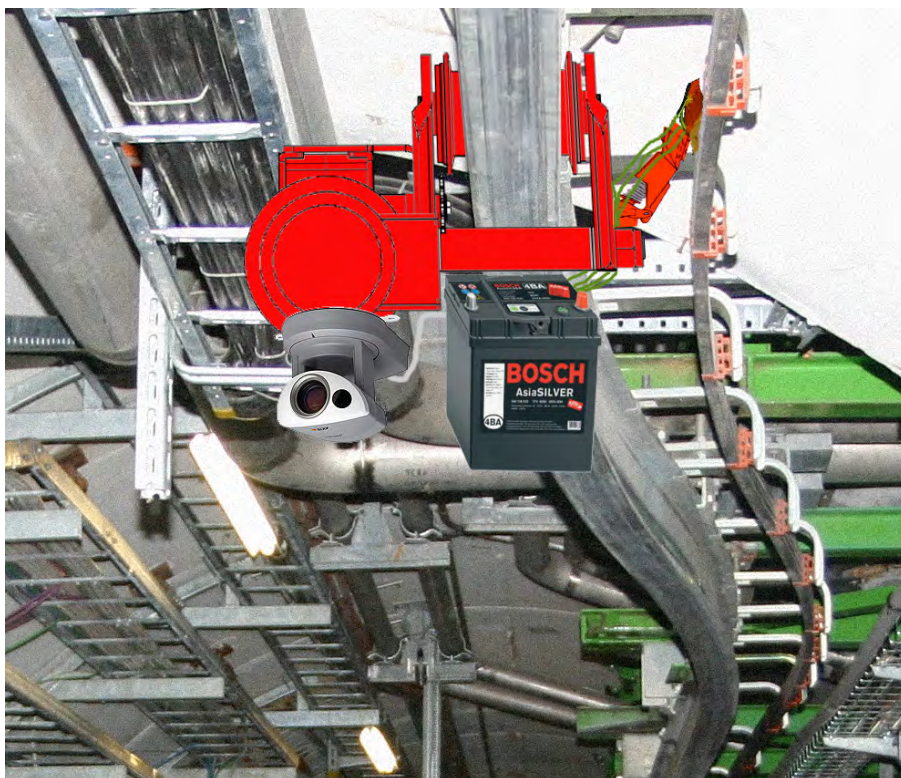


Figure 4.10: Conceptual sketch



(a) The surveillance system inside the tunnel



(b) A close-up of the system

Figure 4.11: Visualization of the proposed system

4.5.1 Camera

The Axis 213 PTZ network camera satisfies the requirements, and is possible to modify and adapt for a possible later change of requirements, for example with adding IR capabilities. For the prototype, the embedded web-server will be used to relay information via the RS232-port of the Axis 213CM connection module and to the motor control system. This will also enable us to receive data from the motor control system, in the form of hexadecimal values, which is good enough for testing and technology validation purposes. By using this strategy, we already have the interface to the Ethernet, and do not need to program this ourselves.

4.5.2 Trolley

We wish to use the trolley made by TKS AS (2006) as described in chapter 4. A speed up to 282m per min ($\approx 17\text{km/h}$) should be good enough for our purpose, since it is above normal walking speed. With this top speed, the trolley could make it across a section in less than 12 minutes. For this trolley to be accepted for use, it needs to have polyurethane wheels, which needs to be custom made.

For motor, the MY1018E2-500W, produced by Shenzhen Unite Industries Co Ltd., should be sufficient.

The trolley will be controlled with the Atmel AVR microcontroller on the AT-AVRMC100 board. This will use a RS-232 serial connection to connect to the camera connection module.

Positioning is not taken into this proposal. It is considered that this can be added at a later stage of development. Shielding is also absent from this proposal, since this is best implemented by building a cage for the trolley to rest in while the LHC is running.

4.5.3 Communication

The proposed solution is to use the FABA rail for data transmission as well as power supply. An enquiry to Maxim-IC (Serpa, 2006) that makes the MAX2980 and MAX2986 chips, confirms that the typical application circuit, as described in the MAX2980 and MAX2986 datasheets from Maxim (2005, 2004), should work for this application, just as it does for the 230V AC net. Unfortunately, there is no documentation available for an application similar to this, so the range and effective bandwidth needs to be tested.

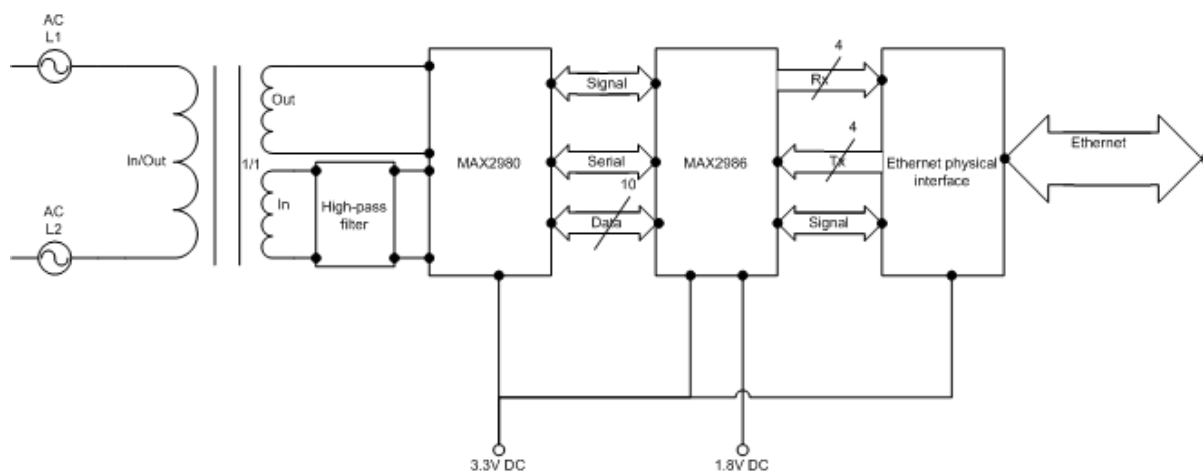


Figure 4.12: Concept sketch of the powerline to Ethernet device

4.5.4 Power

The FABAs power rail will supply 3 phase power. This will be drawn from the rail with 4 power collector shoes. For a prototype, it is most flexible to use a transformer from 400V 3 phase to 230V single phase. This way, the camera can use the power supply that it was supplied with. Similarly, it is simple to find power supplies for the other components as well.

For the times when the trolley is not connected to the power rail, it is necessary to have a battery pack. This is not researched in depth, since the prototype will work without. This way, the battery pack can be adapted at a later stage.

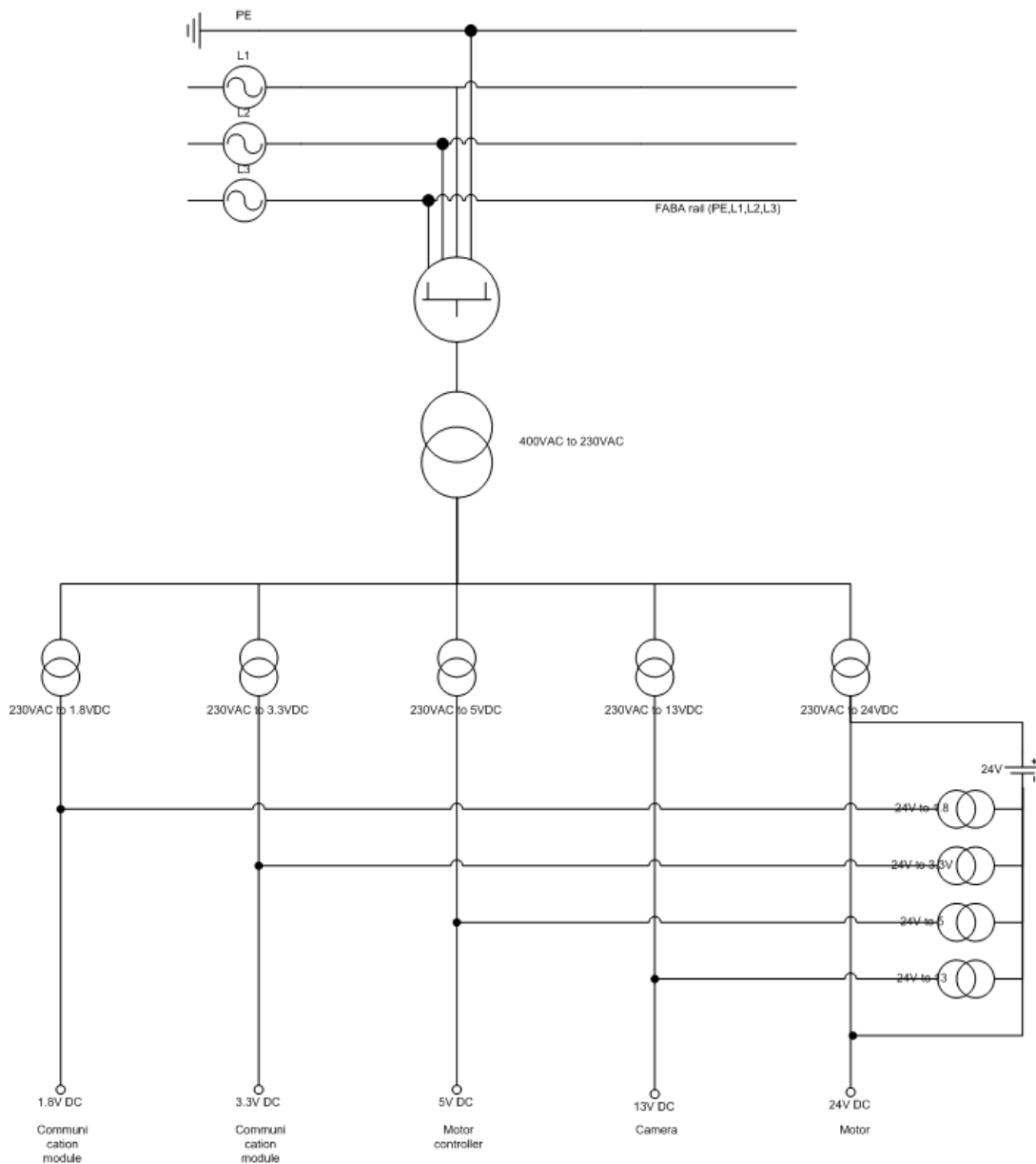


Figure 4.13: Concept sketch of the power-distribution

4.6 Limitations

When pushing the technological limits, one is certain that some limitations will be revealed. Some are already known.

Since the power supply has dead-zones it is not possible to achieve continuous network coverage in the entire tunnel. This means that there are some places where the trolley will need to be placed in a not ideal position in order to monitor some points.

Because of the experienced speed limits on the power rail, battery power will be needed in order for the system to be tested at full speed. The use of batteries will limit the operating time in the way that running long distances and only doing short stops will drain the battery power so that the system will not be available as much as desired.

Turns in the IPN-beam can reduce the theoretical maximum speed. However, this effect is very small because of the large diameter of the tunnel.

When the LHC is operating, the system will not be able to run because of high levels of radiation in the tunnel. Also, the power rail will be shut off, so both communication and power will be unavailable to the system.

The total system is assembled as modules, so that a change in the requirements does not require a total redesign. Most of the modules can easily be changed or modified to new requirements.

5.1 Hardware

5.1.1 Camera

The camera was already present at CERN, so no action was needed to get that up and going. In order to be able to utilize the RS232-interface, it was needed to get the connection module for the camera. This was done, and it started working once it was connected.

Also, a simple test of the camera capabilities was done. This consisted of printing a paper with text, 12 point size, and using the camera to read this. The camera was capable of zooming and focusing clearly at a distance of more 5m.

5.1.2 Trolley

Because of the problem getting the modified wheels to the trolley, this part of the project was not implemented. Neither was the powerful electromotor or the power collector system, since this all depended on the trolley as a platform to mount it on.

The trolley was, however, modeled and simulated in Matlab Simulink, with a DC motor and a position controller.

5.1.3 Power

This part was not implemented, since the original plan was to test all other components with 230V power supply in the lab first. When the trolley is not implemented, then there is no point in getting a 400V to 230V power supply for testing.

5.1.4 Communication

For the communication module, some electric circuit design was needed. The goal was to make a device that had a power line input on one side, and an Ethernet interface on the other side. The MAX2986 chip had the possibility of using several different interfaces, both USB

and RS-232 would work. However, only the Ethernet interface was implemented. Design of the communication module was mostly done as instructed by the various datasheets for the components used. For more sophisticated communication functions, there was the possibility of reprogramming the powerline chip, but this system was only supposed to provide the elementary function, so the programming interface is not implemented.

The parts of the circuit

The power line signal comes in on the high-voltage side of the high-pass filter. This filter, along with the transformer, cuts away the high voltage low frequency part of the input, which leaves only the signal, which has low voltage and high frequency. This, then is input into the MAX2980 powerline analog front-end chip that makes the analog signal into a digital 10-bit signal that then goes into the MAX2986 chip. After that, the MAX2986 sends this further to the Ethernet PHY chip that will take care of the timing needed when the signal will go on into the Ethernet through the RJ45-connector. The same happens when a signal is to go the other way, but it then does not have to go through the high-pass filter, but can be injected right into the transformer as a high-frequency signal. The timing and resending of lost data on a lower level is taken care of by the MAX2986 chip which also controls what is going which way through the system.

The high-pass filter

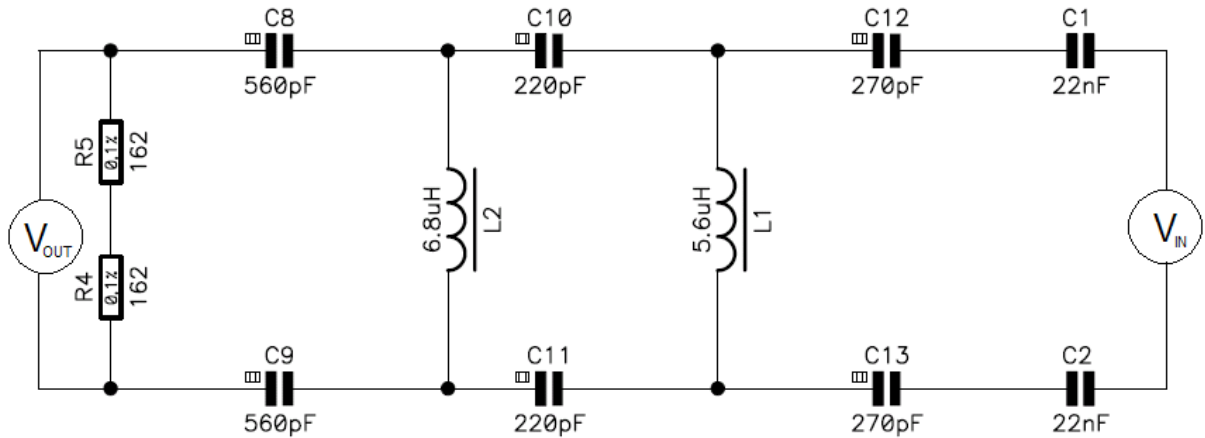


Figure 5.1: The simplified high-pass filter

The high-pass filter used is the one recommended in the datasheet for the MAX2986. In order to prove that this will be right for us, we can look at a simplified version of the filter, as drawn in figure 5.1. By calculating the transfer function from V_{IN} to V_{OUT} , we get the expression in equation 5.1.

$$\frac{V_{IN}}{V_{OUT}} = 4.408 \cdot 10^{-91} s^{14} \cdot (4.408 \cdot 10^{-91} s^{14} + 2.040 \cdot 10^{-83} s^{13} + 1.659 \cdot 10^{-75} s^{12} \quad (5.1)$$

$$\begin{aligned} &+ 1.158 \cdot 10^{-68} s^{11} + 6.429 \cdot 10^{-61} s^{10} + 1.804 \cdot 10^{-55} s^9)^{-1} \\ &= 4.408 \cdot 10^{-91} s^5 \cdot (4.408 \cdot 10^{-91} s^5 + 2.040 \cdot 10^{-83} s^4 + 1.659 \cdot 10^{-75} s^3 \quad (5.2) \\ &+ 1.158 \cdot 10^{-68} s^2 + 6.429 \cdot 10^{-61} s^1 + 1.804 \cdot 10^{-55})^{-1} \end{aligned}$$

The transfer function is of the 14th order, even though 9 zeros and poles cancel out mathematically. We then look at the bode diagram in figure 5.2, and calculate the magnitude at

the frequencies we are interested in. At 50Hz, the magnitude is -542dB, which means that the frequency that the power line sends the 400V on will be cancelled out. Between 4MHz and 20MHz, the magnitude is close to 0dB, so the communications signal gets through and can be picked up by the MAX2980.

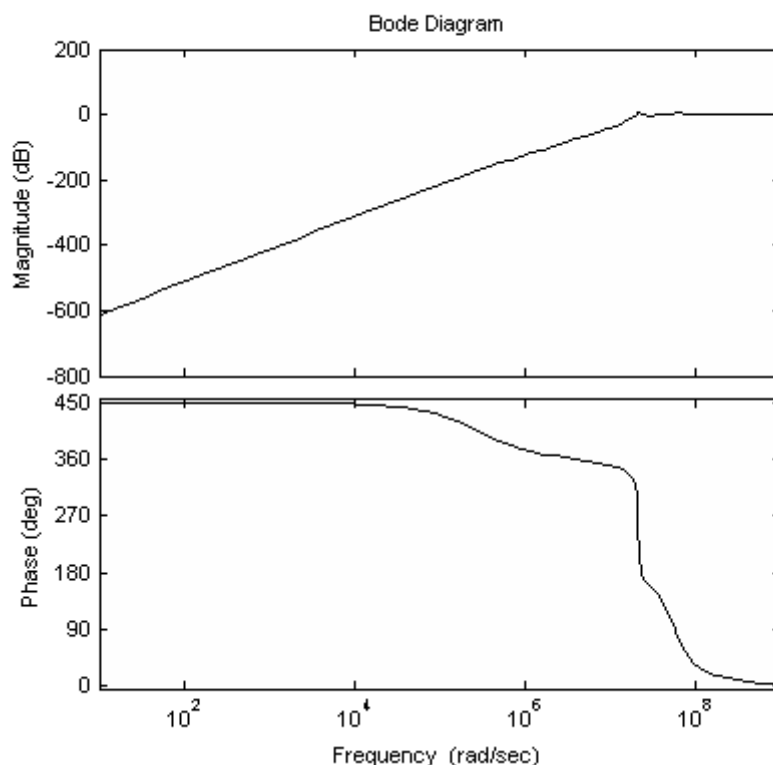


Figure 5.2: Bode diagram of the high-pass filter transfer function

Schematics

The schematics for the communication module is in appendix B, as well as the design of the printed circuit board (PCB) and the part list for the module. This is also published in the CERN Electronic Document Management System (EDMS) and is publicly available as Houge (2006).

5.2 Software

In order to simplify the control system, from the operator's point of view, all communication will go through the camera web server. This way, only one device will need to connect directly to the Ethernet. The communication between the camera and the trolley will use the RS-232C standard, as both the camera and the trolley will have a RS232-interface.

The software in the camera is already implemented when delivered. On the AVR microcontroller, there was already installed software for simple control of the DC motor, but this was rewritten to be able to use an Open Source licensed compiler, and changed to fit our needs. A description of what commands the microcontroller will respond to, and how the software is modified, is offered in appendix C.

In summary, the motor starts when the controller receives the character "r", and stops when it receives "s". It has functions to change direction, to change speed, and to report the current speed back to the device controlling it. When something goes wrong, for example an over-current, the system has a function for reinitializing itself on command.

5.2.1 Camera

Along with their camera systems, Axis has published what they call the AXIS VAPIX API, HTTP - Interface Specification (2005). By using this, it is simple to create a website with links that commands the trolley.

For example, entering this line into the url-field of a web-browser with access rights to the camera:

```
http://camera-ip/axis-cgi/com/serial.cgi?  
port=2&writestring="s"&wait=2&read=2
```

will send the character "s" from the camera and out the RS-232C-port, then wait up to 2 seconds to get 2 characters in return, and return them to the web-browser. In effect, this should turn the motor on, and return the speed of the motor that the controller sends to the camera as a response to the command.

The trolley control system can then be programmed to handle this as a command sequence that makes it go to the position defined as point 1, then stop there and start observing. With this system, the camera is able to send control signals instructing the trolley to go forward, backwards, to a position along the rail, to stop, or to return information about its state, position or speed. The limitations mostly depend on how the microcontroller is programmed to react on the commands received. Some commands can be preprogrammed into a website in the camera web server, while others can be written directly by the operator when it is needed to use them.

5.2.2 Microcontroller for the trolley

The motor would be controlled with the Atmel AVR AT90PWM3 microcontroller mounted on the ATAVRMC100 motor controller card. When delivered, this comes preprogrammed with a demonstration program. When connecting the card to the computer with RS-232 connection, a terminal program (like MS Hyper Terminal) can be used for control of the motor by giving it simple commands.

The demonstration program is written in IAR Workbench. Unfortunately, this program is not free, so in order to be able to reuse code from the demonstration program, we need to port the code to the free WinAVR GCC format. We wish to be able to reuse most of the code, because it has all the I/O-handling finished. All that have to be modified is which characters as input that will control the motor, and what will be returned to the unit that sends commands. Also, the controller itself will need to be implemented if we are to use feedback control. For the purpose of the prototype demonstration, however, all we want to do is to use this to prove that we can send signals from a computer, via the Ethernet connection, through the camera, and finally that the camera will relay the commands to the microcontroller. Also, we want to see that the controller sends back information about its status. For now, we are satisfied with controlling the speed, and reading back measurements of that speed.

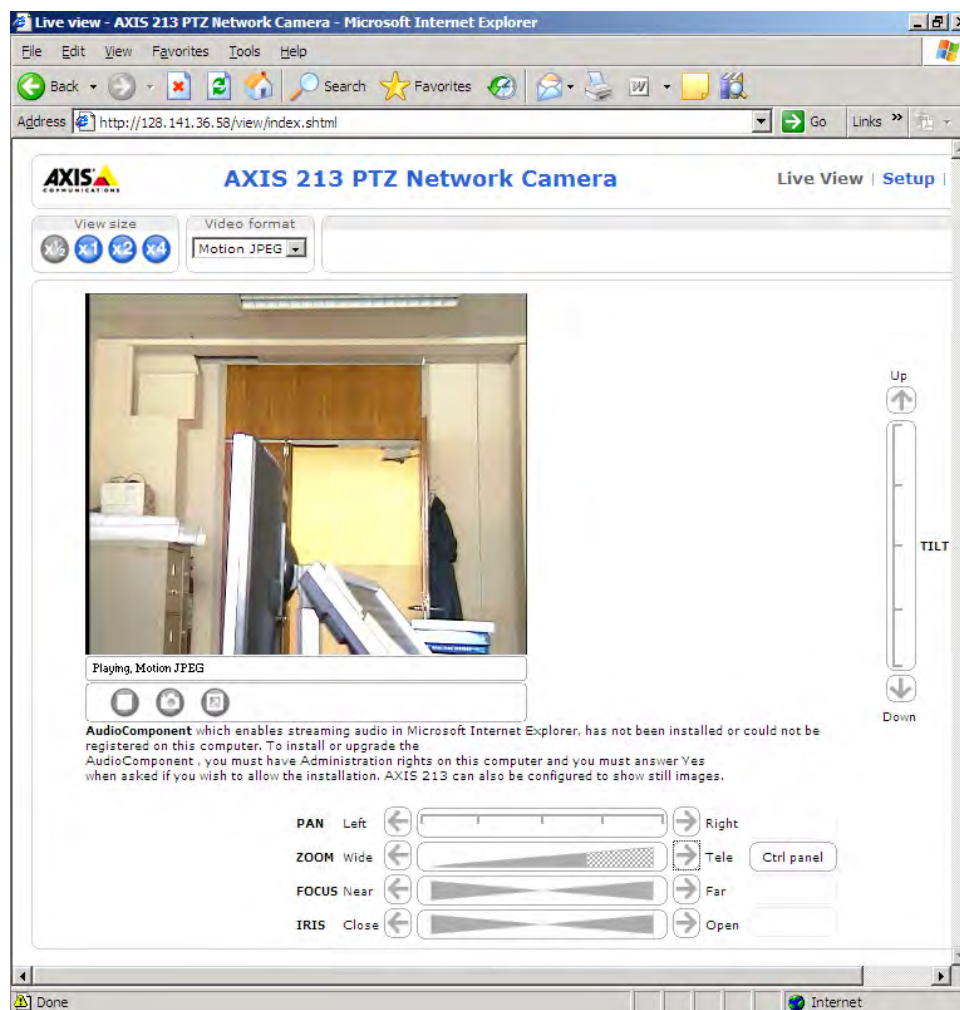


Figure 5.3: The camera interface in Internet Explorer

The modeling is split into two parts, the motor model and the model of the trolley. In Simulink, they are connected together with the controller. The control strategy will be explained in the section about the controller. All variables are variables of time, if not specified otherwise.

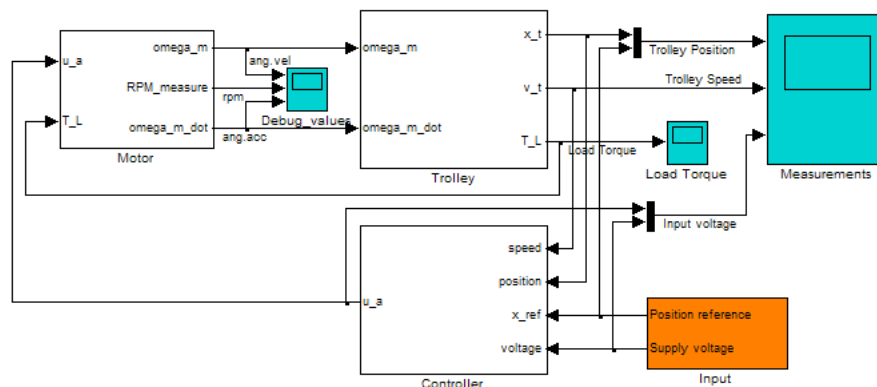


Figure 6.1: The motor and trolley in Simulink

6.1 Modeling

6.1.1 Dimensions to consider

A full model of this system could include a 6DOF mathematical model. This, however, is not necessary. Even though the tunnel is turning, it is so large, that this does not make the trolley rotate in any significant way. So we choose to neglect the rotational states roll, pitch and yaw.

We know that the tunnel is on an incline of maximum 1.4%. For our purpose, this is practically flat, so we can neglect this vertical state. Then we are left with two states, the forward/backward direction, and the sideways one.

If we look at the description of the tunnel, we find that it turns in 8 sections. These are approximately 2800m each. The total lengths of the curved sections then are 22400m, or 22.4km. Looking at these sections together as one complete circle, we can calculate the radius this would

have, which is the effective turning radius for the trolley when it is in a curved section:

$$\begin{aligned} r &= \frac{8 \cdot 2800}{2\pi} \\ &\approx 3565[\text{m}] \end{aligned} \quad (6.1)$$

Considering the estimated maximum speed, v_{max} , of the trolley, 4.7m/s, and a weight, m , of 40kg (trolley: 20kg, battery pack: 20kg), we can calculate the maximum centripetal force on the trolley. From Knight (2004), we have that the centripetal acceleration is expressed as $a_c = \frac{v_{max}^2}{r}$, and directed inward towards the centre of the circle. Using this to calculate the centripetal force, F_c , gives us:

$$F_c = ma_c \quad (6.2)$$

$$= m \frac{v_{max}^2}{r} \quad (6.3)$$

$$= 40 \frac{4.7^2}{3565}$$

$$\approx 40 \cdot 6.25 \cdot 10^{-3}$$

$$= 0.25[\text{N}]$$

Considering that if nothing holds it in place, the trolley will get a sideways acceleration of $6.25 \frac{mm}{s^2}$. For our application, this acceleration is insignificant, so we neglect this in our model, and ends up with just needing to consider the forward and backward motion.

6.1.2 Mathematical model of the motor

We will use the simple DC motor model from Egeland (1993), and calculate the parameters from the datasheet provided by the manufacturer (Shenzhen Unite Industries Co Ltd., 2005). The motor model is:

$$L_a \frac{di_a}{dt}(t) = -R_a i_a(t) - K_E \omega_m + u_a(t) \quad (6.4)$$

$$J_m \frac{d\omega_m}{dt}(t) = K_T i_a(t) - T_L(t) \quad (6.5)$$

$$\frac{d\theta_m}{dt}(t) = \omega_m(t) \quad (6.6)$$

The constants will be defined in table 6.1. In the equations, we have the motor armature current i_a and the motor armature voltage u_a , were the latter will be our input to control. ω_m is the engine shaft speed, given in radians per second, and θ_m is the engine shaft position, which we will not be concerned with, since we will care about the position of the trolley, not the engine shaft. The load torque T_L is the load put on the engine from the trolley, and will be treated as a process disturbance when we start controlling the total system.

From Aveox DC Permanent Magnet Brushless Motors (2006), we find some rules of thumb for estimating the motor parameters based on the information given by the supplier. These rules gives us help calculating the voltage constant, K_E , torque constant, K_T and the terminal resistance, R_a .

$$K_E = \frac{u_a}{\omega_{RPM}} \frac{60}{2\pi} \quad (6.7)$$

$$K_T = \frac{T_{max}}{u_{a,RL}} \quad (6.8)$$

$$R_a = \frac{u_{a,RL}}{i_{a,RL}} \quad (6.9)$$

In the datasheet, we look at the measurements done with the rated load and the maximum torque possible. The information we then have is

$$\begin{aligned} u_{a,RL} &= 24.12[\text{V}] \\ \omega_{RPM,RL} &= 2635[\text{rpm}] \\ i_{a,RL} &= 21.17[\text{A}] \\ T_{max} &= 2.69[\text{Nm}] \end{aligned}$$

ω_{RPM} is the rotational speed at the rated load, measured in revolutions per minute.

This helps us calculate the constants we are looking for. After calculating these constants, we are missing only the values for the moment of inertia, J_m , and the inductance in the motor, L_a . Based on available models, we propose the constants to be $J_m = 0.25\text{mkgm}^2$ and $L_a = 15\text{mH}$. These will not affect the steady state conditions of the motor, but will affect how the speed converges towards this steady state. All the motor parameters are summed up in table 6.1, with the calculated ones above, and the estimated ones below the line.

Voltage constant	$K_E = 0.0874$	[V/rad/s]
Torque constant	$K_T = 0.1115$	[Nm/V]
Terminal resistance	$R_a = 1.1393$	[Ω]
Electrical inductance in the motor	$L_a = 1.5$	[mH]
Inertia of the engine shaft	$J_m = 0.25$	[mkgm ²]

Table 6.1: Motor parameters

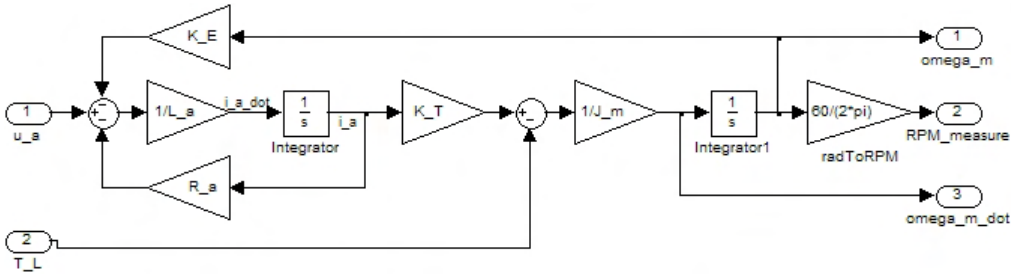


Figure 6.2: Motor model in Simulink

6.1.3 Model of the trolley

From the motor model, we see that the trolley need to take the motor speed, ω_m , as an input, and give a load torque as an output. We are more interested in the speed of the trolley moving along the tunnel, v . The gear ration, r_g , and the wheel radius can be used to calculate the speed. The gear ratio is composed of a transmission, with a ratio of $r_t = 7 : 1$, and a large and small cog wheel with a chain between. The small wheel, with $c_s = 14$ cogs, is connected to the transmission, and the large wheel is also the drive wheel of the trolley, with $c_l = 36$ cogs.

$$r_g = \frac{1}{r_t} \frac{c_l}{c_s} \quad (6.10)$$

$$v(t) = r_g \frac{d}{2} \omega_m(t) \quad (6.11)$$

$$= \frac{c_l}{r_t c_s} \frac{d}{2} \omega_m(t) \quad (6.12)$$

For the trolley, we start by looking at the forces that act upon it in figure 6.3. The sum of

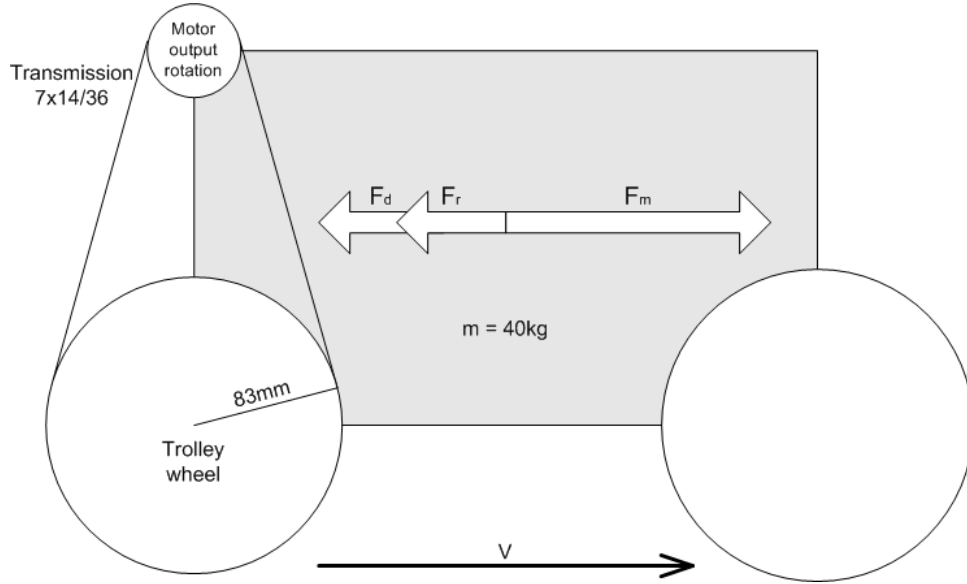


Figure 6.3: Free mass diagram

forces can be set up, as well as the equations for drag, F_d , and rolling friction, F_r . All physical formulas as well as the standard parameters can be found in Knight (2004).

$$\sum F = ma \quad (6.13)$$

$$= F_m - F_d - F_r \quad (6.14)$$

$$F_d = \frac{\rho}{2} AC_d v^2 \quad (6.15)$$

$$F_r = \frac{1}{n_{wheels}} C_{rr} mg \operatorname{sgn}(v) \quad (6.16)$$

$$F_m = ma + \frac{\rho}{2} AC_d v^2 + \frac{1}{4} C_{rr} mg \operatorname{sgn}(v) \quad (6.17)$$

The expression for the drag the system will experience, is the drag coefficient C_d multiplied with the surface area of the trolley, A , multiplied by the half of the density of air, ρ . The drag increases with the square of the increase of speed.

For the rolling friction, the expression does not depend on the magnitude of the speed, just on the direction. As for all frictional forces, it works against the direction of travel. This force is the rolling friction coefficient C_{rr} divided by the number of wheels ($n_{wheels} = 4$) on the trolley. This is multiplied with the mass of the system and the gravitational acceleration g , and finally by the sign of the speed.

The sum of forces is expressed as the mass times the acceleration, a , of the system. Also, it is expressed as the force given to the trolley by the motor, minus the drag and rolling friction. Here, F_m is the force given to the trolley by the motor. Because of Newton's 3rd law, a force with the same magnitude, and opposite direction, will act on the motor from the trolley (Knight, 2004). This will act on the motor as a load torque, T_L . In order to calculate this, we need to first calculate the torque experienced by the wheel shaft on the trolley, which we call T_t . The torque is expressed as the force times the distance from the rotation centre the force is applied. In this case, the distance is the radius of the wheel on the trolley, which is $\frac{d}{2}$. The torque is also geared down through the transmission and the cog wheels, so that the fast motor experiences

significantly less torque than the large, slower wheel on the trolley.

$$T_m = F_m \frac{d}{2} \quad (6.18)$$

$$T_L = r_g T_m \quad (6.19)$$

$$= \frac{c_l}{r_t c_s} \frac{d}{2} F_m \quad (6.20)$$

The parameters used to model the trolley found in table 6.2.

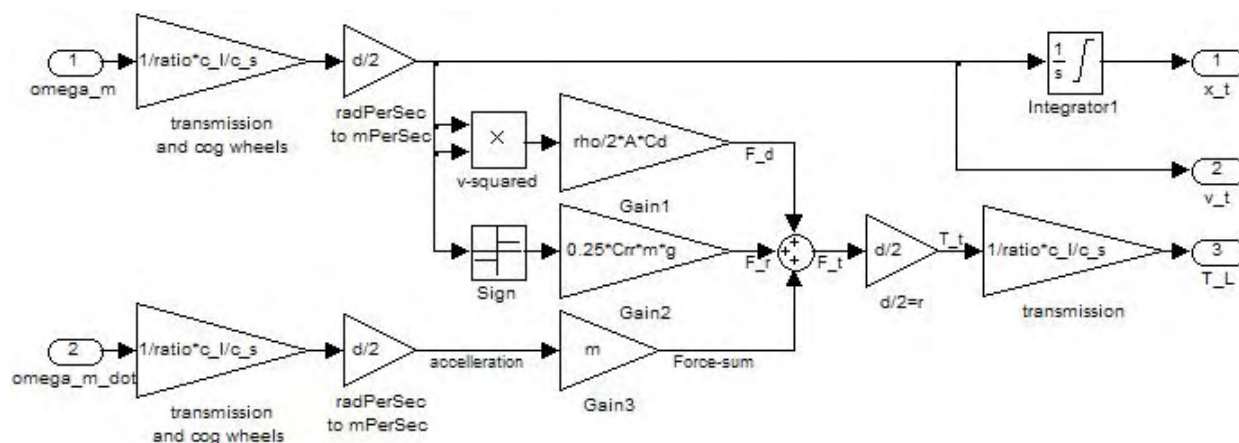


Figure 6.4: Trolley model in Simulink

Diameter of the wheel	$d = 0.083$	[m]
Number of cogs on the small wheel	$c_s = 14$	[cogs]
Number of cogs on the large wheel	$c_l = 36$	[cogs]
Gear ratio of transmission	$r_t = 7$	
Mass of the total system	$m = 40$	[kg]
Frontal area of the trolley	$A = 0.14$	[m ²]
Drag coefficient	$C_d = 0.5$	
Rolling friction coefficient (steel on steel)	$C_{rr} = 0.002$	
Gravity acceleration	$g = 9.81$	[m/s ²]
Density of air	$\rho = 1.28$	[kg/m ³]

Table 6.2: Parameters in the model of the trolley

When we simulate, we want to view both the position and speed of the trolley. The position will be denoted $x(t)$ and is the integrated of the speed $v(t)$.

6.1.4 Verifying the system model

Since we have no real system to test on, we can only look to check if the modeled system responds according to the data we have. Practically, this means that we need to input a known load and voltage into the motor, and see if it reacts the same way as it should according to the datasheet. We try to see how it reacts with no load, and 24.12V. When we simulate this case, we see that the motor goes up to 2602rpm in about 0.1s (as in figure 6.5). It continues to rise even closer to the speed mentioned in the datasheet, which is 2635, but that takes more time.

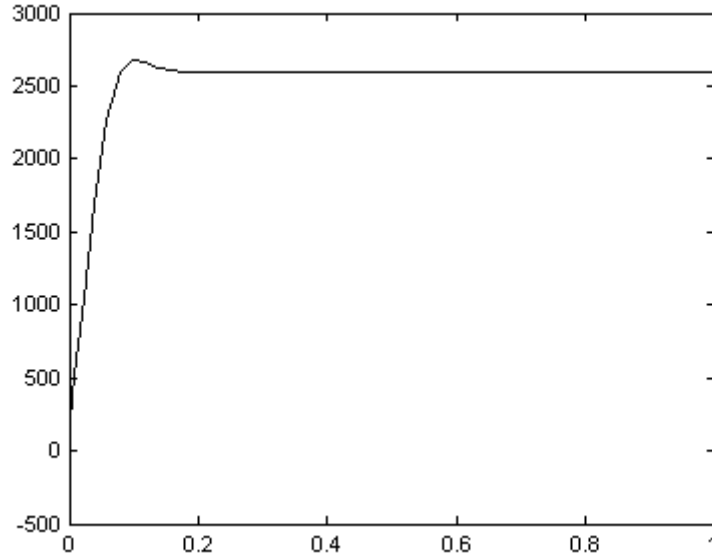


Figure 6.5: Motor performance with no load and full input voltage. The plot show the rotational speed in rpm, as a function of time

We can also take a look at how the full system responds to simply running with full input voltage. It should be able to get up to full speed in not too long time.

By simulating with these conditions, we see that we get a speed of 2618rpm after about 10s. Most of the acceleration is finished after about 5s, as shown in figure 6.6.

We see that the model most likely would be better with more exact parameters and knowledge, but since we do not have the trolley present to measure on, the model seems good enough to use for the further work.

6.2 Controller design and stability

To design the controller, we first set up the system as a state-space model. In order to use standard notation, we introduce a change of variables described in table 6.3. Then we get the state-space model in equation 6.21-6.23.

$$\dot{x}_1 = x_2 \quad (6.21)$$

$$\dot{x}_2 = -\frac{b}{a}x_2^2 \operatorname{sgn}(x_2) - \frac{c}{a} \operatorname{sgn}(x_2) + \frac{d}{a}x_3 \quad (6.22)$$

$$\dot{x}_3 = -ex_2 - fx_3 + \frac{1}{L_a}u \quad (6.23)$$

$$\dot{\mathbf{x}} = \mathbf{f}(\mathbf{x}) + \mathbf{b}u \quad (6.24)$$

$$= \begin{bmatrix} x_2 \\ -\frac{b}{a}x_2^2 \operatorname{sgn}(x_2) - \frac{c}{a} \operatorname{sgn}(x_2) + \frac{d}{a}x_3 \\ -ex_2 - fx_3 \end{bmatrix} + \begin{bmatrix} 0 \\ 0 \\ \frac{1}{L_a} \end{bmatrix} u \quad (6.25)$$

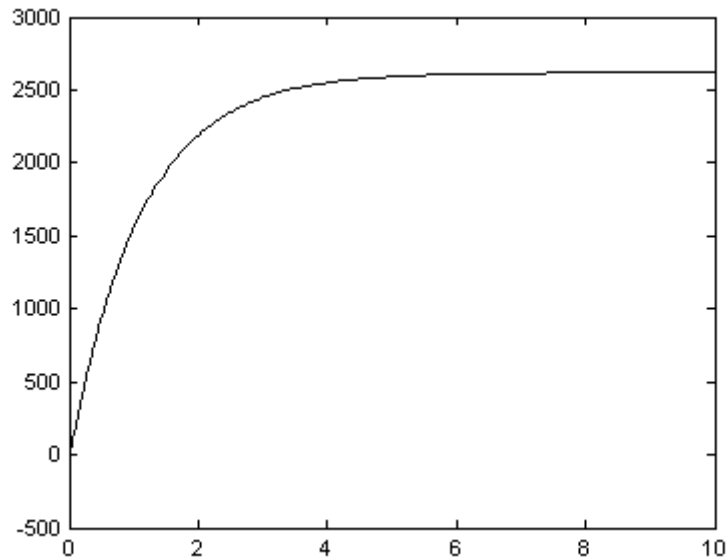


Figure 6.6: Motor rpm speed with full input voltage, as a function of time. The simulation is carried out for the whole system, not just the motor

6.2.1 Linearization

By linearization of the system, we can find the stability properties around a setpoint. We linearize the same way as explained in Chen (1999). First we calculate the equilibrium point with no input.

$$\dot{\mathbf{x}}_0 = \begin{bmatrix} 0 \\ 0 \\ 0 \end{bmatrix}$$

$$\Downarrow$$

$$\mathbf{x}_0 = \begin{bmatrix} x_{1,0} \\ 0 \\ 0 \end{bmatrix}$$

Position	$x_1 =$	$x(t)$
Speed	$x_2 =$	$v(t)$
Acceleration	$\dot{x}_2 =$	$a(t)$
Current	$x_3 =$	$i_a(t)$
Input voltage	$u =$	$u_a(t)$
	$a =$	$\frac{J_m}{r_g d} + \frac{r_g m d}{2}$
	$b =$	$\frac{\rho d r_g A C_d}{4}$
	$c =$	$\frac{d r_g m g C_{rr}}{8}$
	$d =$	K_T
	$e =$	$\frac{2K_E}{r_g d L_a}$
	$f =$	$\frac{R_a}{L_a}$

Table 6.3: Change of parameters and notation

We see that for the position, all points are in equilibrium, when the trolley is at rest. We continue, by calculating the state matrices for this equilibrium.

$$\mathbf{A} = \frac{\partial \mathbf{f}}{\partial \mathbf{x}}(\mathbf{x}_0) \quad (6.26)$$

$$= \begin{bmatrix} 0 & 1 & 0 \\ 0 & 0 & \frac{d}{a} \\ 0 & -e & -f \end{bmatrix}$$

$$\approx \begin{bmatrix} 0 & 1 & 0 \\ 0 & 0 & 0.1707 \\ 0 & -3610 & -759.5 \end{bmatrix}$$

$$\mathbf{B} = \frac{\partial \mathbf{f}}{\partial \mathbf{x}}(u = 0) \quad (6.27)$$

$$= \begin{bmatrix} 0 \\ 0 \\ \frac{1}{L_a} \end{bmatrix}$$

$$\approx \begin{bmatrix} 0 \\ 0 \\ 666.7 \end{bmatrix}$$

Stability of the linearized system

From matrix \mathbf{A} , we can see that the drag and rolling friction is the only part missing when we compare the linearized system with the original system. In general, we know that frictional forces can be considered stabilizing, since they draw energy from the system. Hence, we can make an assumption that the original system is not less stable than the linearized system. We can also define the \mathbf{C} and \mathbf{D} matrices, by saying that we have the speed and the position as our measurements.

$$\mathbf{C} = \begin{bmatrix} 1 & 0 & 0 \\ 0 & 1 & 0 \end{bmatrix} \quad (6.28)$$

$$\mathbf{D} = \begin{bmatrix} 0 \\ 0 \end{bmatrix} \quad (6.29)$$

We plot the bode plots from the input to each of the outputs in the same plot (figure 6.7). Calculating the gain and phase margins, we find that they are both infinite for the transfer function from input to speed. From input to position, the gain margin is $\Delta K = 129\text{dB}$, and the phase margin is $\phi = 87.9^\circ$. The cross frequency is identified as $\omega_c = 0.00132\text{rad/s}$, and $\omega_{180} = 11.4\text{rad/s}$. We see that this system is stable without a controller. By adding a controller, and tuning it, we will be able to make the system converge to the desired position at the correct rate. For the most, that means we wish it to go full speed most of the way, then approaching with a lower speed the last seconds.

Controller design for the linear system

We choose a controller that controls the speed and position towards their setpoints. We found the speed equilibrium point to be 0, and the position equilibrium to be in the desired position.

$$u_a = -\frac{2}{dr_g} (P_d v + P(x - x_{ref})) \quad (6.30)$$

$$|u_a| \leq u_{a,max}$$

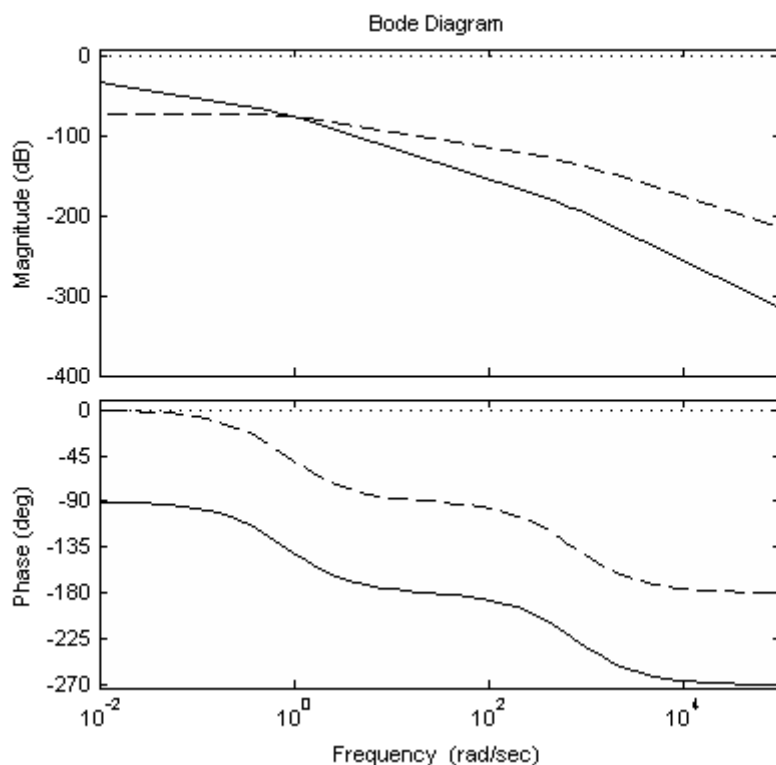


Figure 6.7: Bode plot of the system. Input to speed is the dashed line, input to position is plotted with a solid line. The zero-dB line is plotted with a dotted line

Since the system is stable by itself, any normally stabilizing controller should be able to do the job. For our case, we want the trolley to go fast, but approach the setpoint carefully. By choosing values for the controller so that the P-part is higher than the I-part, then this should be accomplished. Based on simple testing, the values in table 6.4 was chosen. This controller makes the system run at full speed most of the way, and slows down when closing in. It is important that the controller does not make the trolley run past the reference, since that might make it run off the track at the endpoints.

$$\begin{aligned} P_d &= 5 \\ P &= 1 \end{aligned}$$

Table 6.4: Controller parameters

By using the control parameters in table 6.4 and the functions in Skogestad and Postlethwaite (1996), we can set up the sensitivity function and the complimentary sensitivity function for the closed loop system. This tells us about how well it is able to follow a reference.

From Skogestad and Postlethwaite (1996), we know that for good and robust performance of the controlled system, we want S to be much lower than 0dB in order to maintain good control and deal with process noise. We also want T to be much lower than 0dB to achieve good suppression of measurement noise. Since $T = 1 - S$, the demands are clearly not possible at all times. Therefore, a reasonable trade-off is done, requiring S to be small for the frequencies we wish to control, and T to be small in the higher frequency area.

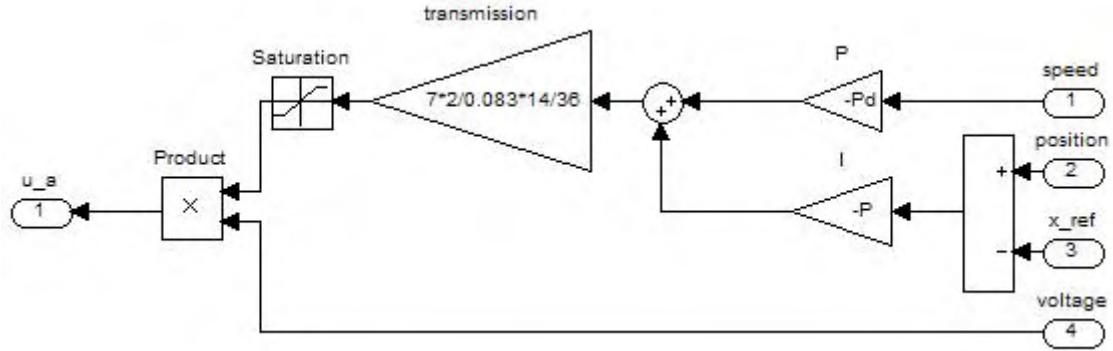


Figure 6.8: The controller implemented in Simulink

Looking at the plot, we see that the two functions cross at a very low frequency, meaning that for sudden changes of position reference, it will not keep up, and the speed will be limited. Considering that the system is rather large, and that we are looking at the control of the position, we can accept this, even though it seems to be a very low frequency.

We have now found that the linearized system is stable, and also found a controller that we believe will provide us with good performance.

6.2.2 Nonlinear stability

To confirm the stability result from the linearized section, we can look at the stability with nonlinear methods. We choose to look at a Lyapunov Function Candidate (LFC), and use this to prove stability as explained in Khalil (2000).

$$V(x_2, x_3) = \frac{1}{2}\alpha x_2^2 + \frac{1}{2}\beta x_3^2 < 0 \quad \forall x_2, x_3 \neq 0 \quad (6.31)$$

$$V(0, 0) = 0 \quad (6.32)$$

$$\dot{V}(x_2, x_3) = \alpha x_2 \dot{x}_2 + \beta x_3 \dot{x}_3 \quad (6.33)$$

$$= -\frac{\alpha b}{a} x_2^3 \operatorname{sgn}(x_2) - \frac{\alpha c}{a} x_2 \operatorname{sgn}(x_2) + \left(\frac{\alpha d}{a} - \beta e\right) x_2 x_3 - \beta f x_3^2 \quad (6.34)$$

$$= -\frac{\alpha b}{a} x_2^2 |x_2| - \frac{\alpha c}{a} |x_2| + \left(\frac{\alpha d}{a} - \beta e\right) x_2 x_3 - \beta f x_3^2 \quad (6.35)$$

$$< 0 \quad \forall x_2, x_3 \neq 0, \alpha \frac{d}{a} = \beta e \quad (6.36)$$

$$\dot{V}(0, 0) = 0 \quad (6.37)$$

For this to be a Lyapunov function, it must satisfy conditions as described in Khalil (2000). First, V must be positive definite for all values of x_2 and x_3 . This is true for our LFC. Second, its derivative with respect to time must be negative definite. We see that this is also true, from equation 6.31. By plotting V and \dot{V} in MatLab, we get a visual confirmation that the calculation is correct.

We see that for correctly chosen values of α and β , V is a Lyapunov function. This means that this system is asymptotically stable. In practical view, this means that the speed of the trolley will converge to a fixed speed that can be controlled. From this, we can deduce that the total system will also be stable, and that the system will converge towards a fixed point. When the speed has converged, we know that $v = x_2 = 0$. From equation 6.21 follows that when $x_2 = 0$, $\dot{x}_1 = 0$, and x_1 is stationary, so it must have converged.

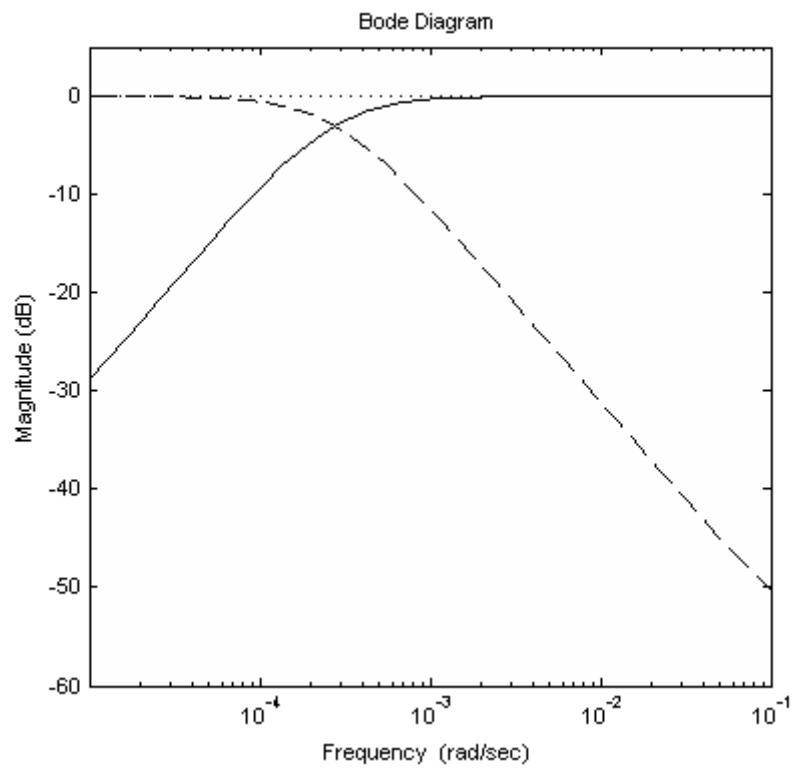


Figure 6.9: Bode magnitude plot of the sensitivity (S) and complimentary sensitivity (T) functions. S is plotted with a solid line, T is the dashed line. The zero-dB line is plotted with a dotted line

We will not design a nonlinear controller, since all nonlinear elements are taking energy out of the system, helping to stabilize it.

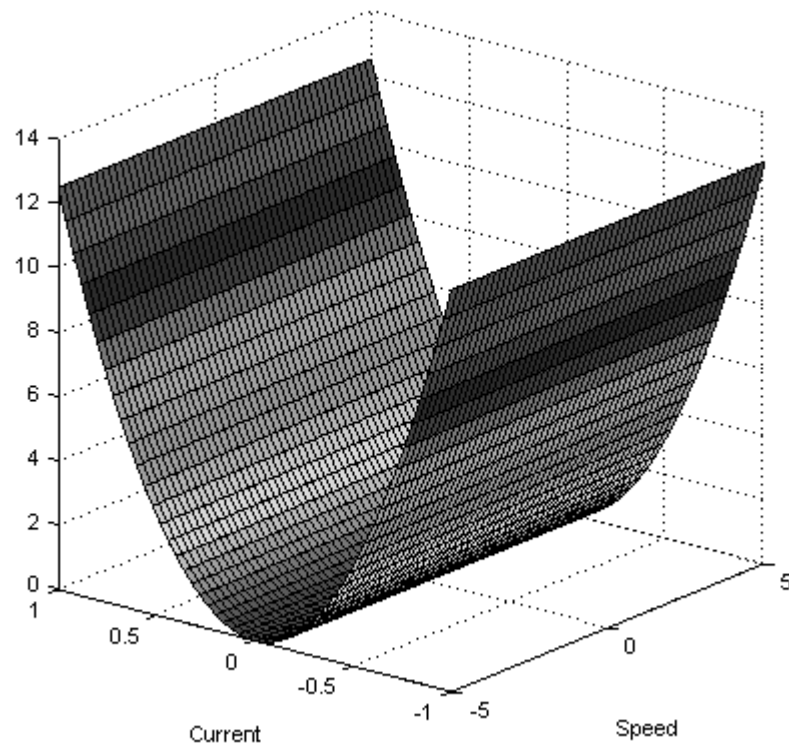
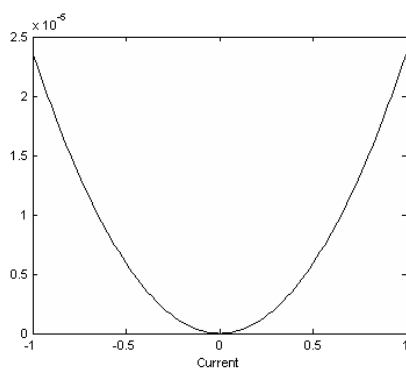
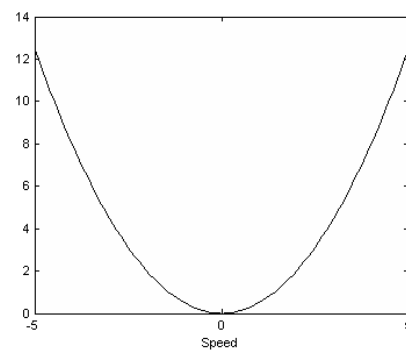
(a) 3-dimensional plot of $V(x_2, x_3)$ (b) Plot of $V(0, x_3)$ (c) Plot of $V(x_2, 0)$

Figure 6.10: The Lyapunov function

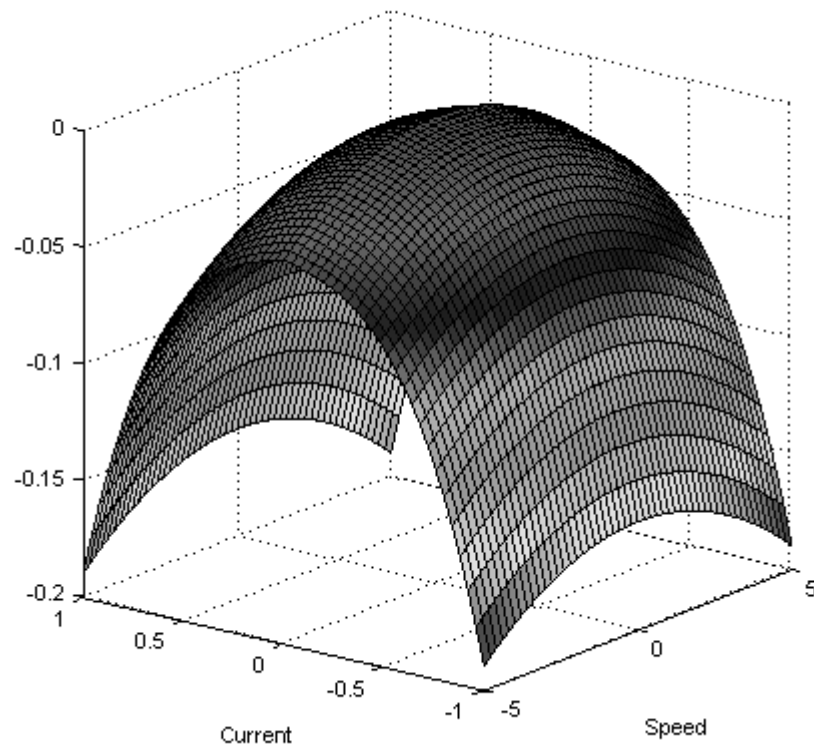
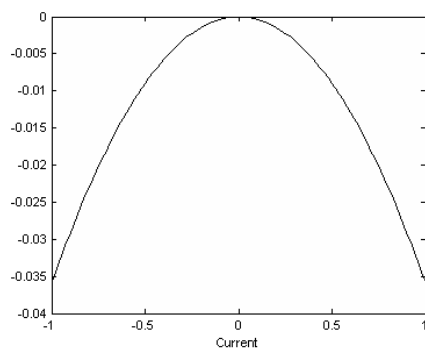
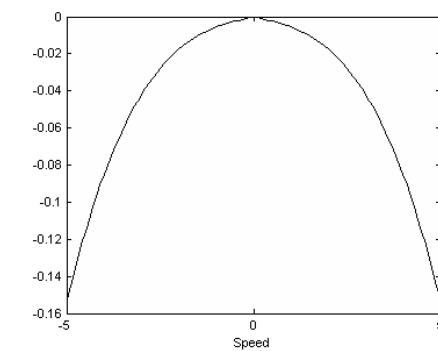
(a) 3-dimensional plot of $\dot{V}(x_2, x_3)$ (b) Plot of $\dot{V}(0, x_3)$ (c) Plot of $\dot{V}(V(x_2, 0))$

Figure 6.11: The time derivative of the Lyapunov function

6.3 Simulations

In order to test the controller, we will simulate it for several scenarios. The first scenario we want to check is the ordinary working situation, where the trolley is instructed to go to a position, and stay there.

Then we will look at how the system behaves when the reference changes while it is moving. Even though the communication most likely will not be available while the trolley is moving, we want to see how the trolley deals with an instruction to reverse direction while at full speed.

In order to see how the system handles a constantly changing position, we input a sine-wave reference. This is an unlikely scenario, but the results can tell us interesting things about our controller.

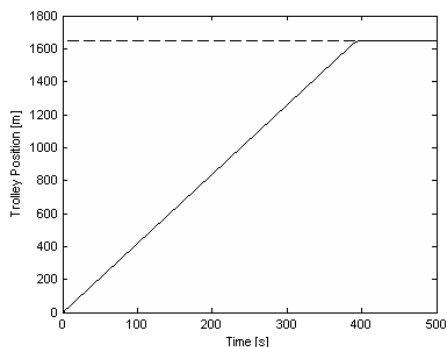
At a later time, it can be interesting to reprogram the system so that it can record video while moving, and then upload this when it is in a place it can communicate. This way, the state of a large tunnel-section can be watched. For this, we are interested in going at a fixed speed. This can be simulated by using a ramp reference for the position.

When running the system in real life, components can malfunction, so we want to check how a varying voltage supply affects the performance. We insert the voltage supply as a sine-wave oscillating around a voltage close to the original supply voltage.

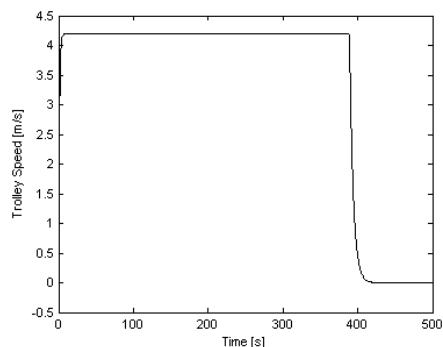
We simulate in Simulink, using the default settings with the ODE45-solver. This is not a problem with extraordinary requirements, so the default works just fine. The time span of the simulations are varying between the simulations, because we choose to simulate for the time span we consider sufficient to observe the effect.

6.3.1 Go to a specified setpoint

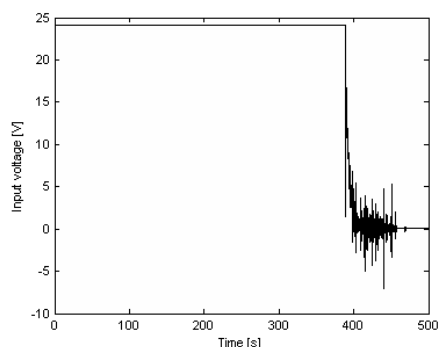
In this simulation, we set the setpoint to be 1650m, that is halfway into the tunnel. We set a steady power supply of 24.12V, as we have used earlier. We see that the speed quickly goes



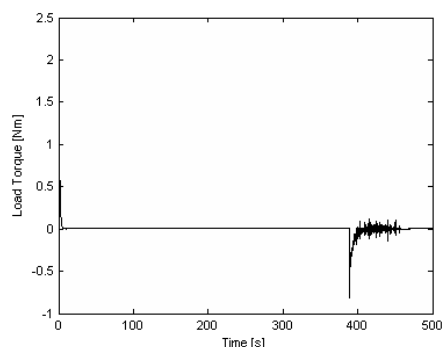
(a) The position is a solid line, the reference is the dashed line



(b) The speed



(c) The input voltage from the controller



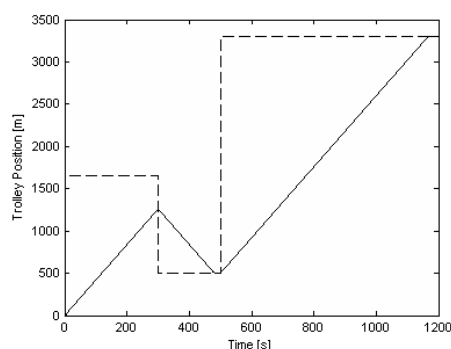
(d) The load torque from the trolley on the motor

Figure 6.12: Simulations with a constant reference at 1650m into the tunnel.

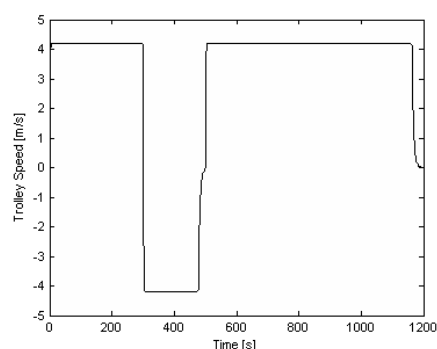
up to the maximum speed. When the trolley arrives, it uses some time slowing down so that it does not overshoot the position. The load torque is quickly changing when accelerating and slowing down, but other than that, it is close to zero. The input voltage from the controller is high when the trolley is at full speed, and goes up and down some when the trolley is slowing down.

6.3.2 Follow a changing setpoint

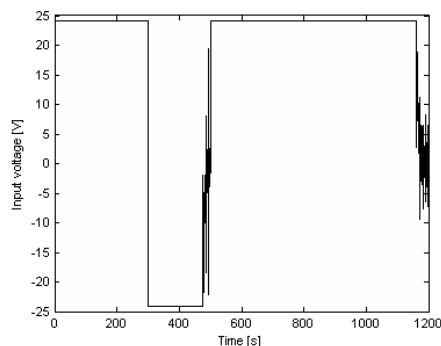
Occasionally, the operator will send the wrong commands to the trolley. If the operator makes a mistake, the trolley will go toward a position in the other side of the tunnel, while the position that is interesting to watch is only a few hundred meters into the tunnel. In such cases, it is interesting to look at how the trolley handles being redirected while moving at full speed. In the simulation, we set the setpoint to be midway into the tunnel (1650m) for 300s. Then the reference changes to 500m, and stays constant for 200s, before it jumps to the endpoint of the tunnel at 3300m. The trolley does not make it to the first setpoint before it is redirected. It



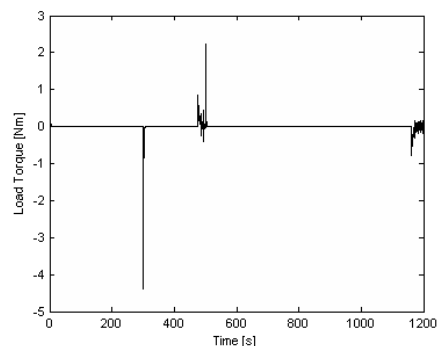
(a) The position is a solid line, the reference is the dashed line



(b) The speed



(c) The input voltage from the controller



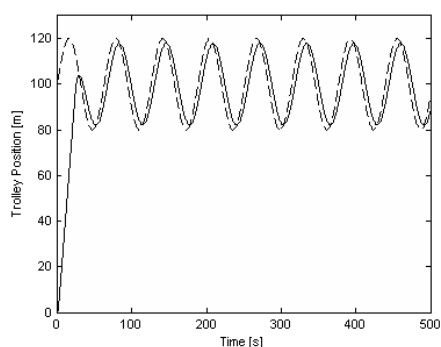
(d) The load torque from the trolley on the motor

Figure 6.13: Simulations with a variable reference.

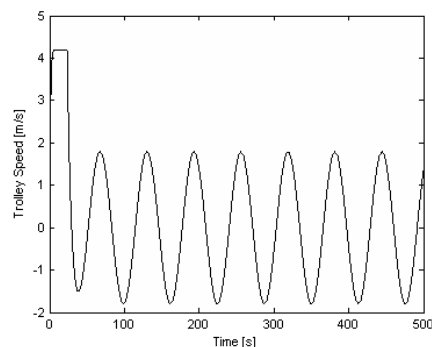
makes it to the second, and it makes it to the third point at the end. The speed changes quickly from maximum one way to maximum the other way when the setpoint changes. The same observation can be done about the input voltage. The load torque peaks at the point where the change of direction occurs, as well as when the trolley slows down when it arrives at the setpoints it is able to come to. In this case, the load peaks at values with a magnitude of more than 4Nm. We also notice, that this peaks very quickly.

6.3.3 Following an oscillating reference

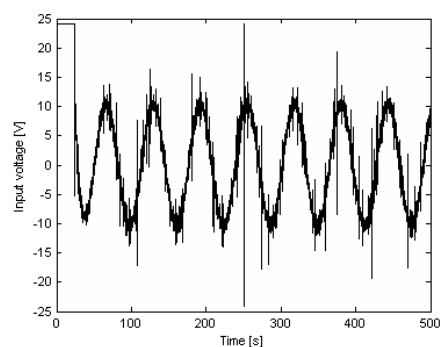
This might not be very relevant as a practical use, but it is still interesting to see how the system responds to a sinusoidal input reference. Here, we have an amplitude of 20m, a frequency of 0.1Hz, and it oscillates around a position 100m into the tunnel. We can measure that the



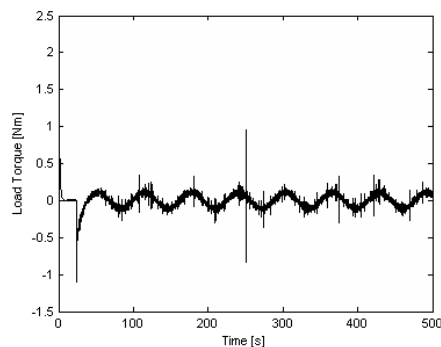
(a) The position is a solid line, the reference is the dashed line



(b) The speed



(c) The input voltage from the controller



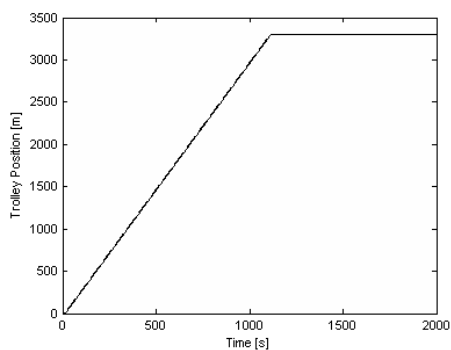
(d) The load torque from the trolley on the motor

Figure 6.14: Simulations with an oscillating reference.

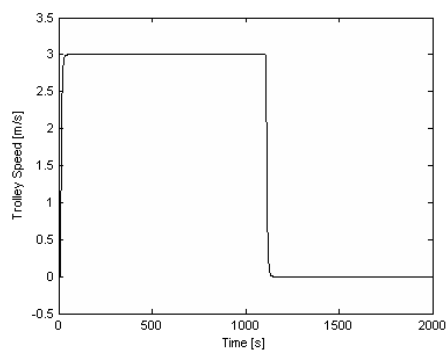
trolley is about 3 seconds behind the signal reference. The speed never peaks when the trolley is oscillating. But it does seem to overshoot a little bit. The torque changes a lot, but is within a small band for the most part. The input voltage is changing just as the torque. All the four measurements oscillate with the same low frequency. In addition, the voltage and torque oscillates with a much higher frequency on top of the low frequency.

6.3.4 Following a constant speed reference

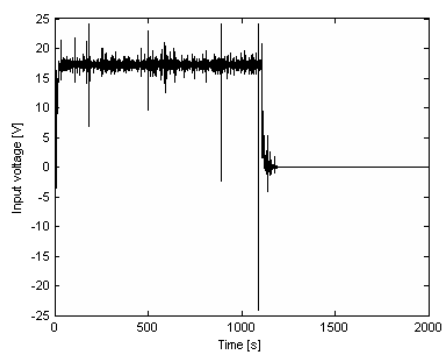
In this case, we choose to make the trolley follow a ramp reference value, with a constant speed of 3m/s. This is a speed we know is below the maximum speed of the trolley. We can see from



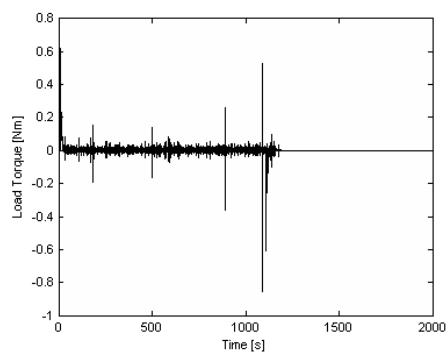
(a) The position is a solid line, the reference is the dashed line



(b) The speed



(c) The input voltage from the controller



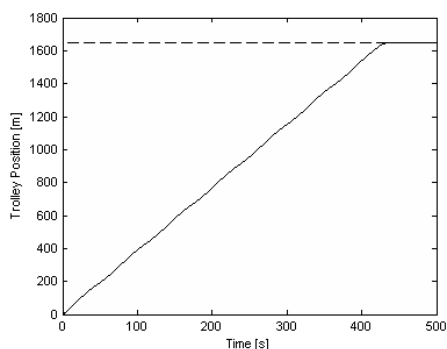
(d) The load torque from the trolley on the motor

Figure 6.15: Simulations with a constantly increasing reference.

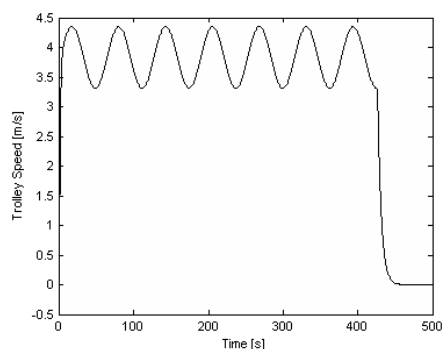
the plot that the trolley is practically staying on target, keeping with the reference value. We can see in the plot for the speed that it keeps the correct speed until the trolley arrives at the saturation point at 3300m. The input voltage is limited to the maximum input voltage, and except for 3 or 4 times, it keeps below that value. The load torque oscillates with high frequency until the speed reference drops to 0.

6.3.5 Varying voltage supply and a constant reference position

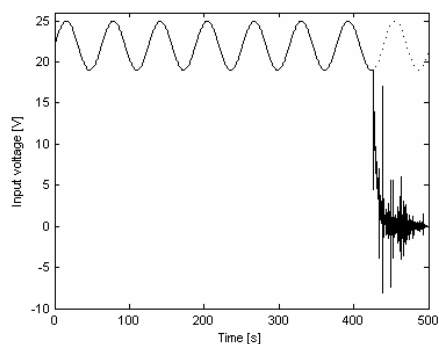
Sometimes, power supply can malfunction. We simulate this case by letting the available voltage oscillate between 19V and 25V, with a frequency of 0.1Hz. This is not really that fast changing, but we want to see how the controller deals with it. We can see that the rate of approach to



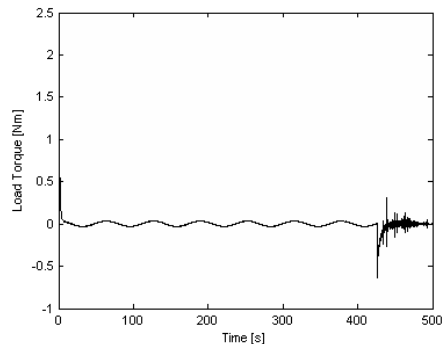
(a) The position is a solid line, the reference is the dashed line



(b) The speed



(c) The input voltage from the controller is drawn as a solid line, and the available voltage is a dashed line



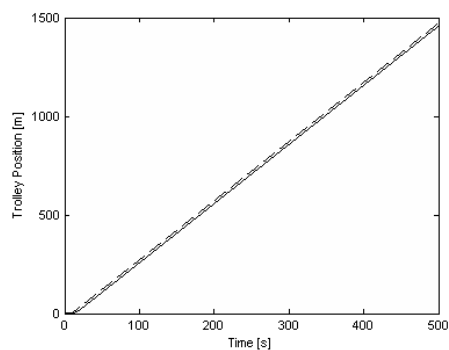
(d) The load torque from the trolley on the motor is drawn as a solid line, and the available voltage is a dashed line

Figure 6.16: Simulations with a constant reference at 1650m into the tunnel, and varying available voltage for the controller.

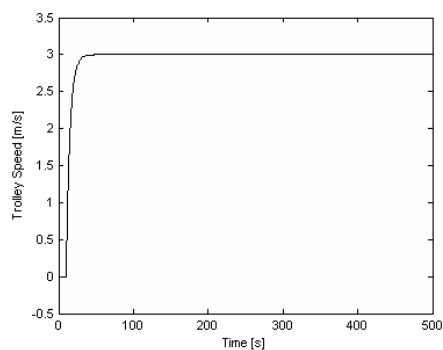
the setpoint position is not as straight as it is for the first simulation. In the plot of the speed, we see that the speed is oscillating. The same is for the input voltage, and we can see that the controller applies the maximum voltage it can almost until it arrives at the setpoint. The load is also oscillating.

6.3.6 Varying voltage supply and constant speed reference

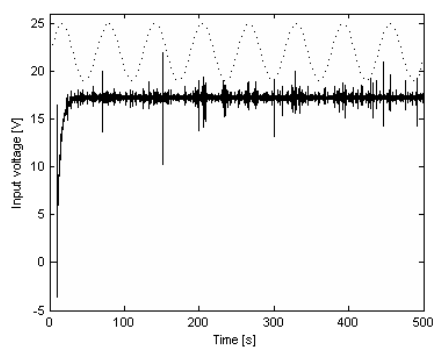
This is the same limitations on the available voltage, but this time the system has the ramp reference. Also this time, the speed is set to 3m/s. The trolley seems to be following the moving



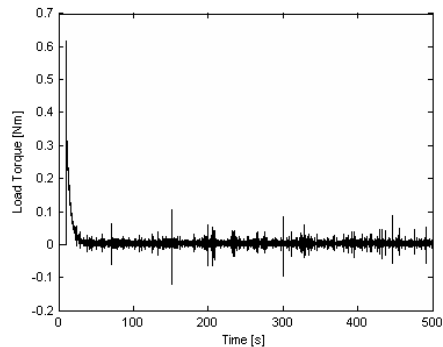
(a) The position is a solid line, the reference is the dashed line



(b) The speed



(c) The input voltage from the controller is drawn as a solid line, and the available voltage is a dashed line



(d) The load torque from the trolley on the motor is drawn as a solid line, and the available torque is a dashed line

Figure 6.17: Simulations with a constant reference at 1650m into the tunnel, and varying available voltage for the controller.

setpoint position, with a fixed deviation. The speed is steady at 3m/s, which is the rate of increase in the setpoint value for the position. The input voltage is mostly below the maximum available voltage. The load is similar to the load at the simulation with ramp reference and constant maximum value of the available voltage. When the trolley is breaking down, the load peaks at about -0.5Nm, and oscillates for about one minute.

In this chapter, we look at the planned design, and the results from the testing and simulations that were performed. This is then compared to the requirements stated in chapter 3.

7.1 Testing

The original plan was to build a complete prototype, and test the entire system in the LHC tunnel. Since it was not possible to get all the components in time, this had to be cancelled.

Practical testing was done of the communication between the camera and the motor controller. Some testing of the powerline communication equipment was done. Also, camera operation was tested.

Simulations in Matlab Simulink were carried out for a model of the trolley with a DC motor.

7.2 Prototype plan and results from tests

7.2.1 Prototype modules

Camera

The camera was already programmed with a web server and a system for use of the RS-232 port on the expansion module. This worked just as it should.

Also, the camera was proven capable of zooming and focusing closely on text written on paper, with size 12points, more than 5m away. The same test was also done with low light conditions, during which it was not possible to read anything.

Trolley

For the motor controller to be able to communicate with the camera, the microcontroller needed to be programmed. The Atmel STK-500 card is well proven, so this worked.

Testing with the motor show that it is possible to communicate with the motor controller by sending commands over the Internet from practically any computer that has the correct password in order to connect to the camera.

It was discovered that some commands were lost in the communication between the camera and the motor controller. The same problem is found with using Ethernet for real-time communication, since packets occasionally get lost. This uncovers the need to make the control system sufficiently smart so that it can avoid running out of the track, or hitting objects that are in the way.

The trolley is the module that has the most requirements. At first it is required to have a large area of operation. In the simulations, the trolley is able to get to the desired position, no matter where in the tunnel this position is. The trolley is to be kept small. An estimate used in the modeling tells us that we can expect it to have a weight of around 40kg. It is also required that the wheels on the trolley are made of polyurethane. This kind of wheels that fit the trolley is not found. A speed of above 12km/h is mentioned as a minimum. Simulations indicate a maximum speed above 15km/h. It is not planned any specific positioning system. For safety, the system is planned to rely on internal programming. The trolley will rely on the camera and communications system to reestablish communication. When it stops in a position without communication, the trolley needs to move to a place with coverage. The parts that require advanced programming is not done, since the complete system is not assembled. If we were to program the microcontroller with all the functions required, it would be no way of testing it properly if we did not have the complete prototype assembled. The shielding of the system is not planned, because the main focus was on the prototype planning, and the shielding is thought to be mounted around a short section of the rail.

Power

Because the trolley was not assembled, the power supply was not obtained, and therefore not tested. The plan was to use a commercially available power supply to convert the power from 400V three-phase to 230V that additional power supplies for the modules. Also, it was planned to add batteries as a backup.

The requirements tell us that we want the system to be able to operate for long periods of time, and also to run for some time without external power. It is not calculated how much power this system would use, so we cannot say how long the system would have worked without external power. It is established from testing on equipment already in the LHC tunnel that the power collector shoes used to provide power to the system, does not work at speeds above 3-4km/h. Also, the power rail in the tunnel has 30cm gaps in the coverage set several places.

Communications

The powerline communication device is not fully tested. A prototype is assembled, but it was too late to do more than basic testing. The only part of the design that is verified at this point, is the voltage regulators, that are found working.

Looking at the requirements set up, we see that remote control is the first requirement. Using the Ethernet to communicate gives us the freedom of placing the operator at any computer connected. The bandwidth of this system is unknown, since it is not tested. We know that using the Ethernet for communication will introduce delays. At certain intervals, there are 30cm gaps in the coverage in the power rail. This means that the communication system also will have gaps in the coverage.

7.2.2 Simulations

Simulations show that the system can achieve a top speed of 4.2m/s. Provided that the position measurement is accurate, it will also stop at the position it is instructed to go to. When going to a specified position, the trolley speeds up to maximum speed in less than 10 seconds, so the acceleration is swift. This means it will pick up speed fast. When approaching its target position, the speed drops when it closes in, and it does not overshoot the position. It uses more than 3 times as much time for breaking as it does for accelerating, as seen in figures 6.12b, 6.13b, 6.14b, 6.15b, 6.16b and 6.17b. For the simulation where we instruct the trolley to go to the center of the section, we see that it uses around 400s. By assuming it will keep the same speed all the way to the end, we get that it will use about 800s, or less than 14 minutes, to go from one endpoint to another.

When the system is instructed to follow a position reference moving with constant speed, or oscillating, it tends to stay between 2 and 5 seconds behind the reference trajectory.

For the case where the supply voltage is simulated as not ideal, the system still is able to get where it is instructed to go. When it is instructed to go to a position far away, the maximum speed will be oscillating. This is because the maximum speed depends on the maximum voltage available. The controller reacts the same way it does for the case where the voltage supply is normal, and outputs the maximum available power. The result of this is more present on the plot of the speed than on the plot of the position, and it does make it to the desired position, even though it uses 100s more than for the case with normal power supply. When following a reference moving slower than the system maximum speed, the speed and position trajectory is similar to the one for the case where the available voltage is normal.

In the simulations, we also observe that the plots of the voltage and load torque are oscillating with a high frequency.

8.1 Camera

Of the parts described in this thesis, only the camera is fully ready to be put in use. In fact, the camera is already in use for surveillance of the LHC cryogenic system. The camera is shown to fulfill all requirements we have listed, except the requirement for functioning in low light conditions. This is not considered very important, since it already is light in the tunnel. An external light source can be added later.



Figure 8.1: A surveillance camera in the LHC

8.2 Trolley

Because of the problem finding wheels made in the correct materials, the trolley was not purchased, and therefore it is not tested.

The motor controller hardware is working well. The problem with not all commands getting transmitted from the camera to the motor controller, is due to the fact that the RS-232 interface uses no common clock. A slight inaccuracy in the clock speed on either of the two devices communicating, and some of the communication is lost. This can be solved by measuring the clock speed on both devices, and adjusting the internal clock in the microcontroller.

However, the software cannot be fully developed until we know exactly what motor will be used, and what kind of positioning system we will use to receive input on where we are in the tunnel. There will also be extra security considerations that need to be made with the controller, since the system is thought to operate autonomously for periods of time.

The simulations show that this system can perform as we want. The controller works, and the system increases its speed faster than it reduces it. Also, it starts the speed reduction far enough away from the setpoint, so that it will not overshoot the position. This means that if the trolley is instructed to travel to one of the endpoints of the rail, it will not run off the rail when it gets there.

The simulation results that are troubling are the effect we observe on the plot of the load torque and input voltage. This high frequency will most likely constitute a significant amount of wear on the motor and the transmission on the trolley. For the design of a prototype, this is possible to accept, but is a factor that needs to be paid attention to in order to see if it actually would become a problem. If this turned out to be a problem, measures must be taken to counter this.

Looking at the requirements, we see that the trolley will have access to the entire section it is to monitor. In simulations, it does get to the setpoint position, and it does achieve a speed well above the minimum required speed. The trolley is expected to weigh twice as much as we initially wanted. This makes it harder to handle. It is not possible to find a lighter system without making a custom design, which is beyond the scope of this work. The shielding and positioning system is missing in the proposed prototype design.

8.3 Power

Because of the unfinished trolley, we have not been able to test the power supply, and see how this will work during operation. Therefore we cannot say that it fills our requirements at this time.

In theory, the power system should provide a steady supply of power. The system will have to rely on battery power when it is in the dead-zones, so the power will not be available at all times at all locations. Also, the proven limitations on speed when using the power rail, is a problem for our system. However, since the power rail is the only infrastructure in the tunnel that can provide coverage along the entire length of each section, this is the only real alternative for us to use.

8.4 Communication

The communication device is not yet fully tested. It looks promising, but until full scale testing is done in the LHC tunnel, we will not know if it will work properly and provide coverage past fuses and disturbances present in the tunnel.

The CERN Control Centre is already operational, and a part of this is reserved for the cryogenic operation and monitoring, so the operator terminal is already ready for use. Ethernet infrastructure at CERN is also in place, so when the system is online, it can be controlled by anyone granted access to control it.

Because of the lack of testing, we do not know if the communication device fulfils all the requirements we have set up. If it works, it will provide access to the system from any computer that is online. It is designed to have high bandwidth, so this requirement is also met. The coverage will have gaps, but these are small, so they will not limit the systems surveillance capabilities.

9.1 The prototype

For this project to be fully tested, the prototype must be assembled. Then the software for the motor controller can be developed.

When the prototype is built, it is possible to improve the theoretical model, and make a better controller. In order to avoid the possible wear the simulations indicate, we can design a robust controller for this system.

In order to reduce the weight of the system, it should be considered to use different types of batteries. It is, however, important to make sure that the batteries will not be a hazard to either people or material in the tunnel.

9.2 More functionality

Since this system will be sent into the tunnel in cases where it is unsafe for personnel to be inside the tunnel, it will be desirable to fit it with equipment that can give more information than the video feed. Such equipment can be for measuring O₂-deficiency or radiation levels. The connection module for the camera has 2 unused inputs that can be read with functions already embedded in the web-server.

An example application of this is if there is a helium leak in the tunnel, but the scope of this leak is not known. Then the system can be instructed to go towards the O₂-deficiency sensor that has warned of the leak, and stop when the onboard sensor warns that there is low levels of O₂ present. It is also possible to connect such equipment to the microcontroller.

Since people will need to lift and move the system manually at times, it would also be good to have measurements for accumulated doses of radiation. This way, they will know what precautions to take when handling it.

List of references

- AM Elektronik (2002), 'Avr libc function reference', Online. Retrieved July 10, 2006, from Amelek.gda.pl.
url: <http://www.amelek.gda.pl/avr/libc/avr-libc-reference.html>
- Atmel (2006), 'ATAVRMC100 - Hardware User Guide', Online datasheet/userguide. Retrieved March 27, 2006 from Atmel Corporation.
url: http://www.atmel.com/dyn/resources/prod_documents/doc7551.pdf
- Aveox DC Permanent Magnet Brushless Motors (2006), 'Technical information, sizing of dc motors', Online. Retrieved June 20, 2006, from Aveox.
url: <http://www.aveox.com/technical/dc.html>
- AVR Libc project group (2006), 'Avr libc 1.4.4', Online. Retrieved July 10, 2006, from Nongnu.org.
url: <http://www.nongnu.org/avr-libc/user-manual/index.html>
- Axis Communications (2005), 'AXIS VAPIX API, HTTP - Interface Specification', Online. Retrieved March 30, 2006, from Axis Communications.
url: http://www.axis.com/techsup/cam_servers/dev/cam_http_api_2.htm
- Axis Communications (2006), 'AXIS 213 PTZ Network Camera', Online datasheet. Retrieved March 29, 2006, from Axis Communications.
url: http://www.axis.com/files/datasheet/ds_213_26598_en_0603_lo.pdf
- Bachy, G. (1989), Engineering and construction experience at LEP (CERN), in 'New Orleans 1989, Proceedings, Supercollider 1', Plenum Press, New York, pp. 711–717.
- Bilstad, H. (2006), Løpekatt. E-mail information about monorail trolley specifications and feasibility.
- Bryson, W. E. (1999), *Cryogenics*, Hanser Gardner Publications, Cincinnati.
- CERN (1984), *LEP design report - Vol 2 - The LEP main ring*, Vol. 2, CERN Geneva.
- CERN (2004a), *LHC Design Report - Vol 1 - The LHC Main Ring*, Vol. 1, CERN, Geneva.

- CERN (2004b), *LHC Design Report - Vol 2 - The LHC Infrastructure and general services*, Vol. 2, CERN, Geneva.
- CERN (2004c), *LHC Design Report - Vol 3 - The LHC Injector Chain*, Vol. 3, CERN, Geneva.
- CERN (2006a), ‘What is CERN?’, Online. Retrieved February 15, 2006, from the CERN website.
url: <http://public.web.cern.ch/public/Content/Chapters/AboutCERN/WhatIsCERN/WhatIsCERN-en.html>
- CERN (2006b), ‘What is LHC?’, Online. Retrieved February 15, 2006, from the CERN website.
url: <http://public.web.cern.ch/public/Content/Chapters/AboutCERN/CERNFuture/WhatLHC/WhatLHC-en.html>
- Chen, C.-T. (1999), *Linear System Theory and Design*, Oxford University Press, New York.
- Chevalley, J. M. (2006), Question about overhead travelling cranes, power and communications. E-mail information about the monorail and power rail installed in the LHC tunnel.
- D-Link (2006), ‘DWL-7700AP > Wireless AG Outdoor AP/Bridge - Specifications’, Online. Retrieved June 28, 2006, from D-Link.
url: <http://www.dlink.com/products/resource.asp?pid=376&rid=1399&sec=0>
- Egeland, O. (1993), *Servoteknikk*, Tapir.
- Encyclopædia Britannica (2006a), ‘CERN’, Online. Retrieved March 27, 2006, from Encyclopædia Britannica Premium Service.
url: <http://www.britannica.com/eb/article?tocId=9360200>
- Encyclopædia Britannica (2006b), ‘DSL’, Online. Retrieved June 20, 2006, from Encyclopædia Britannica Premium Service.
url: <http://www.britannica.com/eb/article?tocId=9363140>
- Encyclopædia Britannica (2006c), ‘Hadron’, Online. Retrieved March 28, 2006, from Encyclopædia Britannica Premium Service.
url: <http://search.eb.com/eb/article-9038748>
- Fahrleitungsbau GmbH (2002), ‘FABA conductor rail systems’, Online. Retrieved February 20, 2006, from Fahrleitungsbau GmbH.
url: http://www.fahrleitungsbau.de/FABA/EN/htm/schleifleitungen/katalog/FABA_Schleifleitungen.pdf
- Faugeras, P. (2002), ‘Voice and data communications in LHC underground areas’, Online. Retrieved February 27, 2006 from CERN EDMS.
url: <https://edms.cern.ch/document/331622/1.0>
- Free Software Foundation, Inc. (2006), ‘Gnu avr-gcc’, Online. Retrieved July 10, 2006, from AVRfreaks.
url: <http://www.avrfreaks.net/AVRGCC/>
- Guerrero, L. (2006), Question about leaky feeder in lhc tunnel. E-mail information about the leaky feeder cable installed in the LHC tunnel, received July 19.
- Houge, T. (2006), ‘Powerline device - eda-01363’, Online. Retrieved June 16, 2006, from CERN EDMS.
url: <https://edms.cern.ch>

- Kershaw, K. (2006), Monorail trolley. E-mail information about monorail trolley requirements.
- Khalil, H. K. (2000), *Nonlinear Systems*, 3 edn, Prentice-Hall Inc., Pearson Education International, New Jersey.
- Knight, R. D. (2004), *Physics for Scientists and Engineers*, Pearson Education Inc., Addison Wesley, San Francisco.
- Krishna, C. and Shin, K. G. (1997), *Real-Time Systems*, McGraw Hill, Singapore.
- Loke, A. and Ali, F. (2002), 'Direct conversion radio for digital mobile phones - design issues, status, and trends', *IEEE Transactions on microwave theory and techniques* **50**(11), 2422–2435.
- Magnetek Electromotive Systems (2003), 'FABA conductor bar system - standard components', Datasheet. Available from Magnetek as publication #FABASC-04.
- Maxim Integrated Products (2004), MAX2986 integrated powerline digital transceiver. Datasheet available on request from Maxim Integrated Products.
- Maxim Integrated Products (2005), MAX2980 powerline communication analog front-end transceiver. Datasheet available on request from Maxim Integrated Products.
- McClaning, K. and Vito, T. (2000), *Radio receiver design*, Noble Publishing Corporation.
- Radio Frequency Systems (2006), 'Product data sheet RLKW114-50J/JFN/JFL', Datasheet. Available from Radio Frequency Systems.
- Schiver, S. W. V. (1986), *Helium Cryogenics*, Plenum Press, New York.
- Serpa, M. (2006), Re: Max2986 data sheet request. Enquiry to Maxim-IC technical support, received by e-mail March 17. 2006.
- Shenzhen Unite Industries Co Ltd. (2005), 'MY1018E-300-500W', Online. Retrieved May 03, 2006, from Shenzhen Unite Industries Co Ltd.
url: <http://www.cn-dcmotor.com/productShows.asp?ArticleID=163>
- Silari, M. and Menzel, H. (2004), *Radiation Protection Group Annual Report 2003*, CERN Geneva.
- Skogestad, S. and Postlethwaite, I. (1996), *Multivariable Feedback Control - Analysis and Design*, Wiley.
- TKS AS (2006), 'TKS Løpekatter', Datasheet. Available on request from TKS AS.
- Weisend II, J. G., ed. (1998), *Hanbook of cryogenic engineering*, Taylor and Francis, Philadelphia, PA.
- Wi-Fi Alliance (2006), 'What is the range of a wireless network?', Online. Retrieved February 25, 2006, from Wi-Fi Alliance.
url: <http://www.wi-fi.org/faqs.php>

APPENDIX A

400V 3-phase AC current

In the powered rail, we have 3 conductors which carry 230V AC power. The challenge is posed when we do not have an N-conductor present. The solution to this is to take the potential between the L1 and L2 conductors. This will introduce a phase change and increase the amplitude of the resulting sine curve.

$$L1 = 230 \cdot \sqrt{2} \sin(2\pi ft) \quad (\text{A.1})$$

$$L2 = 230 \cdot \sqrt{2} \sin(2\pi ft - \frac{2}{3}\pi) \quad (\text{A.2})$$

$$V = L1 - L2 \quad (\text{A.3})$$

$$= 230 \cdot \sqrt{2} \left(\sin(2\pi ft) - \sin(2\pi ft - \frac{2}{3}\pi) \right) \quad (\text{A.4})$$

$$= 230 \cdot \sqrt{2} \left(\sin(2\pi ft) - \sin(2\pi ft) \cos(-\frac{2}{3}\pi) - \cos(2\pi ft) \sin(-\frac{2}{3}\pi) \right) \quad (\text{A.5})$$

$$= 230 \cdot \sqrt{2} \left(\frac{3}{2} \sin(2\pi ft) - \frac{\sqrt{3}}{2} \cos(2\pi ft) \right) \quad (\text{A.6})$$

$$= 230 \cdot \sqrt{2} \left(\sqrt{3} \sin(2\pi ft) \cos \frac{1}{6}\pi - \sqrt{3} \cos(2\pi ft) \sin \frac{1}{6}\pi \right) \quad (\text{A.7})$$

$$= 230 \cdot \sqrt{6} \sin(2\pi ft + \frac{1}{6}\pi) \quad (\text{A.8})$$

$$\approx 400 \cdot \sqrt{2} \sin(2\pi 50t + 30^\circ) \quad (\text{A.9})$$

$$\approx 566 \sin(2\pi 50t + 30^\circ) \quad (\text{A.10})$$

$$(\text{A.11})$$

We see that between the cables, we have 400V AC RMS value, which gives us 566 in amplitude. The frequency is still 50Hz, so this can be used for powerline networking just as good as a powerline at home, we simply need to make our electronic circuits robust enough to take the extra voltage. In figure A.1, this is visualized.

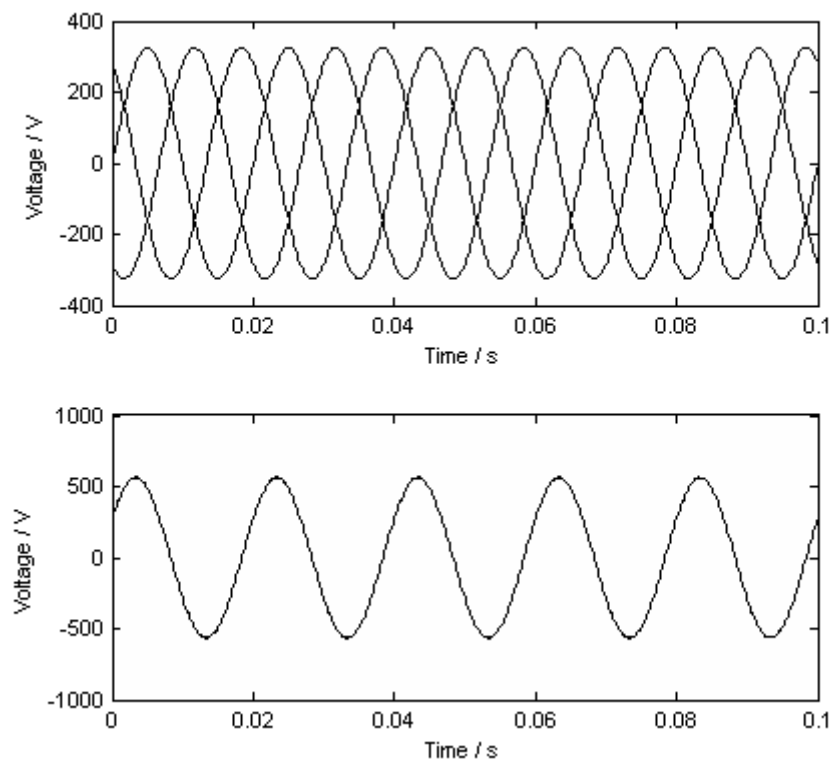


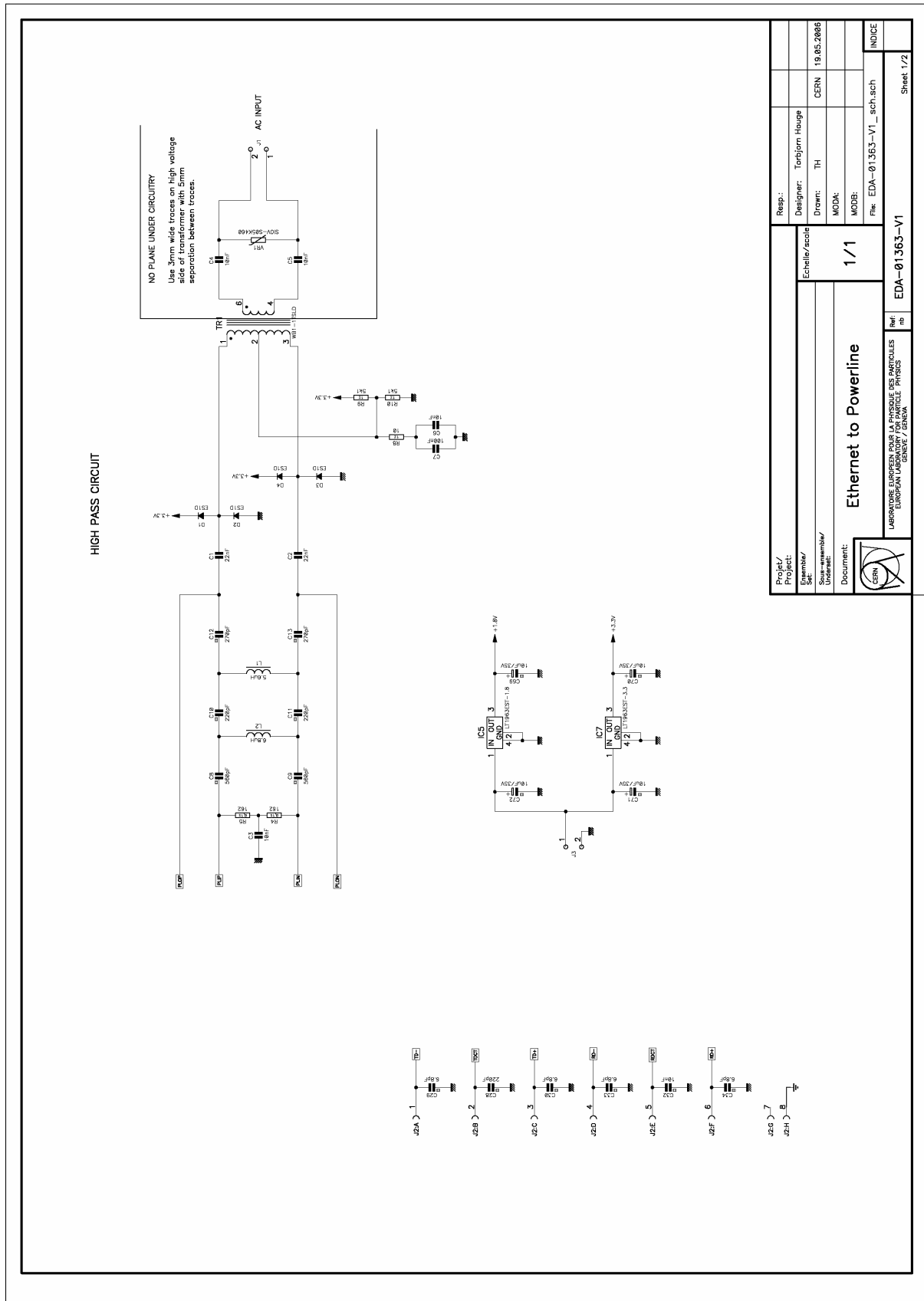
Figure A.1: The 3 phases in the top plot, the difference between phase 1 and 2 in the bottom plot

APPENDIX B

Design of the communication device

This design is also published online in the CERN EDMS system. It is publicly available, and is found at <http://edms.cern.ch> with id EDA-01363 (Houge, 2006). In this appendix, the schematics on 2 pages, the PCB layout on 4 pages, and the 3-page material list is listed.

B.1 P-CAD output



Project/Project:		Resp.:	
Echelle/Scale:		Designer: Torbjorn Houge	
Set:		Drawn: TH	
Undersatt:		MODA:	
Document:		MODB:	
1/1		File: EDA-01363-V1_sch.sch	
Ethernet to Powerline		INDICE	
LABORATOIRE EUROPEEN POUR LA PHYSIQUE DES PARTICULES EUROPEAN LABORATORY FOR PARTICLE PHYSICS GENÈVE / GENEVA		Sheet 1/2	
EDA-01363-V1			

Figure B.1: Schematics for the powerline to ethernet device, made in P-CAD, page 1

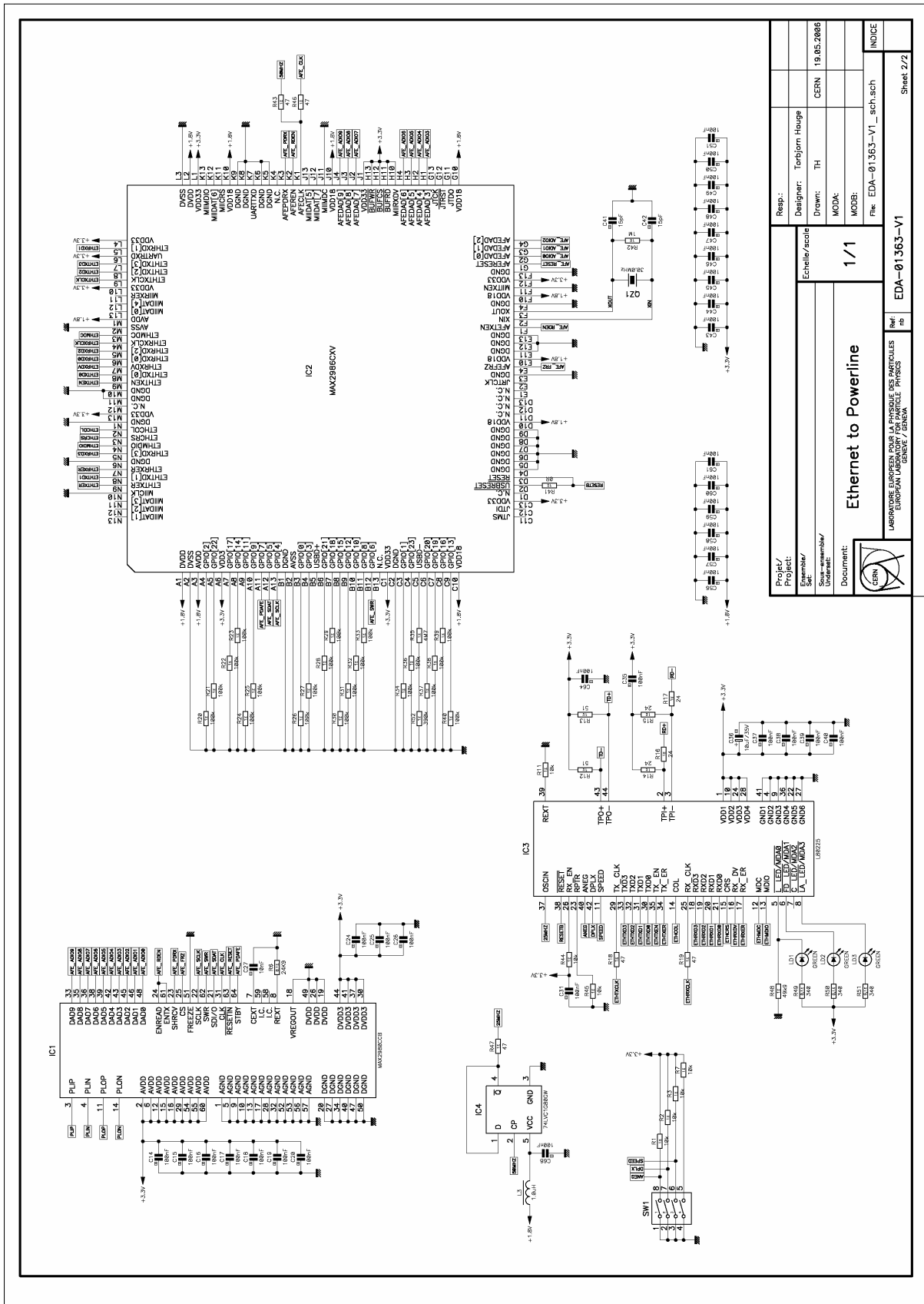


Figure B.2: Schematics for the powerline to ethernet device, made in P-CAD, page 2

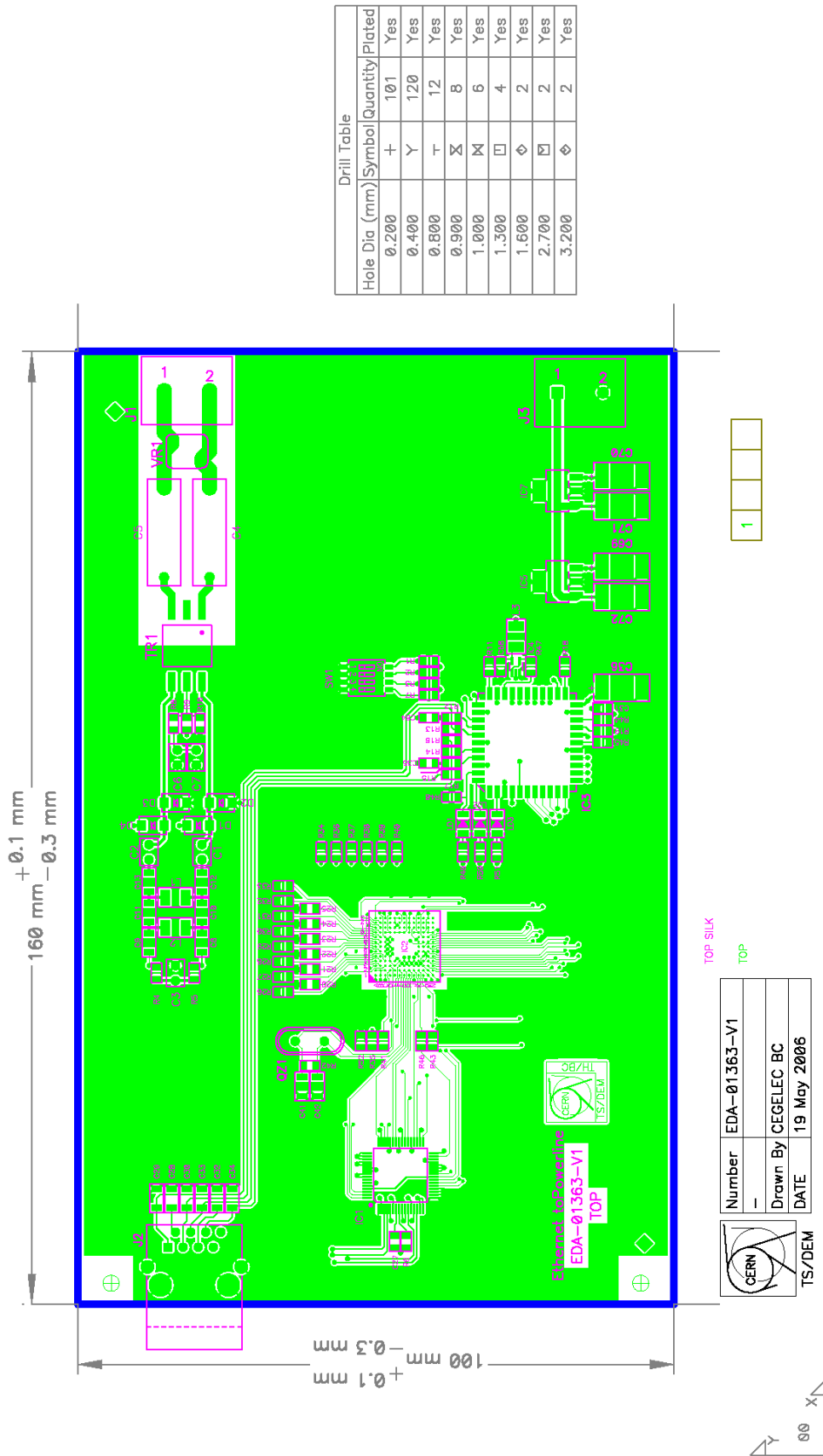


Figure B.3: PCB layout for the powerline to ethernet device, made in P-CAD, page 1

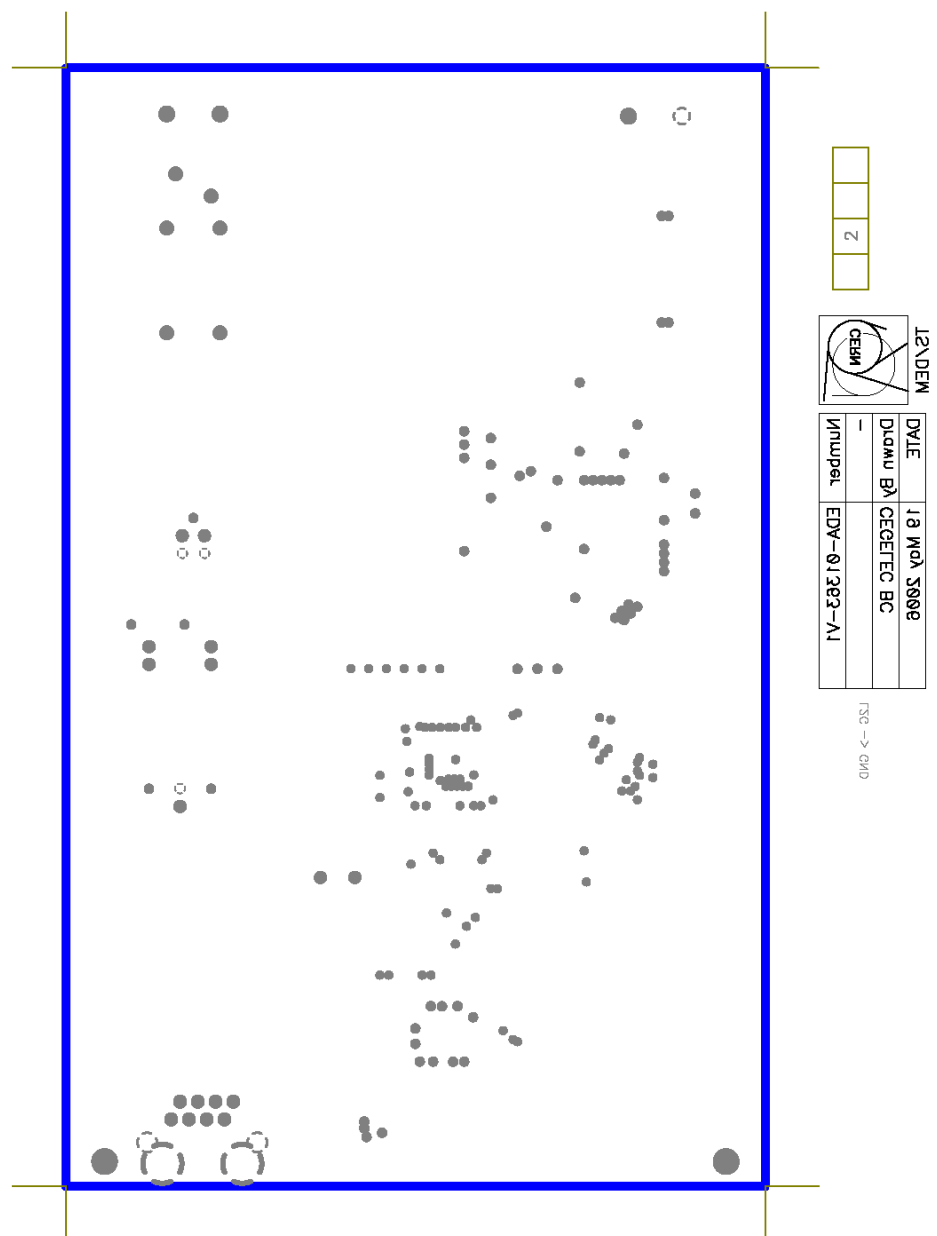


Figure B.4: PCB layout for the powerline to ethernet device, made in P-CAD, page 2

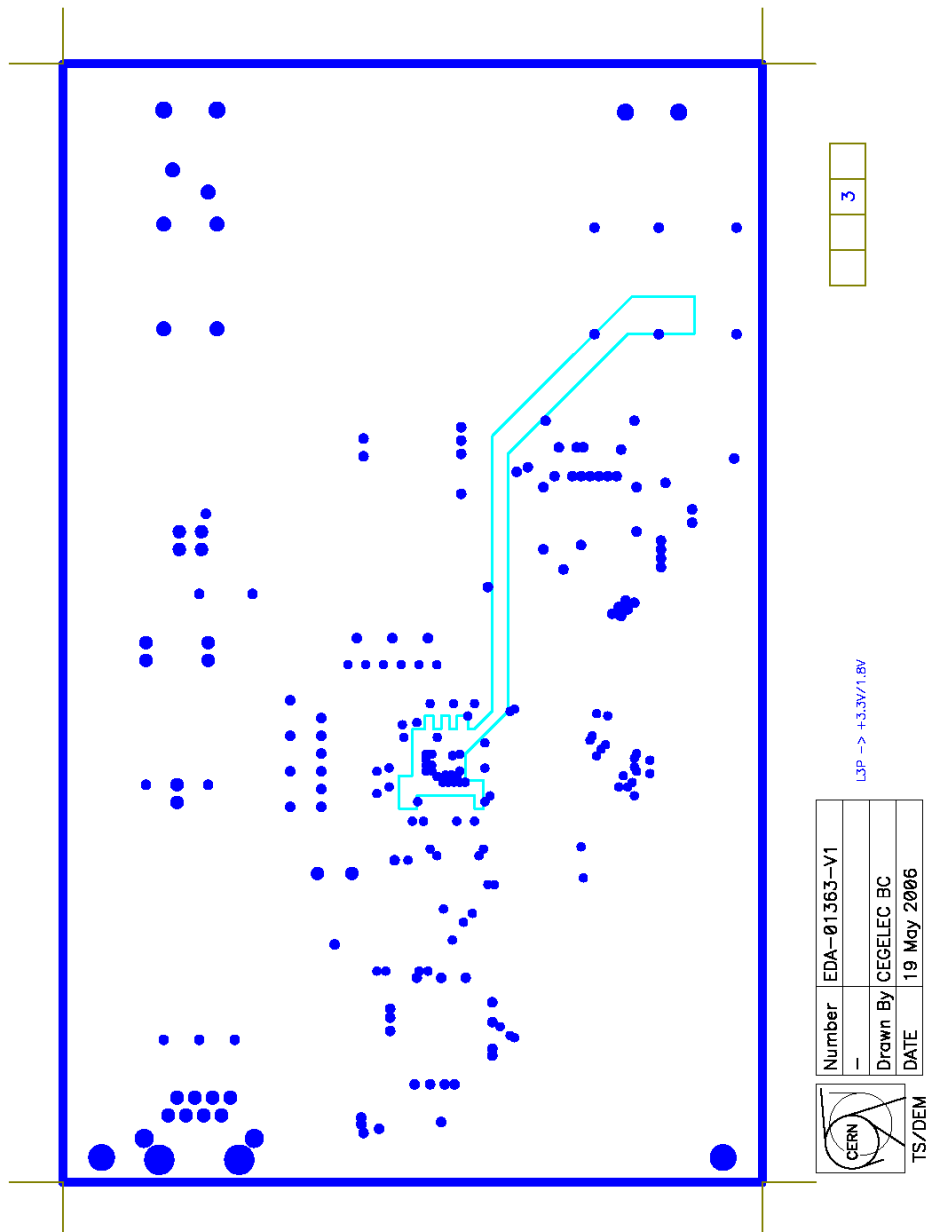


Figure B.5: PCB layout for the powerline to ethernet device, made in P-CAD, page 3

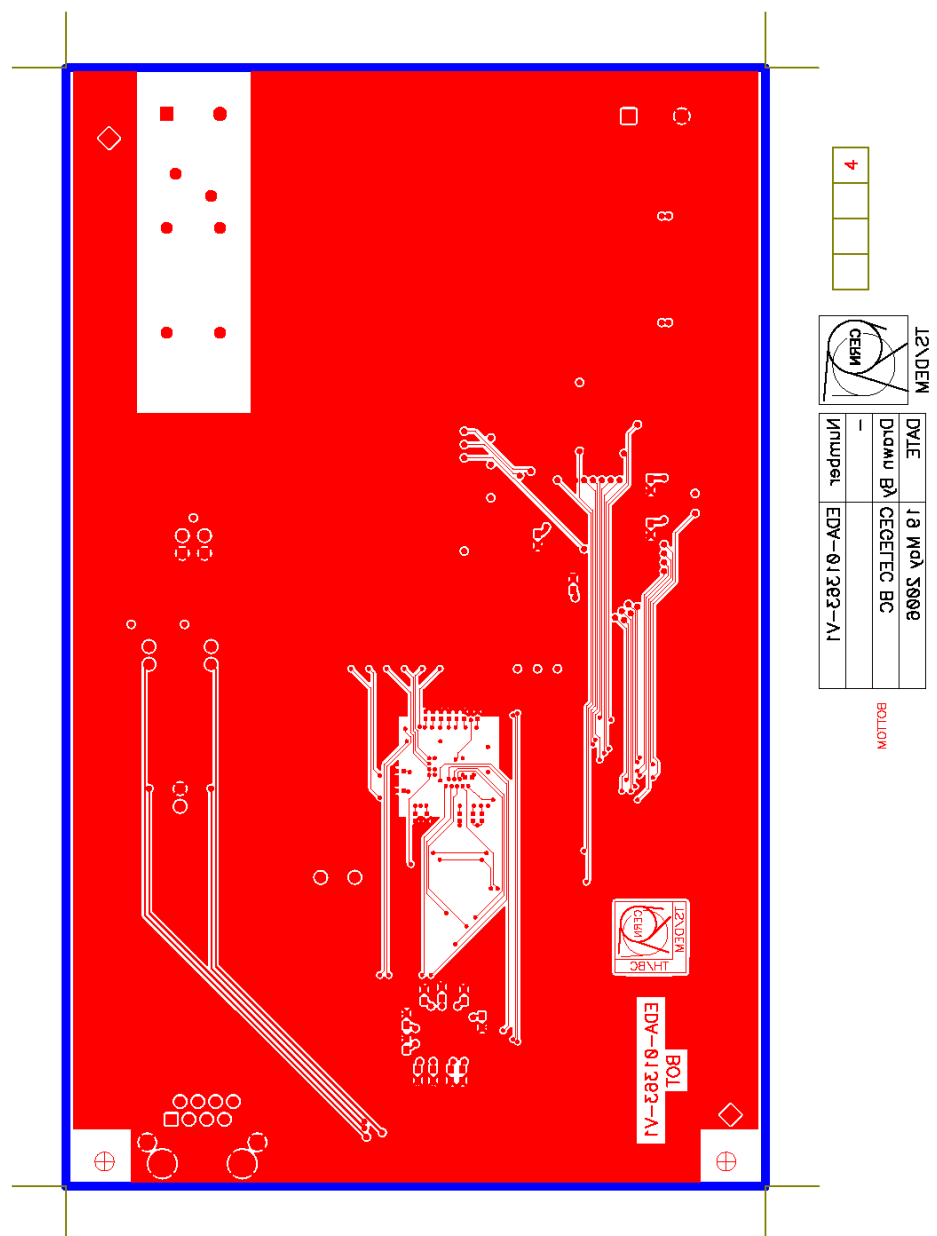


Figure B.6: PCB layout for the powerline to ethernet device, made in P-CAD, page 4

EDA-01363-V1_pcb-mat

Title : Ethernet to Powerline		RefDes		Count	SCEM	Description	VAL & Device	Ref Fabricant	PatternName
N° EDMS : EDA-01363				2	10.35.06.322.1	POLYESTER CAPACITOR 1 STEP	22nF	WIMA TYPE MKS02	CPOL100
Revision : V1				1	10.35.06.400.4	POLYESTER CAPACITOR 1 STEP	100nF	WIMA TYPE MKS02	CPOL100
Date : 30/05/2006				2	10.03.04.400.5	X7R DIELECTRIC SMD MULTILAYER CHIP CERAMIC CAPACITOR	10nF	VISHAY / VITRAMON VJ1206Y103JXAAT	C1206
				2	10.03.04.256.5	NPO DIELECTRIC SMD MULTILAYER CHIP CERAMIC CAPACITOR	560pF	VISHAY / VITRAMON VJ1206A651JXAAT	C1206
				2	10.03.04.115.7	NPO DIELECTRIC SMD MULTILAYER CHIP CERAMIC CAPACITOR	15pF	VISHAY / VITRAMON VJ1206A150JXAAT	C1206
				1	N.S.	±10% 50V X7R DIELECTRIC MULTILAYER CHIP CAPACITOR	10nF	PHYCOMP 2222 580 15636	C0605
				4	N.S.	±10% 50V X7R DIELECTRIC MULTILAYER CHIP CAPACITOR	100nF	PHYCOMP 2222 580 15649	C0805
				5	10.81.02.220.2	±10% 35VDC SPEEDPOWER LOW ESR TANTALUM CHIP CAPACITOR	10uF/35V	EPCOS B45197A6106K409	CMS-CTD
				15	10.03.05.408.1	CLASS 2 ±10% 16V Y5V SURFACE MOUNT MULTILAYER CAPACITOR	100nF	PHYCOMP 04022F104M75B00	C0402
				14	10.03.05.440.2	±5% 16V X7R SURFACE-MOUNT CERAMIC MULTILAYER CAPACITOR	100nF	PHYCOMP 06032R14J7B00	C0603
				2	10.03.04.227.0	NPO DIELECTRIC SMD MULTILAYER CHIP CERAMIC CAPACITOR	270pF	VISHAY / VITRAMON VJ1206A271JXAAT	C1206
				2	N.S.	± 5% 630V DOUBLE METALLIZED FILM PULSE CAPACITOR	10nF	EVOX-RIFA PHE450MB5100JR06	
				4	10.03.04.088.7	POLYPROPYLENE DIELECTRIC	5.8pF	VISHAY / VITRAMON VJ1206A6R8JXAAT	C1206
						NPO DIELECTRIC SMD MULTILAYER CHIP CERAMIC CAPACITOR			

Figure B.7: List of components for the powerline to ethernet device, made in P-CAD, page 1

EDA-01363-V1_pcb-mat

RefDes	Count	SCEM	Description	VAL & Device	Ref.Fabricant	PatternName
C7	3	10.03.04.222.5	NPO DIELECTRIC SMD MULTY LAYER CHIP CERAMIC CAPACITOR	220pF	VISHAY / VITRAMON VJ1206A221JXAAT	C1206
C3						
C16	2	10.35.06.300.7	POLYESTER CAPACITOR 1 STEP	10nF	WIMA TYPE MKS02	CPOL100
C8->C9	4	N.S.	1A SUPERFAST RECTIFIER	ES1D	FAIRCHILD SEMICONDUCTOR	DO-214AC
D1->D4	1	N.S.	INTEGRATED POWERLINE DIGITAL TRANSCEIVER	MAX2986CXV	MAXIM INTEGRATED PRODUCTS	
IC1	1	N.S.	POWERLINE COMMUNICATION ANALOG FRONT-END TRANCEIVER	MAX2980CCB	MAXIM INTEGRATED PRODUCTS	TQFP64-050
IC2	1	N.S.	10/100Mbps TX/10BT ETHERNET PHYSICAL LAYER DEVICE	L80225	LSI LOGIC	PLCC44
IC3	1	N.S.	SINGLE D-TYPE FLIP-FLOP POSITIVE-EDGE TRIGGER	74LVC1G80GW	PHILIPS SEMICONDUCTORS	SOT353-1
IC4	1	N.S.	1.8V 1.5A LOW NOISE FAST TRANSIENT RESPONSE LDO REGULATOR	LT1963EST-1.8	LINEAR TECHNOLOGY	SOT223
IC5	1	N.S.	3.3V 1.5A LOW NOISE FAST TRANSIENT RESPONSE LDO REGULATOR	LT1963EST-3.3	LINEAR TECHNOLOGY	SOT223
IC6	1	N.S.	CONNECTING TERMINALS 7.62mm 500V 32A		PHOENIX CONTACT GMKDS 3/2	GMKDS3-2
J1	2	N.S.				
J3						
J2	1	N.S.	1 PORT NO LED RJ45 10/100Base-TX MAGJACK CONNECTOR MODULE		BEL STEWART CONNECTOR SI-10148	
L1	1	N.S.	SMT INDUCTOR SIMID 1210	6.8uH	EPCOS B82422-A1682	L1210
L2	1	N.S.	SMT INDUCTOR SIMID 1210	5.6uH	EPCOS B82422-A1562	L1210
L3	1	N.S.	SMT INDUCTOR SIMID 1210	1.0uH	EPCOS B82422-A1102	L1210
LD1->LD3	3	N.S.	GREEN SMD LED (1206 PACKAGE)		FAIRCHILD SEMICONDUCTOR	LED1206
QZ1	1	N.S.	QUARTZ CRYSTAL	30.0MHz	JAUCH Q30.0-SS4-30-30/50-FU-T1	SS4
R1	2	N.S.	0.1W ±0.1% PRECISION CHIP RESISTOR	162	MEGGITT CGS TYPE RN73C2A162RBTDF	R0805
R4						
R15	1	N.S.	0.125W ±1% THIN-FILM RECTANGULAR CHIP RESISTOR	1M	VISHAY CRCW 0805 1M F 100	R0805
R2	1	N.S.	0.125W ±1% THIN-FILM CHIP RESISTOR (Pb FREE)	10	PHYCOMP YAGEO RC0805FR-0710R	R0805
R25	1	11.24.09.168.9	0.125W ±1% THIN-FILM CHIP RESISTOR (Pb FREE)	390k	PHYCOMP YAGEO	R0805
R27	1	N.S.	0.125W ±1% THIN-FILM CHIP RESISTOR (Pb FREE)	4M7	PHYCOMP YAGEO RC0805FR-074M7	R0805
R29	1	N.S.	0.125W ±1% THIN-FILM CHIP RESISTOR (Pb FREE)	0R	PHYCOMP YAGEO RC0805FR-070R	R0805
R3	2	N.S.	0.125W ±1% THIN-FILM CHIP RESISTOR (Pb FREE)	5k1	PHYCOMP YAGEO RC0805FR-075K1	R0805
R5						
R31	1	N.S.	0.1W ±0.1% PRECISION CHIP RESISTOR	24K9	MEGGITT CGS TYPE RN73C2A24K9BTDF	R0805
R32	5	11.24.09.154.8	0.125W ±1% THIN-FILM CHIP RESISTOR (Pb FREE)	47	PHYCOMP YAGEO	R0805
R37					RC0805FR-0747R or 232273464709	
R49->R50						
R52	7	N.S.	0.125W ±1% THIN-FILM CHIP RESISTOR (Pb FREE)	10k	PHYCOMP YAGEO RC0805FR-0710K	R0805
R33->R36						
R47						
R51						
R53						
R38	1	N.S.	0.125W ±1% THIN-FILM CHIP RESISTOR (Pb FREE)	49k9	PHYCOMP YAGEO RC0805FR-0749K9	R0805
R39->R42	4	N.S.	0.125W ±1% THIN-FILM CHIP RESISTOR (Pb FREE)	24	PHYCOMP YAGEO RC0805FR-0724R	R0805
R43->R44	2	N.S.	0.125W ±1% THIN-FILM CHIP RESISTOR (Pb FREE)	51	PHYCOMP YAGEO RC0805FR-0751R	R0805
R45->R46	3	N.S.	0.1W ±0.1% PRECISION CHIP RESISTOR	340	MEGGITT CGS TYPE RN73C2A340RBTDF	R0805
R48						
R6	1	11.24.05.175.3	0.25W ± 1% METAL FILM CHIP RESISTOR	75	BOURNS TYPE CR 1206-FX	R1206

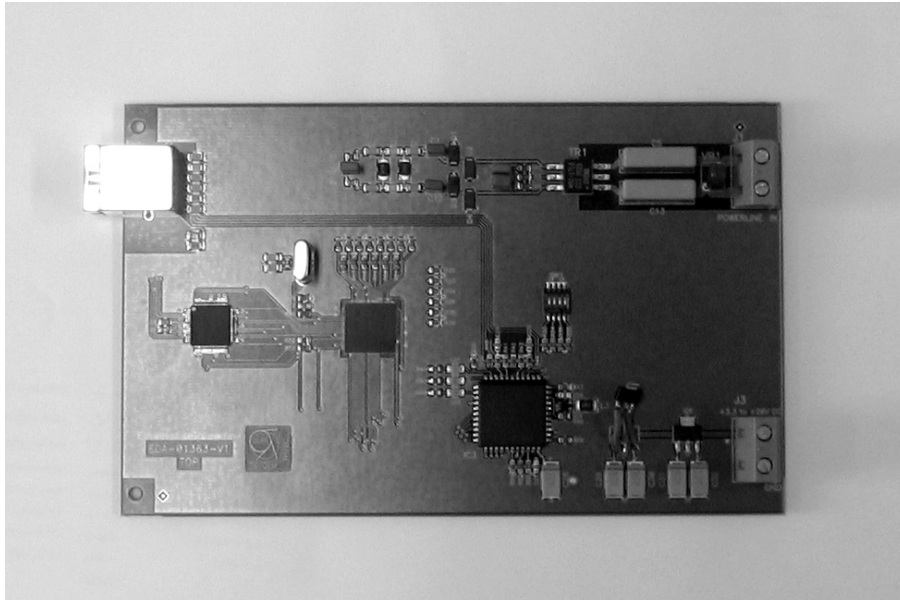
Figure B.8: List of components for the powerline to ethernet device, made in P-CAD, page 2

EDA-01363-V1_pcb-mat

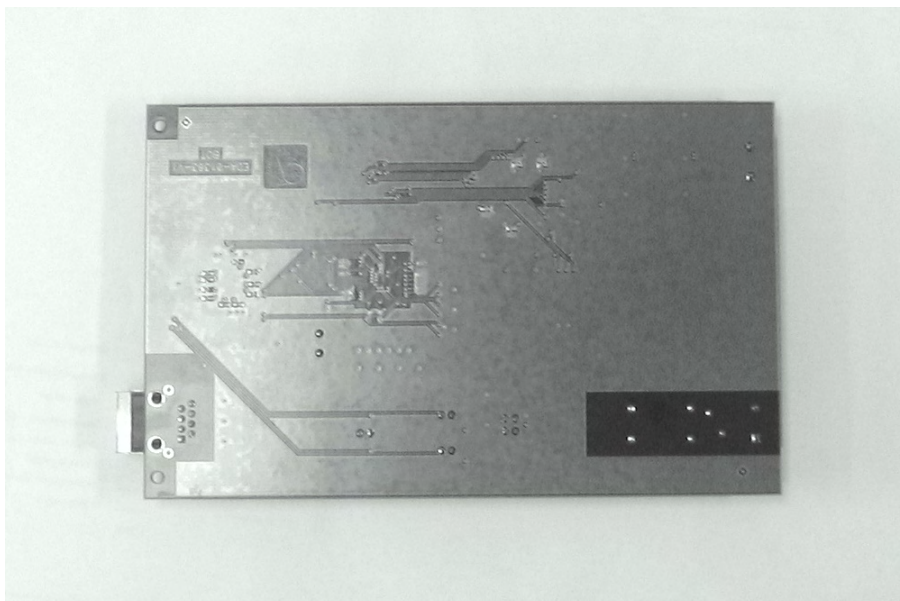
RefDes	Count	SCEM	Description	VAL & Device	Ref.Fabricant	PatternName
R7->R14 R16->R24 R26 R28 R30 R30	20	N.S.	0.125W ±1% THIN-FILM CHIP RESISTOR (Pb FREE)	100k	PHYCOMP YAGEO RC0805FR-07100K	R0805
SW1	1	N.S.	SURFACE MOUNT 050 PITCH LOW PROFILE 4 POLES DIP SWITCH	GDH04S	TYCO ELECTRONICS	
TR1	1	N.S.	WIDEBAND TRANSFORMER 100MHz TO 375MHz	WB1-1TSLD	COILCRAFT	WB1-1TSL
VR1	1	N.S.	460VAC S+M METAL OXIDE VARISTOR	SIOV-S05K460	EPCOS B72205-S461-K101	
Dimension :				34		
160 x 100 mm				457		
Through pins:				60		
SMD pins on TOP:				551		
SMD pins on BOTTOM:						
Total nb of pins:						

Figure B.9: List of components for the powerline to ethernet device, made in P-CAD, page 3

B.2 The finished board



(a) The front of the board



(b) The back of the board

Figure B.10: The PCB, finished with the components mounted

Software for the motor controller

On the ATAVRMC100 motor controller card, with the AT90PWM3 microcontroller, it is already made a demonstration software, that is pre-compiled and can be downloaded from the Internet and used to program the controller. This software is written for the IAR C-compiler, which is costly to purchase, so before the software is used in this project, it is ported to the OpenSource WinAVR GCC compiler. Basically, the functions needed for this is found at the AVR GCC website (Free Software Foundation, Inc., 2006), in the documentation for AVR-libc (AVR Libc project group, 2006), and in the AVR libc function reference page (AM Elektronik, 2002).

The controller will use the RS232 to communicate with the camera, that means that the UART-port on the microcontroller will be used. When the camera sends a `char` to the controller, then the microcontroller receives this with UART, and then executes whatever action it is supposed to take when this char arrives. In most cases for the demonstration, this means changing the speed of the motor, or starting, stopping, changing direction. After that, the controller responds by sending out information about the present set-speed.

The commands available by default is listed in table C.1.

If we want to create a controller for this system, it is already fit with functions to read back the current speed, so that is a simple task to manage.

0	Set speed to 50 out of 255 possible speed values, where 255 is the maximum possible speed
1	Set speed to 100
2	Set speed to 150
3	Set speed to 255
4	Set speed to 15
+	Increase speed by 1
-	Reduce speed by 1
i	Initialize the system (i.e. after an over-current detection in hardware)
?	Read back the set-speed
m	Read back the measured speed
r	Run
s	Stop
f	Direction forward
b	Direction backward

Table C.1: List of Commands

MatLab and Simulink code and diagrams

In this appendix, the MatLab code and Simulink diagrams used to produce bode diagrams and simulations are shown.

D.1 MatLab code

The calculations for the simplified high-pass filter in chapter 5.1.4 is written in the file named `HPfilter.m`.

The file `stability.m` calculates the sensitivity function, the complimentary sensitivity function, and plots them. In addition, it plots the LFC used to prove stability, and the time derivative of the LFC, both used in the report as figures 6.10 and 6.11. At last, the code used to plot the 400V 3-phase power (figure A.1) is displayed as file `power.m`.

```
%% Initialization
C1 = 22e-9;
C2 = 270e-12;
C3 = 220e-12;
C4 = 560e-12;
C5 = 10e-9;
Cs1 = (2/C1+2/C2)^-1;
%
R1 = 162;
R = 2*R1;
%
L1 = 5.6e-6;
L2 = 6.8e-6;
%% Transfer function of the simplified circuit
s = tf('s');
SYS = ((s*L2+1/(s*Cs1))*(1/(s*L2)+2/(s^2*L2*C2*R)
+2/(s^2*L2*C1*R)+2/(s^3*L1*L2*C2)*(2/(s*C1*R)+1))
+(1/(s^2*Cs1*L1))*(2/(s*C1*R)+1)+1/(s*Cs1*R))^-1;
%% Bode plot of the function
WMIN= 10; % 10Hz
WMAX= 1e9; % 1GHz
bode(SYS,{WMIN,WMAX});
```

HPfilter.m

```

%% Initialization
PI = 1;
P = 5;
a = 0.00025/(0.083*7/18)+40*0.083*7/(18*2);
b = 36/14/7*1.28*0.083*0.14*0.5/4;
c = 0.083*40*9.81/8*36/14/7*0.002;
d = 0.1115;
e = 2*0.0874/(0.083*0.0015*7/18);
f = 1.1393/0.0015;
A = [0 1 0;0 0 d/a; 0 -e -f];
B = [0 0 1]';
C = [1 0 0;0 1 0];
D = [0 0]';
SYS = ss(A,B,C,D);
%% Sensitivity function and complementary sensitivity function
s = tf('s');
H = SYS(1);
K = PI+P*s;
L = K*H;
S = 1/(1+L);
T = L*S;
%% Plotting of S and T
WMIN= 1e-5;
WMAX= 1e-1;
figure(1);subplot(2,1,1);bodemag(S,{WMIN,WMAX});
figure(1);subplot(2,1,2);bodemag(T,{WMIN,WMAX});
figure(2);bodemag(tf(1),'k:');hold on;
bodemag(S,'k-',{WMIN,WMAX});bodemag(T,'k--',{WMIN,WMAX});hold off;
%% Plotting the Lyapunov function
alpha= 1;
beta= d/a/e*alpha;
x2 = -5:0.2:5;
x3 = -1:0.04:1;
V = zeros(length(x2),length(x3));
Vdot= V;
for i=1:length(x2)
    for j=1:length(x3)
        V(i,j)= 0.5*alpha*x2(i)^2 + 0.5*beta*x3(j)^2;
        Vdot(i,j)= -alpha*b/a*x2(i)^3*sign(x2(i))
            -alpha*c/a*x2(i)*sign(x2(i))
            +(alpha*d/a-beta*e)*x2(i)*x3(j)-beta*f*x3(j)^2;
    end
end
end
figure(1);surf(x2,x3,Vdot);colormap(hsv);xlabel('Speed');ylabel('Current');
figure(4);surf(x2,x3,V);colormap(hsv);xlabel('Speed');ylabel('Current');

```

```
%% Initialization
Vrms = 230;
phase = 120*pi/180;
time = 0:0.0002:0.1;
%% Voltage init
l1 = Vrms*sqrt(2)*sin(time*50*2*pi);
l2 = Vrms*sqrt(2)*sin(time*50*2*pi-phase);
l3 = Vrms*sqrt(2)*sin(time*50*2*pi-2*phase);
%% Plotting of the original voltages
figure(1);subplot(2,1,1);
plot(time,l1,time,l2,time,l3);
xlabel('Time / s');ylabel('Voltage / V');
%% Calculation and plots of the rest
l1=l1-l2; % Calculating the resulting waveform
        % from the difference between l1 and l2
lt=400*sqrt(2)*sin(time*50*2*pi+1*pi/6);
subplot(2,1,2);
plot(time,l1,'g',time,lt,'k--');
xlabel('Time / s');ylabel('Voltage / V');
```

powerline.m

D.2 Simulink diagram

Below is the diagrams drawn in Simulink for simulating the total system. The system is put together in blocks, in order to make it easier to see the effects of the different parts, and also to enable us to scope the different signals in a more intuitive way.

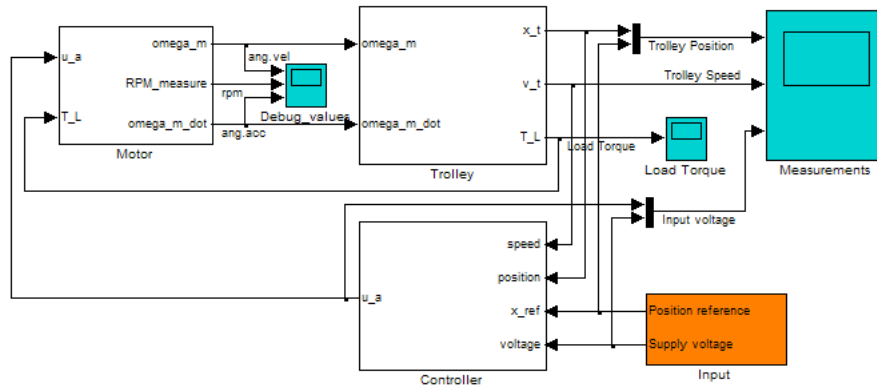


figure D.1: The overall system

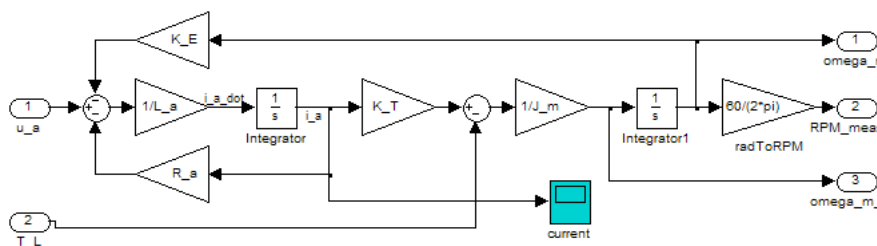


figure D.2: The motor model

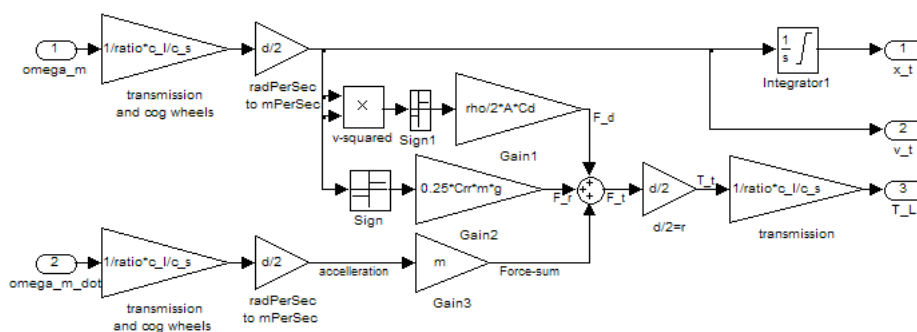


figure D.3: The trolley model

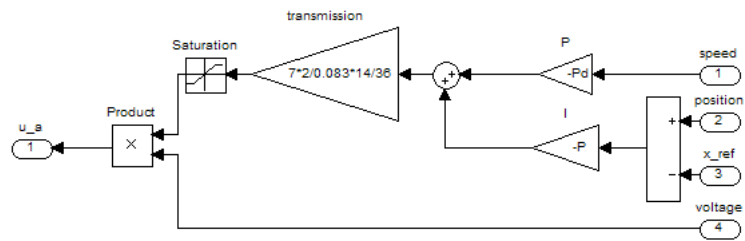


figure D.4: The controller

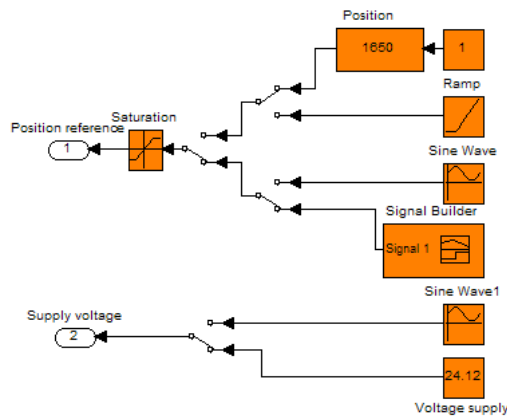


figure D.5: The block for choosing inputs to simulate

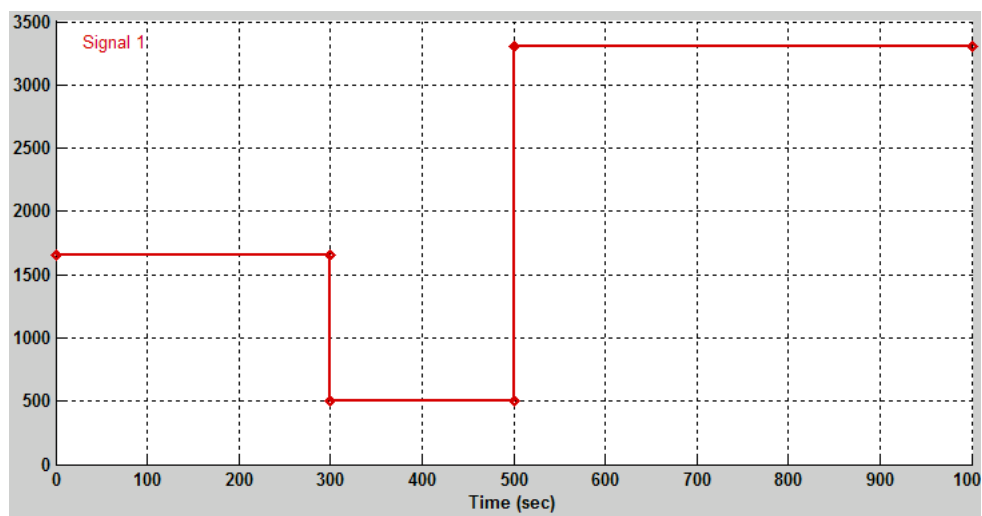










figure D.6: The input made from the signal builder block, the y-axis is the number of meters into the tunnel


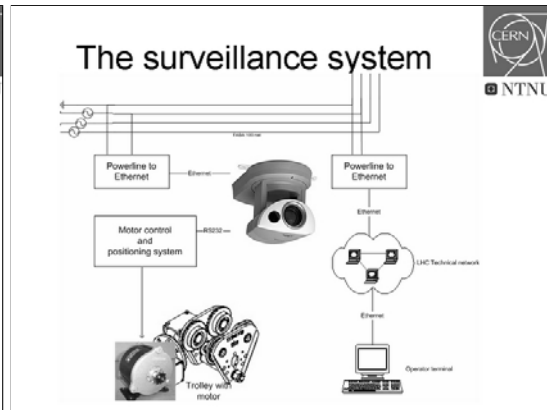
Project presentation

This presentation was presented at the CERN AT-ACR group meeting on July 13. 2006. The presentation was done with PowerPoint, the file is on the CD described in Appendix F

<p>Mobile remote surveillance system for the CERN LHC cryogenic system</p> <p>And visual inspection of cryogenic pipelines after installation</p> <p> </p>	<p>Requirements  </p> <ul style="list-style-type: none">• View small objects (1cm) in 3m distance• Flexibility• Long range of operation, 3.3km• Size & weight to be kept small• Material considerations• Speed• Position• Safety
<p>Project components  </p> <ul style="list-style-type: none">• Camera• Trolley• Communications• Power	<p>Technologies for communication  </p> <ul style="list-style-type: none">• Wireless<ul style="list-style-type: none">– WLAN<ul style="list-style-type: none">• Distance• Line of sight– GSM<ul style="list-style-type: none">• Bandwidth– Leaky feeder<ul style="list-style-type: none">• Link budget looks negative• Requires a lot of power



Technologies for communication

- **Wired**
 - VDSL
 - Discrete coverage
 - Complicated
 - Powerline networking
 - Continuous coverage where there is power
 - Not adapted for 400V, must design

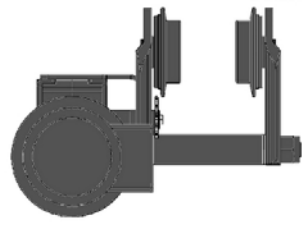

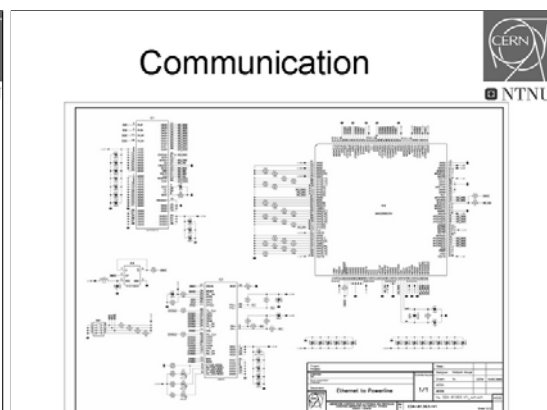
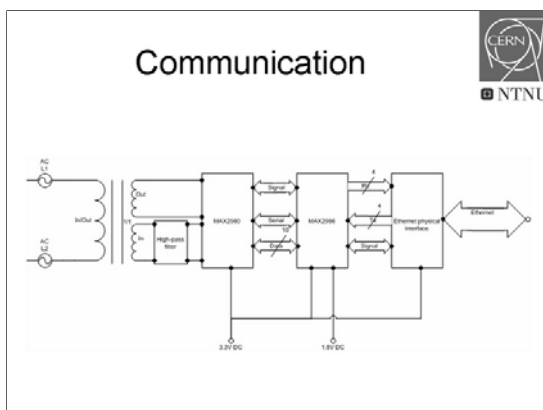
Camera

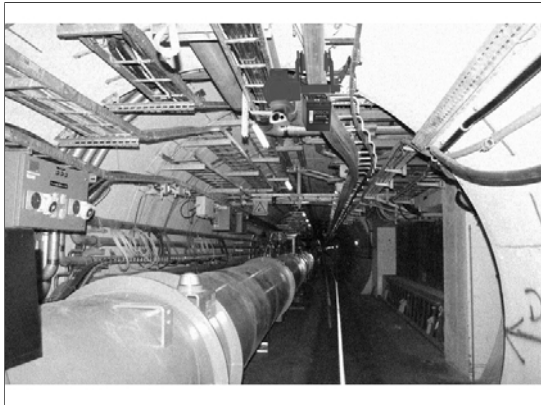
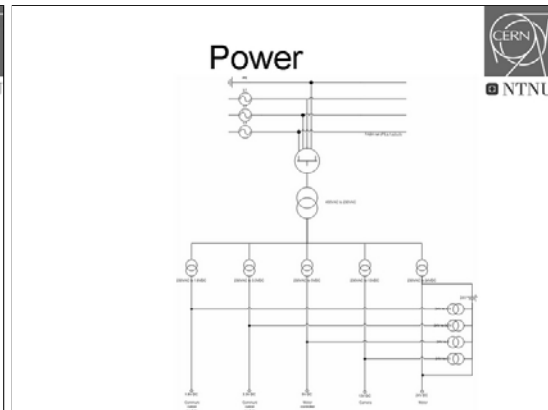
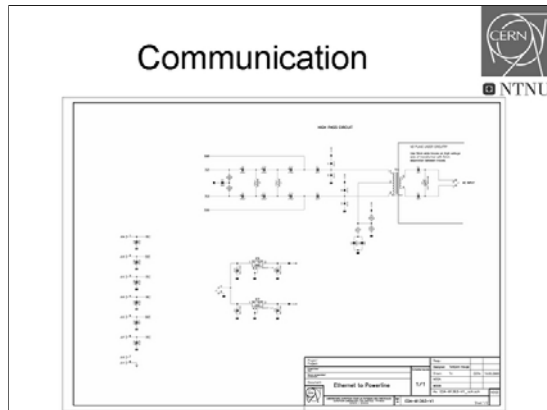
- The Axis 213 PTZ is already in use at CERN
- Has an onboard webserver, can be programmed

Trolley

- Manufacturer say it can go up to 17km/h
- Can be controlled if fitted with a DC motor
- Need to change steel wheels into polyurethane




Constraints

- Power-supply
 - Dead-zones
 - Possibly unreliable at times
 - Experienced speed might not be equal to theoretical speed
- If the trolley is offline when moving, it might not establish contact before it is arrived, and the operator will not know its position at all times
- Operation while LHC operation is not likely because of radiation
- Real-time control of the trolley is not possible, since the communication over ethernet will have delays

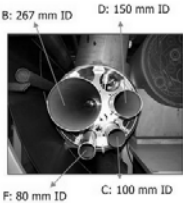
Status

- Communication device is designed
 - PCB finished
 - Most components has arrived, not all
 - Not finished
- Not found wheels for trolley
 - Not finished
- Camera
 - Was already here
 - Communicates nicely with microcontroller
- Motor controller
 - Works good
 - Communicates with camera server and controls the motor
- Power


Inspection of cryogenic pipelines



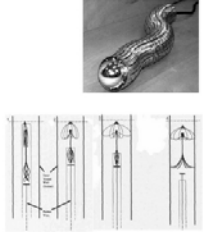
- Length of pipes
- Sensors inside the pipes
- Bends




Inspection of cryogenic pipelines




- Prototype systems
 - Snake robots
 - Move as snakes, no wheels
 - Need space
 - Still being researched
 - Jumping robot
 - Jumps and holds
 - Still on research stage




Inspection of cryogenic pipelines



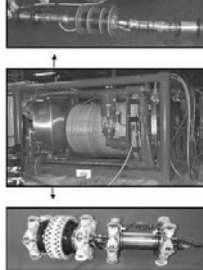
- Prototype systems
 - Explorer
 - Carnegie Mellon and New York Gas Group and NASA
 - 150-200mm diameter pipes
 - 90 deg bends ok
 - Goes up/down well
 - Wireless communication, large battery pack
 - Has been proven, but will not get past sensors very well



AGR



- AGR is a Norwegian company experienced in pipe inspection for international oil companies



APPENDIX F

Video and files

Attached to this report is a CD with documentation on parts of the project.

- A version of this report, in pdf format (`MobileSurveillance.tex`)
- A video with a demonstration of the communication from the camera to the motor controller, and a demonstration of use of the camera (`Camera_control_demo.wmv`)
- Code for the Atmel microcontroller on the ATAVRMC100 motor controller (folder `Motor Control Software`)
- A PowerPoint presentation about this project presented at CERN on the 13. July 2006 (`Project_presentation_2006_07_13.ppt`)
- PDF-files with output from P-CAD, as described in appendix B (`EDA-01363-V1_sch.pdf`, `EDA-01363-V1_pcb.pdf` and `EDA-01363-V1_pcb-mat.pdf`)

